ISTANBUL TECHNICAL UNIVERSITY ★ GRADUATE SCHOOL

ENZYMATICALLY SYNTHESIZED POLY(δ-VALEROLACTONE) AND POLY(δ-VALEROLACTONE) NANOHYBRID USAGE IN CONTROLLED DRUG DELIVERY SYSTEMS

M.Sc. THESIS

ZEYNEP KEÇE

Department of Chemical Engineering

Chemical Engineering Programme

JANUARY 2025

ISTANBUL TECHNICAL UNIVERSITY ★ GRADUATE SCHOOL

ENZYMATICALLY SYNTHESIZED POLY(δ-VALEROLACTONE) AND POLY(δ -VALEROLACTONE) NANOHYBRID USAGE IN CONTROLLED DRUG DELIVERY SYSTEMS

M.Sc. THESIS

Zeynep KEÇE
(506211042)

Department of Chemical Engineering

Chemical Engineering Programme

Thesis Advisor: Prof. Dr. F. Yüksel GÜVENİLİR

JANUARY 2025

İSTANBUL TEKNİK ÜNİVERSİTESİ ★ LİSANSÜSTÜ EĞİTİM ENSTİTÜSÜ

ENZİMATİK OLARAK SENTEZLENMİŞ POLİVALEROLAKTON VE POLİVALEROLAKTON NANOHİBRİTİNİN KONTROLLÜ İLAÇ SALIM SİSTEMLERİNDE KULLANIMI

YÜKSEK LİSANS TEZİ

Zeynep KEÇE
(506211042)

Kimya Mühendisliği Anabilim Dalı

Kimya Mühendisliği Programı

Tez Danışmanı: Prof. Dr. F. Yüksel GÜVENİLİR

OCAK 2025

Zeynep KEÇE, a M.Sc. student of ITU Graduate School student ID 506211042, successfully defended the thesis/dissertation entitled "ENZYMATICALLY SYNTHESIZED POLY(δ-VALEROLACTONE) AND POLY(δ-VALEROLACTONE) NANOHYBRID USAGE IN CONTROLLED DRUG DELIVERY SYSTEMS", which she prepared after fulfilling the requirements specified in the associated legislations, before the jury whose signatures are below.

Thesis Advisor :	**Prof. Dr. F. Yüksel GÜVENİLİR** Istanbul Technical University	.....
Jury Members :	**Prof. Dr. Didem SALOĞLU DERTLİ** Istanbul Technical University	……..
	Asst. Prof. Dr. Cansu ÜLKER TURAN Gebze Technical University	…….

Date of Submission : 10 January 2025
Date of Defense : 23 January 2025

To my family,

FOREWORD

I would like to express my gratitude and huge respect to my esteemed thesis advisor, Prof. Dr. Fatoş Yüksel GÜVENİLİR, who gave me both academic and life discipline with her mentorship, supported me in every times and kept my motivation and interest alive.

I would like to thank and appreciate Asst. Prof. Dr. Cansu ÜLKER TURAN, who helped me in every way possible with the problems I encountered, both laboratory experiments and methods of the thesis and during my studies. Her valuable comments and evaluations played a major role in determining the roadmap of this study.

Also, I would like to express my gratitude and appreciation to Asst. Prof. Dr. Yasemin KAPTAN for giving me every information that she already knew and for always helping my experiments with pleasure.

I am deeply thankful to my dear friend Mete DERVİŞCEMALOĞLU for his kind support.

In addition, I would like to express my gratidue to HAYAT, who supported me for conducting characterization tests (FT-IR, UV-Vis, SEM, DSC, TGA) and allowing me to use their laboratories.

Finally, I would like to thank my entire family, who encouraged me to continue my graduate education and always supported me throughout my graduate studies.

January 2025

Zeynep KEÇE
(Chemical Engineer)

TABLE OF CONTENTS

Page

ABBREVIATIONS

3-APTES **:** (3-Aminopropyltriethoxysilane
3-APTMS **:** (3-Aminopropyl)trimethoxysilane
3-GPTMS **:** (3-Glycidyloxypropyl)trimethoxysilane
CALB **:** *Candida antarctica* Lipase B
DNA **:** Deoxyribonucleic acid
DSC **:** Differential Scanning Calorimetry
FT-IR **:** Fourier Transform Infrared Spectroscopy
PBS **:** Phosphate Buffered Saline
PBT **:** Poly(buthylene therephthalate)
PCL **:** Poly(ε-caprolactone)
PET **:** Poly(ethylene therephthalate)
PGA **:** Polyglycolic acid
PHB **:** Polybutylene terephthalate
PLA **:** Poly(lactic acid)
PLGA **:** Poly(lactic-co-glycolic acid)
PVA **:** Polyvinyl alcohol
RHA **:** Rice Husk Ash
RNA **:** Ribonucleic acid
ROP **:** Ring Opening Polymerization
SEM **:** Scanning Electron Microscope
TC **:** Trans-chalcone
TGA **:** Thermo Gravimetric Analysis
XRD **:** X-Ray diffraction analysis
δ-VL **:** δ-Valerolactone
ε-CL **:** ε-Caprolactone

SYMBOLS

ΔH_m	**:** Melting Enthalpy
K_H	**:** Higuchi Dissolution Constant
K_{KP}	**:** Korsmeyer-Peppas Release Rate Constant
M_n	**:** Number Average Molecular Weight
n	**:** Release Exponent
R^2	**:** Coefficient of determination
Q_0	**:** Initial Concentration of Drug
Q_t	**:** Cumulative % Drug Release at Any Time
Q_t / Q_∞	**:** Fraction of Drug Released at Any Time
t	**:** Time
T_g	**:** Glass Transition Temperature
T_m	**:** Melting Temperature
v/v	**:** Volume to volume ratio
W_0	**:** Initial Weight
W_t	**:** Dry Weight at Any Time

LIST OF TABLES

Page

LIST OF FIGURES

Page

ENZYMATICALLY SYNTHESIZED POLY(δ-VALEROLACTONE) AND POLY(δ-VALEROLACTONE) NANOHYBRID USAGE IN CONTROLLED DRUG DELIVERY SYSTEMS

SUMMARY

There is an increasing interest for the biopolymers these days, because oppose to synthetically/artificially formed ones, they are generated by renewable resources. It is clear that with the increasing population and the times when we need to pay more attention to the world's depleting resources, why the people are tending to use biopolymers instead of synthetic polymers, which are petroleum-based. In other words, with the developing technology, oppose to fossil resources, which are very traditional, people started to care to eliminate their carbon footprint. In order to make this valuable approach happen, they beginned to use natural resources. Due to their better biodegradability, reproducable, biocompatibility and chemical degradability, they indicate non-toxicity and they have low-weight. These qualities lead them to be used in not only packaging, textile, medical, agricultural industries, but also wearable devices, sensors and mostly in drug delivery systems. Due to their many benefits, including biocompatibility, nontoxicity, thermoplasticity, semi-crystalline and hydrophobic form, flexibility, along with controlled decomposition, PVL is an intriguing option and frequently utilized in biomedical implementations. PVL is a fundamental component in the production of anthracycline type of antibiotics and the controlled medications (like doxorubicin (DOX)), which are prescribed to avoid different types of cancer. Nanohybrid systems are composite substances constructed up of two or more different nanoscale constituents that are closely joined or blended at the molecular or atomic scale. When these elements are combined, a fresh substance with specific qualities that may be superior to those of the constituent parts individually can be produced. The resultant nanohybrids frequently show mutually beneficial impacts, which enhance efficiency across a range of applications. Having particle sizes varying from one to thousand μm in diameter, microspheres are a form of particle dispersion mechanism, where molecules of drug are incorporated in a polymer matrix by adsorption or dispersion. Numerous medical compounds, including peptides, proteins, nucleic acids and molecules of small size medicine could be encapsulated in microspheres and have the relevant therapeutic properties. The microspheres have garnered a lot of interest lately upon account of their tiny size of particles, unique surface features, and substantial surface-to-volume ratio. Chalcones are polyphenolic chemicals of various structures found in plants. There are several possible uses for chalcone-based compounds, including antibacterial, antiviral, antioxidant, anti-inflammatory, antidiabetic, antiulcer, anticancer properties. The remarkable chemical structure and intriguing pharmalogical properties of trans-chalcone (TC), also known as 1,3-diphenyl-2-propen-1-one, make it a prominent focus of scientific investigation alongside other chalcones.

In this study, physical adsorption was employed in the first part to immobilize lipase on surface-modified rice husk ash (RHA) to be used in enzymatic ring opening

polymerization. The silica based material underwent surface modification when amine groups were added to its surface by utilizing 3-aminopropyltriethoxysilane (3-APTES). Then, pysical adsorption methodology was used to immobilize the free form of Candida antarctica lipase B. By using the monomer ratios from prior study, poly(δ-valerolactone) and poly(δ-valerolactone) nanohybrid were generated by enzymatic ring opening polymerization. The reactions are conducted at 80^{o}C for 24 hours to get the highest molecular mass for both polymer and nanohybrid. These resultant materials were ultimately found to be applied in the fabrication of microspheres. As following, the methodology of O/W emulsion was employed to fabricate TC-loaded PVL microspheres, TC-loaded PVL nanohybrid microspheres, drug-free PVL microspheres and drug free PVL nanohybrid microspheres. Afterwards, drug release mechanism of these fabricated microspheres were investigated. For this investigation, with three different PVA concentrations (0.1, 0.5, 1 (w/v)%), there different TC:PVL ratio (10, 20, 40%) and TC:PVL nanohybrid ratio (10, 20, 40%) have been evaluated in order to ascertain greatest encapsulation efficiency, and thereby drug release profile. To define the thermal, chemical and mechanical properties, TGA, DSC, SEM and XRD were applied to these microspheres. The greatest encapsulation efficiencies were observed with specimen A-2 (1% PVA and 20% ratio of TC:PVL) as 98.6 ± 8.4 (%) and specimen C-2 (1% PVA and 20% ratio of TC:PVL nanohybrid) as 82.7 ± 6.4 (%). This research, also demonstrates that drug release mechanisms are not affected majorly by the pH-changes. The DSC analysis shows that addition of TC into microspheres has lowered the melting points but there were no any extra TC-peak on the curves, so it is concluded that TC is successfully encapsulated and molecularly dispersed into PVL and PVL nanohybrid microspheres. TGA analyses were used to compare the thermal degradation pattern of drug-free and TC-loaded PVL microspheres with PVL. Additionally, TGA analyses were used to compare the thermal degradation pattern of drug-free and TC-loaded PVL nanohybrid microspheres with PVL nanohybrid. Decompositions and weight losses have been evaluated and interpreted based on the scientific literature and the analyses that were conducted. The chemical groups that indicate the existence of TC, PVL, TC-loaded PVL microspheres, drug-free PVL microspheres, PVL nanohybrid, TC-loaded PVL nanohybrid microspheres, and drug-free PVL nanohybrid microspheres were all observed by using FT-IR as characterization technique. Since FT-IR spectras are alike, it shows that TC was determined to be encapsulated within the microspheres. XRD analyses were used besides to several other characterizations to investigate the impact of TC loading on the crystalline structures and the crystallinity of microspheres. The SEM images reveal that every single one of the microsphere formulations had spherical shape. To observe the drug release behaviour of the microspheres fabricated in various surroundings, pH-dependent drug release investigations were conducted in the present research by employing two pH levels that were 5.6 and 7.4. The total cumulative release of TC was enhanced by the PVL microsphere formulations, reaching 42.1% in pH 7.4 ambient and 43.5% in pH 5.6 ambient. Moreover, the total cumulative release of TC was enhanced by the PVL nanohybrid microsphere formulations, reaching 39.4% in pH 7.4 ambient and 34.2% in pH 5.6 ambient. The TC release was conducted for an overall duration of 744 hours in each case. Finally, the release kinetics were examined. The release was found to be compatible with the kinetic model of Korsmeyer-Peppas. All microsphere formulations had TC release that was controlled by Fickian diffusion, according to the calculated n value. In conclusion, the goal of this study is to develop new controlled drug delivery systems by integrating a transchalcone into biological in origin polymeric carriers. A biocompatible, environmentally friendly, high-molecular-

weight polymer and nanohybrid containing home-made immobilized enzymes that are compatible for human body will be produced in order to fabricate microspheres. Transchalcone will be incorporated with the polymer and nanohybrid generated by biocatalyst for use in therapy. Following the completion of all characterization tests and investigation of drug release profiles, it can be clearly said that this research's findings suggest that PVL microspheres or PVL nanohybrid microspheres may find implementation in prolonged therapeutic applications.

ENZİMATİK OLARAK SENTEZLENMİŞ POLİVALEROLAKTON VE POLİVALEROLAKTON NANOHİBRİTİNİN KONTROLLÜ İLAÇ SALIM SİSTEMLERİNDE KULLANIMI

ÖZET

Günümüzde biyopolimerlere olan ilgi giderek artmaktadır, çünkü sentetik/yapay olarak oluşturulanların aksine, yenilenebilir kaynaklardan üretilmektedirler. Artan nüfus ve dünyanın tükenen kaynaklarına daha fazla dikkat etmemiz gereken bu zamanlarda, insanların petrol bazlı sentetik polimerler yerine biyopolimerleri kullanmaya yönelmesinin nedeni açıktır. Başka bir deyişle, gelişen teknoloji ile birlikte, geleneksel olan fosil kaynakların aksine, insanlar karbon ayak izlerini ortadan kaldırmaya özen göstermeye başladılar. Bu değerli yaklaşımı gerçekleştirmek için doğal kaynakları kullanmaya başladılar. Biyopolimerler, daha iyi biyolojik olarak parçalanabilirlik, yeniden üretilebilirlik, biyouyumluluk ve kimyasal parçalanabilirlik nedeniyle, toksik değildirler ve düşük ağırlığa sahiptirler. Bu nitelikleri, biyopolimerlerin yalnızca paketleme, tekstil, tıp, tarım endüstrilerinde değil, aynı zamanda giyilebilir cihazlarda, sensörlerde ve çoğunlukla ilaç dağıtım sistemlerinde kullanılmasına yol açmıştır. Biyouyumluluk, toksik olmama, termoplastisite, yarı kristal ve hidrofobik form, esneklik ve kontrollü ayrışma gibi birçok faydası nedeniyle poli(δ-valerolakton)(PVL) ilgi çekici bir seçenektir ve biyomedikal uygulamalarda sıklıkla kullanılır. PVL, antrasiklin tipi antibiyotiklerin ve farklı kanser türlerinden kaçınmak için reçete edilen kontrollü ilaçların (doksorubisin (DOX) gibi) üretiminde temel bir bileşendir. Nanohibrit sistemler, moleküler veya atomik ölçekte yakından birleştirilmiş veya harmanlanmış iki veya daha fazla farklı nano ölçekteki bileşenden oluşan kompozit maddelerdir. Bu elementler birleştirildiğinde, bileşen parçalarının ayrı ayrı özelliklerinden daha üstün olabilecek belirli niteliklere sahip yeni bir madde üretilebilir. Elde edilen nanohibritler sıklıkla çeşitli uygulamalarda verimliliği artıran, karşılıklı olarak faydalı etkiler gösterir. Çapları bir ila bin μm arasında değişen parçacık boyutlarına sahip olan mikroküreler, ilaç moleküllerinin adsorpsiyon veya dispersiyon yoluyla bir polimer matrisine dahil edildiği bir parçacık dispersiyon mekanizması biçimidir. Peptitler, proteinler, nükleik asitler ve küçük boyutlu ilaç molekülleri de dahil olmak üzere çok sayıda tıbbi bileşik mikrokürelere kapsüllenebilir ve ilgili terapötik özelliklere sahip olabilir. Mikroküreler son zamanlarda küçük parçacık boyutları, benzersiz yüzey özellikleri ve önemli yüzey-hacim oranları nedeniyle çok ilgi görmüştür. Kalkonlar, bitkilerde bulunan çeşitli yapıların polifenolik kimyasallarıdır. Kalkon bazlı bileşiklerin antibakteriyel, antiviral, antioksidan, anti-inflamatuar, antidiyabetik, antiülser, antikanser özellikler dahil olmak üzere çeşitli olası kullanımları vardır. 1,3-difenil-2-propen-1-on olarak da bilinen transkalkonun (TC) dikkate değer kimyasal yapısı ve ilgi çekici farmakolojik özellikleri, onu diğer kalkonların yanında bilimsel bir araştırmanın önemli bir odağı haline getirir.

Bu çalışmada, enzimatik halka açma polimerizasyonunda kullanılmak üzere yüzey modifiye edilmiş pirinç kabuğu külü (RHA) üzerinde lipazı immobilize etmek için ilk

bölümde fiziksel adsorpsiyon kullanılmıştır. Silika bazlı malzeme, 3-aminopropil trietoksisilan (3-APTES) kullanılarak yüzeyine amin grupları eklendiğinde yüzey modifikasyonuna uğramıştır. Daha sonra, *Candida antarctica* B lipazının serbest formunu immobilize etmek için fiziksel adsorpsiyon metodolojisi kullanıldı. Önceki çalışmalardaki monomer oranları referans alınarak, poli(δ-valerolakton) ve poli(δ-valerolakton) nanohibriti enzimatik halka açma polimerizasyonu ile üretildi. Reaksiyonlar, hem polimer hem de nanohibrit için en yüksek moleküler kütleyi elde etmek için 24 saat boyunca 80ºC'de gerçekleştirildi. Bu elde edilen polimer ve nanohibrit, ilaç taşıyıcı sistem olarak kullanılacak mikroküre lerin üretiminde kullanıldı. Aşağıdaki gibi, O/W emülsiyon metodolojisi, TC yüklü PVL mikroküreleri, TC yüklü PVL nanohibrit mikroküreleri, ilaç içermeyen PVL mikroküreleri ve ilaç içermeyen PVL nanohibrit mikroküreleri üretmek için kullanıldı. Daha sonra, üretilen bu mikroküre lerin ilaç salım mekanizması araştırıldı. Bu araştırma için, üç farklı PVA konsantrasyonu (%0.1, 0.5, 1 (w/v)) ile, en büyük kapsülleme verimliliğini ve dolayısıyla ilaç salım profilini belirlemek için farklı TC:PVL oranları (%10, 20, 40) ve TC:PVL nanohibrit oranları (%10, 20, 40) değerlendirildi. Termal, kimyasal ve mekanik özellikleri tanımlamak için, bu mikroküre lere TGA, DSC, SEM ve XRD uygulandı. En büyük kapsülleme verimlilikleri, A-2 numunesinde (%1 PVA ve %20 TC:PVL oranı) %98.6 ± 8.4 ve C-2 numunesinde (%1 PVA ve %20 TC:PVL nanohibrit oranı) %82.7 ± 6.4 olarak gözlendi. Bu araştırma, ilaç salım mekanizmalarının pH değişimlerinden büyük ölçüde etkilenmediğini de ortaya koymaktadır. DSC analizi, transkalkonun mikroküre lere eklenmesinin erime noktalarını düşürdüğünü, ancak eğriler üzerinde ekstra ilaç (transkalkon) pikinin olmadığını göstermektedir, bu nedenle transkalkonun başarılı bir şekilde kapsüllendiği ve moleküler olarak PVL ve PVL nanohibrit mikroküre lerinde dağıldığı sonucuna varılmıştır. TGA analizleri, ilaç içermeyen ve transkalkon yüklü PVL mikroküre lerinin termal bozunma davranışını PVL ile karşılaştırmak için kullanıldı. Ek olarak, ilaç içermeyen ve transkalkon yüklü PVL nanohibrit mikroküre lerinin PVL nanohibrit ile termal bozunma davranışını karşılaştırmak için TGA analizleri kullanıldı. Bozunmalar ve ağırlık kayıpları, bilimsel literatür ve yapılan analizlere göre değerlendirilmiş ve yorumlanmıştır. TC, PVL, TC yüklü PVL mikroküreleri, ilaç içermeyen PVL mikroküreleri, TC yüklü PVL nanohibrit mikroküreleri ve ilaç içermeyen PVL nanohibrit mikroküre lerinin varlığını gösteren kimyasal gruplar bir diğer karakterizasyon tekniği olan FT-IR kullanılarak gözlemlendi. FT-IR spektrumlarının benzer oluşu da, transkalkonun mikroküreler içinde başarılı bir şekilde kapsüllendiği ortaya koydu. XRD analizleri, TC yüklemesinin kristal yapılar üzerindeki etkisini ve mikroküre lerin kristalliğini araştırmak için diğer birkaç karakterizasyonun yanı sıra kullanıldı. SEM görüntüleri, mikroküre formülasyonların her birinin küresel şekle sahip olduğunu ortaya koymaktadır. Çeşitli ortamlarda üretilen mikroküre lerin ilaç salım davranışını gözlemlemek için, bu araştırmada pH'a bağlı ilaç salım araştırmaları 5.6 ve 7.4 olan iki pH seviyesi kullanılarak yapılmıştır. TC'nin toplam kümülatif salımı, PVL mikroküre formülasyonları ile arttırılmış olup, pH 7.4 ortamında %42.1'e ve pH 5.6 ortamında %43.5'e ulaştı. Ayrıca, TC'nin toplam kümülatif salımı, PVL nanohibrid mikroküre formülasyonları ile arttırılmış olup, pH 7.4 ortamında% 39.4'e ve pH 5.6 ortamında %34.2'ye ulaştı. TC salımı, her durumda toplam 744 saat süreyle gerçekleştirildi. Son olarak, ilaç salım kinetiği incelendi. İlaç salım kinetiğinin Korsmeyer-Peppas'ın kinetik modeli ile uyumlu olduğu bulundu. Tüm mikroküre formülasyonları, hesaplanan n değerine göre Fickian difüzyonu ile kontrol edilen TC salımına sahipti. Sonuç olarak, bu çalışmanın amacı, transkalkon ilacını polimerik taşıyıcılara biyolojik olarak entegre ederek yeni kontrollü ilaç

dağıtım sistemleri geliştirmektir. Mikroküreleri üretmek için, insan vücudu ile uyumlu olan ev yapımı hareketsizleştirilmiş enzimler içeren biyouyumlu, çevre dostu, yüksek moleküler ağırlıklı bir polimer ve nanohibrit üretilecektir. Transkalkon, çeşitli tedavilerde kullanımı için biyokatalizör ile üretilen polimer ve nanohibrite entegre edilecektir. Tüm karakterizasyon testlerinin tamamlanmasının ve ilaç salım profillerinin araştırılmasının ardından, bu araştırmanın bulgularının, PVL mikrokürelerinin veya PVL nanohibrit mikrokürelerinin, hastalıkların uzun süreli terapötik uygulamalarında potansiyel ilaç taşıyıcı sistem olarak kullanılabileceğini ortaya konulmuştur.

1. INTRODUCTION

With regard to their functional characteristics and manufacturing costs, the emergence of biopolymers has created a perfect rivalry with their counterparts derived from fossil fuels. Although the cost of producing biopolymers is relatively acceptable, ongoing efforts are being made to improve their functional features. Recent years have seen the realization of a wide range of applications for biopolymers, including blends and additives in bioplastics, personal hygiene products, food items, pharmaceuticals, all while providing the advantage of environmentally friendly breakdown [1]. Novel and intentive applications of materials based on biopolymers have produced a significant advancement in sustainable biotechnology and the bioeconomy in the past few years [2]. Biopolymers could be divided into two subcategories, which are biodegradable and non-biodegradable polymers. Aliphatic polyesters are the majority of biodegradable polymers. They show non-toxic behavior and they are also lightweight and biocompatible. The greatest number of aliphatic polyesters have semi-crystalline structure, which leaves them vulnerable to natural deterioration and hydrolysis by enzymes[3]. Two prevalent processes for producing aliphatic polyesters are polycondensation or ring opening polymerization (ROP), which is often accomplished by metallic, cationic, or anionic catalysts. Organocatalysts and biocatalysts have been the subject of numerous recently conducted investigations owing to the increasing worry over remaining metallic substances in polyesters for utilization in food or medicine. A lot of research has been done on the polycondensation of diacid compounds and diols, or oxyacid compounds, in addition to the ring opening polymerization of lactides and other lactones, employing biocatalysts like lipases and esterases [4]. The implicit seek for substitutes to traditional manufacturing pathways, which need metallic catalysts and/or harsh manufacturing conditions, motivates enzymatic polymer production. In addition to being toxic to biomedical components, metal catalysts can have a detrimental impacts on the environment. Besides, harsh manufacturing circumstances can result in undesirable adverse reactions and significantly restrict an integration of biological substances (drugs, proteins etc.) and several intriguing but heat-sensitive functional compounds (vinyl, epoxy, etc.) [5].

Thus, in recent decades, enzymatic polymerization has become a crucial method for the formation of biodegradable polymers, particularly aliphatic polyesters, with remarkable structures that can meet the requirements of cutting-edge implementation domains like biomedicine, where the toxicity of solvents and cataylsyt remainings must be taken into account, especially when biological decomposition procedures take place. Due to the substantial enantioselectivity, regioselectivity and chemoselectivity of the catalysts as well as the minimal number of byproducts produced during the manufacturing procedure, the primary benefits of enzymatic polymer production are associated with the relatively mild reaction circumstances required to fine-tune and control the polymerization procedures [6,7]. With benefits including minimal energy usage, no by-products, and atomic productivity, enzymatic ring opening polymerization (eROP) of lactones is an extremely widely employed approach to produce biodegradable polyesters with great molecular weight [8]. In the enzymatic polymerization of aliphatic polyesters, hydrolases – more especially, lipases – are efficient catalysts [9]. In consequence of its excellent catalytic activity in polymer synthesis, *Candida antarctica* lipase B (CALB) is an exceptionally prevalent enzyme type [10]. The research area of biological systems has given major consideration to nanohybrids that combine organic and inorganic components due to their advantageous physicochemical properties. Hetero-nanoparticles featuring distinct parts composed of inorganic as well as organic materials are known as organic/inorganic nanohybrids. The organic parts of the nanohybrids may generally offer controlled medication release, biodegradability, foreign substance loading and selectivity [11].

Particular emphasis has lately been paid to the design and fabrication of drug delivery systems by using biopolymers. To guarantee that an exceptional particular medication is available for targeting the diseased area with the fewest possible adverse impacts, drug delivery systems are a method for incorporating medicinal compounds. The loaded medicine can be targeted and its release controlled by using the optimal drug delivery system. Before reaching the diseased area, drug delivery carriers serve as a means of preventing the medications from breaking down, while they are being transported through the body [12]. The production of microsphere as a drug carrier can successfully increase the drug's stability, while also lowering its toxic impact to the organ because of the carrier substance's defensive action. The microspheres can be in

immediate proximity with the mucosal layer at the area of absorption and extend the duration of retention because of their large surface area to volume ratio when compared to conventional preparations. Consequently, it may yield controlled released and targeted medications [13]. For a long time, flavonoids, which are a broad class of naturally occurring substances that are plentiful in plants, have been valued for their numerous biological functions. The chalcones are among the many different types of flavonoids that exhibit an extensive variety of pharmalogical characteristics, including antioxidant, analgesic, antibacterial, anticancer, antifungal, anti-inflammatory, and antimalarial features. The remarkable chemical structure and intriguing pharmalogical properties of trans-chalcone (TC), also known as 1,3-diphenyl-2-propen-1-one, make it a prominent focus of scientific investigation alongside other chalcones [14,15].

The main objective of this research was to fabricate drug-loaded microspheres that were biocompatible to the human body. The medication was chosen as a trans-chalcone. According to the previous studies, the agent 3-APTES was first used to silanize the support material's surface. Then, as stated earlier, CALB was immobilized on surface-modified RHA using a physical adsorption strategy [16]. By employing the methods and the settings from the previous researches, poly(δ-valerolactone)(PVL) and poly(δ-valerolactone) (PVL) nanohybrid were successfully synthesized from δ-valerolactone with CALB immobilized to RHA in the second phase of the research [17]. Trans-chalcone loaded PVL microspheres, drug-free PVL microspheres, trans-chalcone loaded PVL nanohybrid microspheres, and drug-free PVL nanohybrid microspheres were all attempted to be made by using the O/W emulsion technique throughout the third phase of the research. The drug release profiles were investigated by using the microspheres that had the greatest encapsulation efficiency. To be able to gain insight into the thermal, morphological and mechanical characteristics of PVL, PVL nanohybrid, TC-loaded PVL microspheres, drug-free PVL microspheres, TC-loaded PVL nanohybrid microspheres and drug-free PVL nanohybrid microspheres, a number of characterization analyses were employed upon completion of microspheres were fabricated. These analyses included the use of scanning electron microscope (SEM), differential scanning calorimetry (DSC), fourier transform infrared spectroscopy (FT-IR), thermal gravimetric analysis (TGA), and X-Ray diffraction analysis (XRD). Drug release experiments were additionally carried out for TC-loaded PVL microspheres and TC-loaded PVL nanohybrid microspheres. Besides, in order to

gain a better understanding of the drug release mechanism, the drug release profiles were fitted to a various kinds of kinetic models. Given the outcomes of the characterization analyses and drug release behaviour, this research indicates that microspheres may be employed prolonged treatment of illnesses.

2. LITERATURE REVIEW

2.1 Biopolymers

Polymers are defined by the units, which resemble to the bricks of the house, called monomers. When approximately a hundred of the monomers get together like a repetitive chain, they form a polymer. Like the cement between the bricks, in this case, they covalently bond each other. There are two ways of this formation; one of them can be naturally and other one can be artificially or synthetically. If the formation occurs as naturally, it is called biopolymer. There is an increasing interest for this type of polymers these days, because oppose to synthetically/artificially formed ones, they are generated by renewable resources. It could be seen the advantages and the disadvantages of the natural polymers and synthetic polymers in Table 2.1 and Table 2.2, respectively.

Table 2.1 : Advantages and disadvantages of natural polymers [18].

Polymer	Advantages	Disadvantages
Natural polymers	Water-soluble, abundance, less toxic, biocompatible, biodegradable, less side effects, exerts less toxicity along with drugs, chemical modification possible, low cost, low angiogenesis, low immunogenesis, mucoadhesiveness	Chemical molecules are very based on climate, geographical conditions, availability of nutrients, and thus chemical constituents different from batch to batch, microbial contamination is high, adulteration needed, heavy metal contamination, time consumption for extraction and purification, low mechanical strength, sensitive to heat and chemicals, recycling and reuse not possible

Table 2.2 : Advantages and disadvantages of synthetic polymers [18].

Polymer	Advantages	Disadvantages
Synthetic polymers	Mechanical stability	Intrinsic biocompatibility and bioactivity are absent
	Durability	Toxic
	Inertness	Oncogenesis
	Tunable	Inflammation and immune response
	Beneficial tailoring properties	High-production cost
	Reproducibility	Water-insoluble
	Bioadsorbable	
	Environmental stability	
	Biocompatible	

It is clear that with the increasing population and the times when we need to pay more attention to the world's depleting resources, why the people are tending to use biopolymers instead of synthetic polymers, which are petroleum-based. In other words, with the developing technology, oppose to fossil resources, which are very traditional, people started to care to eliminate their carbon footprint. In order to make this valuable approach happen, they beginned to use natural resources who are derived from living species, such as trees, animals, microbes, plants, agricultural wastes[19]. Biopolymers could be produced as natural or synthetic according to their resources or their manufacturing process. In other words, they could be completely biosynthesized by living species or chemically synthesized via several reactions from biological reactants [20].

Natural biopolymers are classified as three categories. The first category is polynucleotides. It means they occur by nucleotides as a monomer, bonded by phosfodiester bonds. Deoxyribonucleic acid (DNA) and ribonucleic acid (RNA) could be given as an example for the first category. The second category is polypeptides/proteins. Peptides, which is combination of many aminoacids as a building block, are the monomer of polypeptides. They are bonded by peptide linkages. Collagen, fibrinogen, silk, soy protein, zein, elastin, resilin, wheat gluten, gelatine, casein, gluten, serum albumin could be given as an example for the second category. The third category is polysaccarides/carbohydrates. They are combination of

many monosaccarides, which could be ketones and hydroxy aldehydes. In addition, they are bonded by α-(1,4)-glycosidic linkages. Cellulose, starch, chitosan/chitin, hemicellulose, hyaluronic acid, alginate, pectin, dextran could be given as an example for a third category [21,22].

Synthetic biopolymers are classified as two categories, which are biodegradable and and non-biodegradable biopolymers. The classification could be seen from the Figure 2.1.

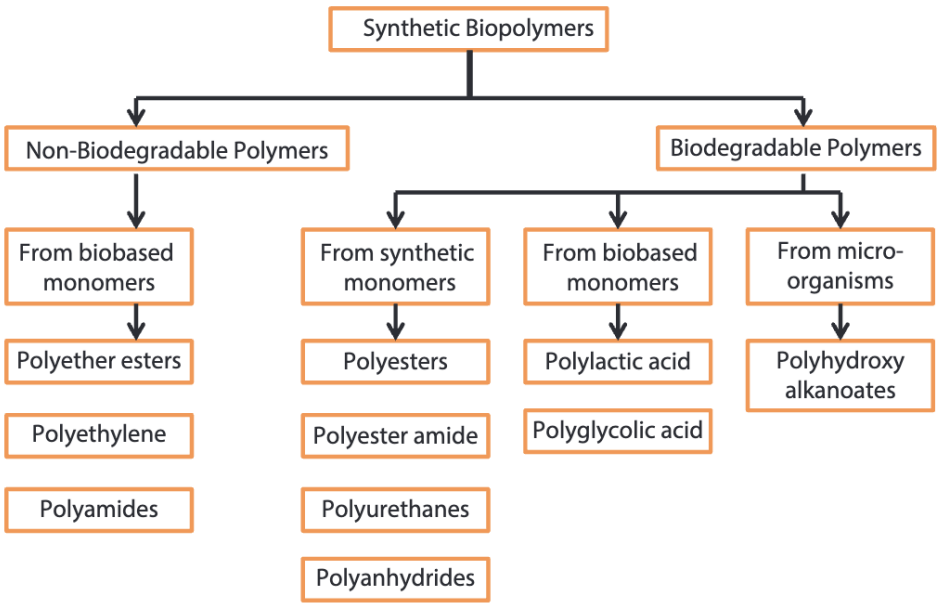

Figure 2.1 : Classification of synthetic biopolymers [23].

They can be also classified according to their manufacturing process, which are addition and condensation polymerization. Polyesters are the subcategory, that attracts the most attention and is therefore researched. This subcategory divided into two categories, which are poly-(hydroxy acid)s and poly-(ether ester)s in terms of the molecular structure and the functional groups [23]. There are three primary groups in terms of molecular structure for the polyesters, which are aliphatic, aromatic and aromatic-aliphatic polyesters. The aliphatic polyesters are known as green plastics with the semi-crystalline structure. Poly(lactic acid)(PLA), poly(hydroxyalkanoate)(PHA), poly(buthylene succinate)(PBS) and poly(ε-caprolactone)(PCL) could be the main examples for this group, due to their better biodegradability, biocompatibility and chemical degradability [24,25]. They indicate non-toxicity and they have low-weight. These qualities lead them to be used in not only packaging, textile, medical, agricultural industries, but also wearable devices and

sensors [26]. The aromatic polyesters are known with their ascendant thermal properties. Besides, poly(ethylene therephthalate)(PET) and poly(butylene therephthalate)(PBT), which are the widespread aliphatic-aromatic polyesters, known with their exceptional mechanical features, high degradation temperatures and electrical insulation characteristics. These qualities lead them to be used as thermoplastics especially in an engineering area [27].

There are multifarious fields, which we use biopolymers. Packaging, environmental field, agriculture, medical field, pharmaceutical and cosmetic fields are the areas we encounter most frequently. These areas are shown in Figure 2.2. Among all of them, drug delivery is the outstanding one. Especially, the features of biocompatibility, biodegradability, bioavailability and cost-effectiveness of the biopolymers highlight this field. Moreover, being non-toxic, environmental-friendly and non-carcinogenic are additional reasons for the prevalent use of biopolymers in this area. There are also several types of usage of the biopolymers in drug delivery area, such as nanofibers, films, capsules, microcapsules, tablets, micro/nanospheres and hydrogels [28].

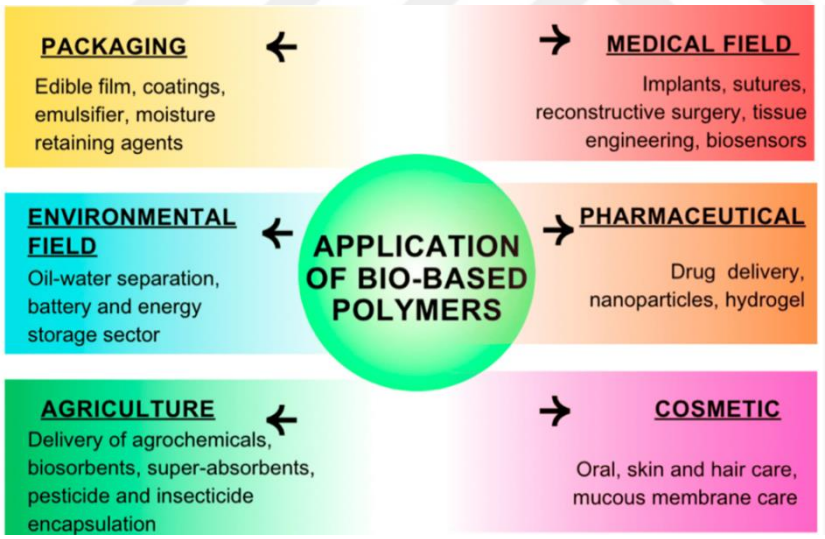

Figure 2.2 : Applications of bio-based polymers [29].

2.2 Lipase Enzyme

Enzymes are basically a macromolecule based on proteins. They are a biocatalyst, which are responsible for many chemical reactions in living species. They are admirable applicants for pharmaceutical implementations owing to their natural uniqueness and suitability for mild reaction terms [30]. Because of this suitability, the necessity for the energy is less. Additionally, enzymes are biodegradable and non-

toxic, which means they are eco-friendly. What is more, they are reusable. As exceptional biocataylsts, Lipases (EC 3.1.1.3), are defined as triacylglycerol acylhydrolases, which are a member of hydrolase family [31]. They are able to catalyze hydrolysis of various substrates into mono-, di-glycerides, glycerol and fatty acids. They are also capable of esterification, transesterification, acidolysis, alcoholysis as a number of other reactions [32]. Besides, they show limited sensitivity to product inhibition, excellent efficacy in non-aqueous settings, and durability to temperature and pH changes. They function well without the aid of cofactors and are stable in organic solvents [33]. When lipases come into contact with hydrophobic ambients, which can be substrates or supports, sorts of acts are designated by them. Generally, lipases have a polypeptide chain, which contains hydrophobic and hydrophilic surface. Furthermore, they specify by their "entry gate" or "lid". This lid is in charge of the active site of the enzyme and covers this site. It can be opened or closed according to the type of the environment, where lipases are. For instance, if they are in a hydrophobic ambient, their active sites appear. In other words, the site is influenced by the hydrophobic regions of the lid, which is already enclosing of the active site. In this way, the active site is isolated from the rest of the ambient. The structure of lipase undergoes a adjustable transition when coming into contact with an interface, causing this lid move away and reveal the residues, which are left by biocatalysis(open/active form). If lipases are in a hydrophilic ambient, they become unstable and prone to stay like a in-active form (closed form) [34,35]. This catalytic mechanism of the lipases is described as "interfacial activation" and it could be seen in detail from Figure 2.3.

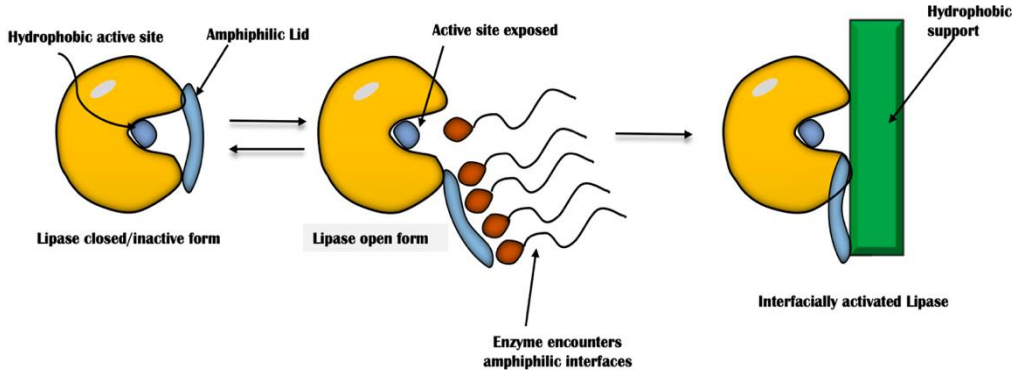

Figure 2.3 : Interfacial activation of free lipases [35].

Lipases have numerous usage areas in industry. With the help of lipases, detergents can work in lower temperatures in detergent industry. They can be used not only for

fermentation, but also fat-removal from meats in food processing industry. Since they are the cost-effective solution and also have enantioselectivity and regioselectivity, they are crucial to be used in pharmaceutical industry. Apart from these benefits, there are still some restrictions for the lipases. Being easy to inactivate and instability are the some points, where these restrictions are grounded on. To increase the stability, and optimize the activity of the lipases, enzyme immobilization method is used. This method gives us the economic way to be able to get the bio-catalyst back to be used repetitively [36]. *Candida antarctica* lipase B(CALB) is a kind of lipase enzyme. It has a shape that assists the substrate specifity and noteworthy catalytic afficiency. The three essential amino acid remainings, which are serine, histidine and aspartate, exist in the active site. They are substantial for formation of ester bonds and catalyzing the hydrolysis [37]. In the market, there is a commercial form of CALB to make polymer synthesis or modification happen. It is called Novozyme 435®. It uses macroporous acrylic resin as a immobilization support by interfacial adsorption immobilization method [38]. In this study, free CALB was used, and immobilized onto a new support, which is different than the commercial one in the market (Novozyme 435®).

2.3 Enzyme Immobilization

A vital allowing breakthrough in the shift to a sustainable chemical industry is enzme biocataysis. Numerous industries, such as environmental industry, biomedicine, food and biomedical production(particularly pharmaceutical industry), currently use enzymes. Because of their origin and the link between their structure and functionality, enzymes present both beneficial paths and obstacles for their applications. The typical benefits consist excellent selectivity, considerable catalytic turnover and wide spectrum of substrates; the typical adverse effects start with the expenses and challenges on the design of the biocatalyst [39]. As a solution for this design problem, two ways emerge. One of them is defined as homogenous catalysis. It is possible to use the enzyme in free form, embedded within the same aqueous environment as the substracts and the products in this catalysis type. Since the enzymes shows instability in the free form, and separation between substrates and products become intricated, the interest is shifted to other type. The other one is defined as heterogeneous catalysis. In this type, there is a enzyme in an immobilized form, which means its movement in space has been restricted either completely or to a small limited region [39,40]. This

restriction is made by using solid supports [36]. By stabilizing their structure, solid support materials generally aid in maintaining the activity of enzymes. Thus, compared to free enzymes, fixed enzymes are more resilient to changes in the environment [41].

There are several upsides of enzyme immobilization. With the resusability of the enzyme, enzyme usage can be continuous. Also, reaction time can be made shorter and it is likely to get elevated enzyme-substrate ratio with low cost by using the immobilized enzymes [41]. Currently, there are many implementations to perform enzyme immobilization. These implementations are divided to two main methodologies, which are physical methodologies and chemical methodologies [42]. Chemical methodologies are identified as covalent-bonding and cross-linking. An enzymatic immobilization technique called cross-linking has been proven to raise the stability of enzymes by enabling them to attach without the requirement for support. In order to manufacture cross-linked enzymes, this methodology relies on a material called a cross-linking agent, which forms connections with particular amino acid groups located on the surface of enzymes [36]. The covalent-bonding method uses covalent bonds to bind enzymes together. Chemical operations that are consisting of specific amino acid residuals (like those of cysteine, lysine etc.), along with functional groups of amino acids including carboxylic, phenolic and hydroxylamine groups generate these bonds. This method, which adds a substantial amount of enzymes to the supports and provides enzymatic stability, guarantees rigidity in the structure owing to the intrinsic durability of the covalent bond [36]. Physical methodologies are identified as entrapment/encapsulation and adsorption. Entrapped enzymes are distributed throughout a solid or semi-solid matrices rather than the ability to move freely. Connections among molecules or size impacts induce the enzymes to become trapped within the cross-linked matrices. A variety of materials, including hydrogels, fibers, and other solid matrices, have been employed to entrap ezymes. The slowing down of the diffusion could be regarded as the entrapment method's drawback [40]. Encapsulation method permits substrates and products to enter and exit, while confining the enzymes in a tiny cage. The enzyme could move or less freely inside the cage's pore via this method. Metal-organic/covalent-organic/hydrogen-bonded complexes have all received a lot of interest lately as encapsulating-carriers[40]. Physical adsorption is the most basic/oldest procedure among all the immobilization methodologies.When an enzyme immobilized by physical adsorption, it either stays

unable to dissolve in aqueous solution or is held on the hydrophobic area of the support (via ionic, hydrophobic, hydrogen-bonding or Van der Waals connections) [41,43]. As opposed to other methodologies, it is straightforward to use, affordable, and permits the reuse of enzymes without the need for support activation. On top of that, it could help minimize the inhibition of enzymes. This methodology is influenced by several factors. The surface of support, porosity, size of the pores, concentration of enzyme and adsorbed enzyme amount on support could be the examples for these factors [43]. One of its benefits is that it may immobilize a biomolecule in mild circumstances without causing major conformational alterations. The potential for the desorption of the enzyme due to fluctuations in temperature, pH and disorientation is a downside, nonetheless, and dictates strict process control. Yet, physical adsorption remains as the preferred approach for lipases owing to their hydrophobic features, decreased strength of ionic interactions and the stabilization procedure of the enzyme [43]. Advantages and disadvantages of lipase immobilization methodologies could be seen from the Figure 2.4.

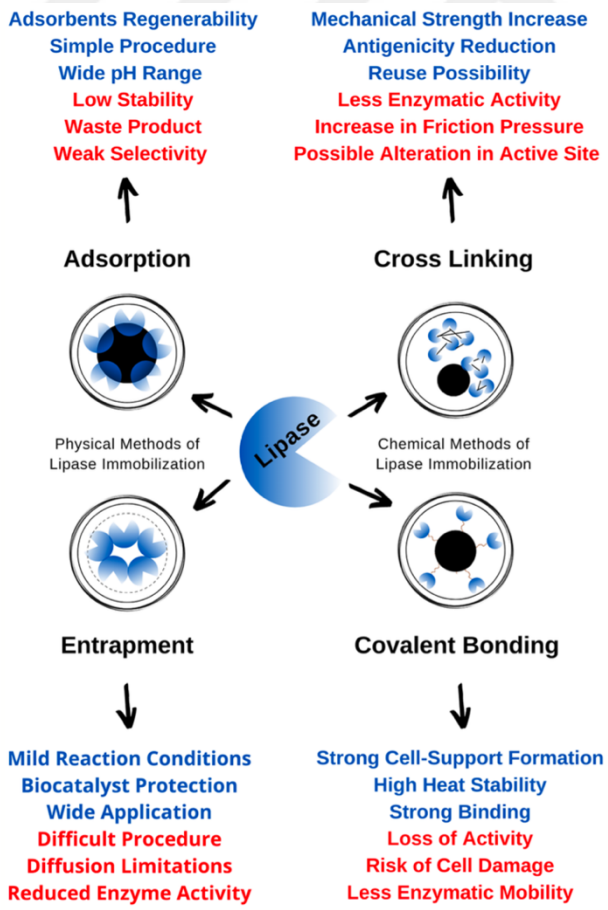

Figure 2.4 : Advantages, disadvantages and techniques of the lipase immobilization [42].

Because of its high level of selectivity, as well as its resilience to severe surroundings, CALB is one of the most valued lipases. However, due to its costly price, challenging recovery, free CALB's prevalent application in industry is constrained. Still, the methodologies of immobilization bypass these constraints. The features of supports have been proven to have a major impact on the functionality and utilization of immobilized CALB. The immobilized CALB(Novozyme 435®), which is sold on a commercial scale, originates by physical adsorption on macro-porous acrylic polymer resin [44].

2.3.1 Support materials for enzyme immobilization

An intriguing scientific challenge has been how to properly utilize or transport enzymes. Multiple substances or methods have been used in extensive research on the immobilization and distribution of enzymes throughout the decades that have passed [45]. Through enzyme immobilization implementing various support matrices, breakthroughs in the practical use of enzymes have improved the effectiveness of the enzymes under unfavourable circumstances, including excessive temperatures and pH differences. The characteristics of the generated catalytic system and the performance of the enzymes depend critically on the support matrix selection [46].

Despite the fact that using supports could appear like an extra expense, there are numerous comprehensive financial advantages and gains. The capacity to restrict an enzyme to a solid matrix through physical and chemical clinkages does, in fact, result in improved stability towards breaking down chemicals, heat, and pH, thereby avoiding the enzyme from being lost throughout processes. Apart from that, it permits the employing of a multi-enzymatic mechanism once necessary and can offer enhanced accuracy in regulating the parameters of the catalytic procedure. Yet, what's greatest is that the enzyme can be recovered and used again for a number of purposes [47]. The creation of unique support materials with ideal porosity, surface area, along with hydrophilic/hydrophobic composition is necessary for optimizing the immobilization of enzymes. Certain properties consisting of thermal and chemical stability, inertness, ability to regenerate, heterogeneousity, interacting groups of functional compounds, physical durability, accessibility, and affordability should all be present in these types of support materials [48].

The support materials divided into two main groups, which could be organic and inorganic. Silica, ceramics, glass and activated carbon could be given as an example for an inorganic support. Organic supports also stem from two primary sources, which could be biopolymers or synthetic polymers [46]. The basic scheme for this division could be seen from Figure 2.5.

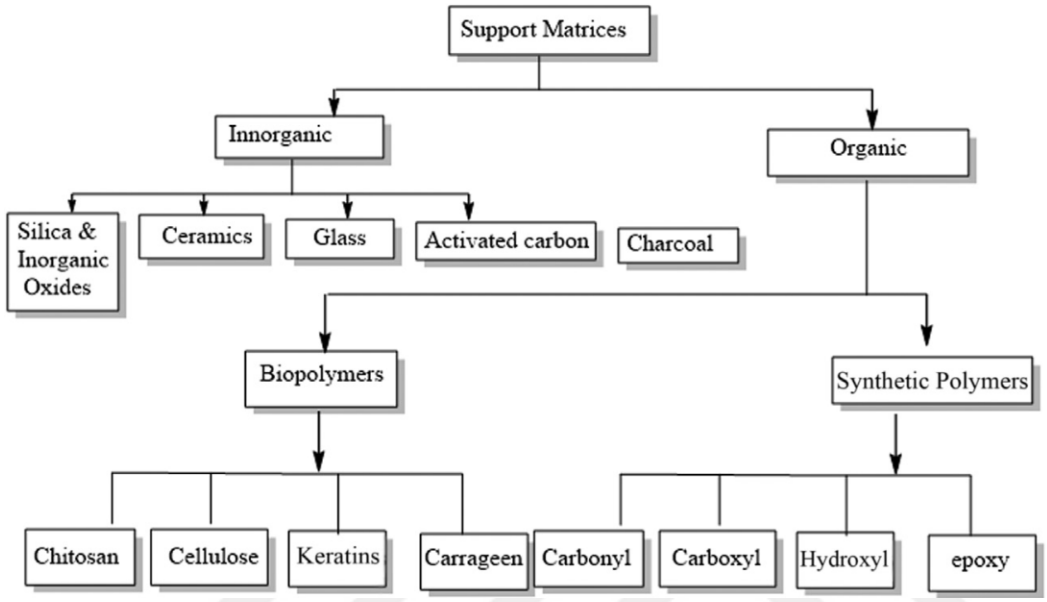

Figure 2.5 : The classification of the solid support materials [46].

Due to its excellent mechanical qualities and remarkable resistance to heat and chamicals, silicon dioxide, also known as silica, is one of the more popular inorganic support materials for lipase immobilization. Since it has its advantageous surface area and beneficial structure of pores, silica is a suitable support material for a variety of applications with good adsorption characteristics. Optimal lipase binding is made possible by these unique characteristics, which also minimize diffusion limits [49]. Silica is generally more affordable and eco-friendly than many other materials [45].

Silica occurs not only naturally as quartz and sand, but also can be found in the exterior layer of the earth as gel, cyristalline and amorphous formations. There are many sources of the silica. For instance, 88.8 wt. % of sorghum, 90.6 wt. % of wheat, 64.3 wt. % of corn, 57.4 wt. % of bamboo, 73 wt. % of bagasse, 93 wt. % of rice husk, 82 wt. % of rice straw and 81.8 wt. % of bread fruit tree are silica [50].

As it could be seen from the Figure 2.6, silica has multiple tetrahedral assemblies, which contains siloxane(represented by Si-O-Si connection) and silanol(represented by Si-OH connection) groups. These tetrahedra assemblies are significant to specify

some characteristics, which could be visuality(glass-like or quartz-like) or like being heterogeneous(stems from broken Si-O bonds) as a surface properties [51].

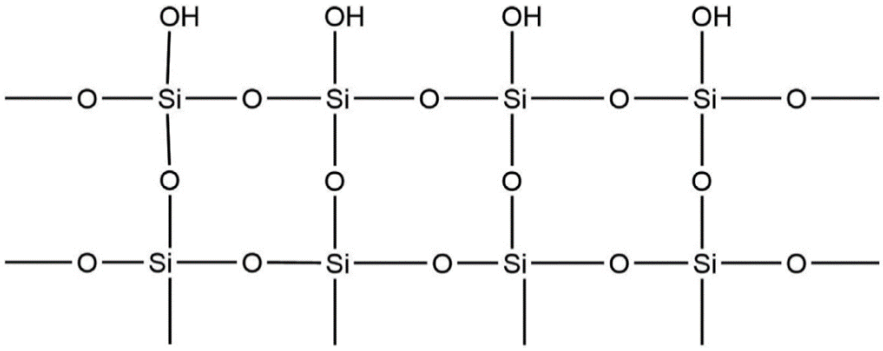

Figure 2.6 : The structure of silica [46].

Since the raw material is inexpensive, and the quantity of silica present is considerable, and the silica manufactured is of excellent standard; residue from agriculture is regarded as an adequate supply of silica with an opportunity for industrial use [52]. One of the most revenue-generating harvest is rice. The outer part of the rice grain, referred to as rice husk, which could be seen from Figure 2.7, is an organic waste that is left over after rice is ground. Rice husk ash is a remaining created, when rice husk is burned under ideal combustion circumstances. It leads to produce amorphous silica, with nanoscale dimensions, a wide surface area and great reactivity [53].

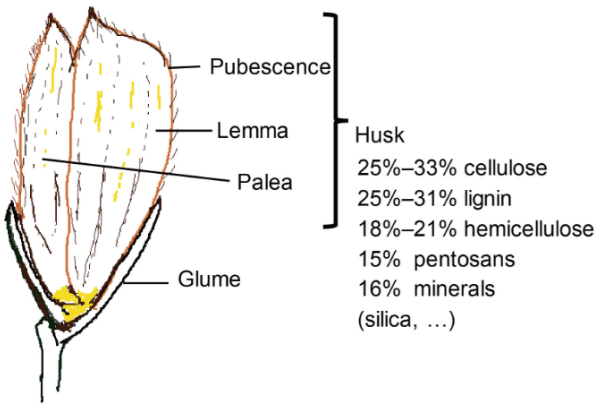

Figure 2.7 : The components of rice grain [54].

Regarding modifying oxide surfaces for binding biomolecules to the surfaces, organosilane compounds are the most popular equipments. 3-aminopropyl triethoxysilane(3-APTES) is widely employed in silane-functionalization procedures by integrating amino groups onto the silica(SiO_2) surfaces through surface modification. It has three ethoxy and aminopropyl groups. Oxide surfaces like silica, due to having hydroxyl groups(-OH), can quickly build up a covalent connection with

organosilane agents as part of the modification process owing to their high surface energy. As a result, amino groups are added onto the surface. In that case, these surfaces may have better ability to dispersion endurance and adaptability with the polymer matrices [55–57]. The silica functionalized with 3-APTES and the covalent attachment of enzyme on silica surface could be seen from Figure 2.8.

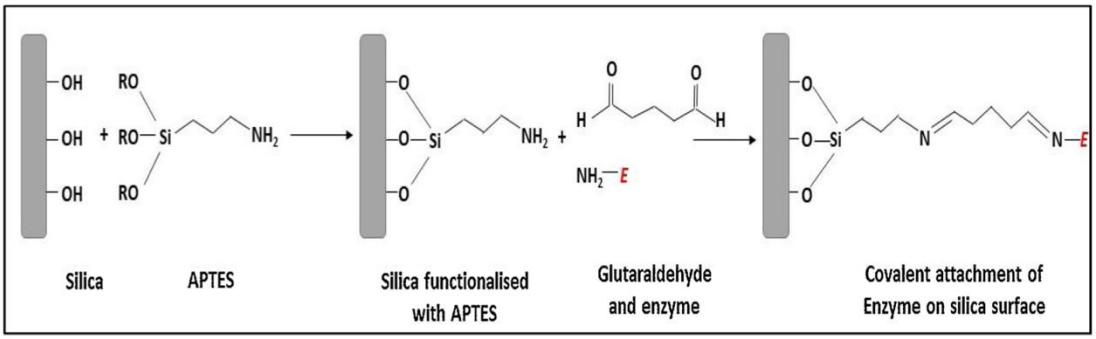

Figure 2.8 : Surface modification of silica by using 3-APTES and glutaraldehyde as a linker [58].

2.4 Biopolymer Production

To synthesize biopolymers, three main sources can be used. They can be synthesized from synthetic monomers, biobased monomers or microorganisms. There are also various synthesis ways to produce biodegradable polymers. They can be modified from natural polymers (hydroxylation, alkylation etc.), chemically synthesized, microbiologically synthesized, enzymatically synthesized and chemoenzymatically synthesized [23]. Polycondensation and ring-opening polymerization(ROP) of relevant cyclic monomers are the two distinct processes, which are used to create aliphatic polyesters, such as poly(lactic acid)(PLA) and poly(ε-caprolactone)(PCL) [31,59]. The fabrication of limited molecular weight dispersion and foreseeable molecular mass is made possible by ring opening polymerization(ROP)'s extensive level of ability to regulate polymer attributes. Typically, ring opening polymerization(ROP) ensures to produce polyester with substantial molecular weight without byproducts, at low levels of temperatures quickly [31]. The complexes/salts built with alkali group metals (iron, copper, tin, zinc, lanthanides, aluminium etc.) have predominantly proven successful in conducting these ROP processes. Due to their increased activity, applicability, and ease of utilizing, tin(II) complexes (for example: tin(II) bis-2-ethylhexanoate) are at the most commonly employed catalysts within the industrial field at present [59,60]. On the other hand, they have drawbacks, such as

toxicity along with elevated reaction temperatures. These drawbacks encourage transesterification processes, which jeopardize the control of polymerization, between molecules [59]. The simplified synthesis mechanism of ROP and monomer groups that can be used in ROP reaction could be seen from Figure 2.9.

(a)

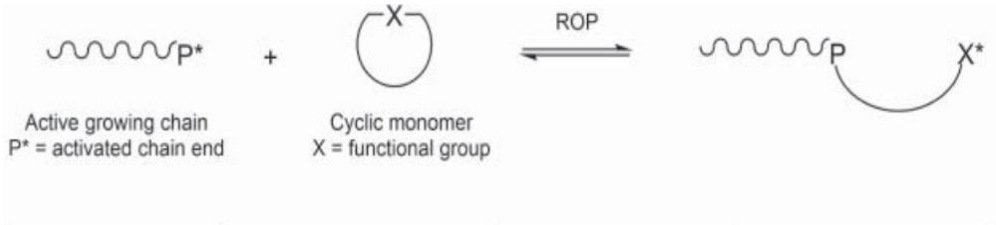

(b)

Oxygen		Nitrogen		Sulfur		Phosphor	
Function	—X—	Function	—X—	Function	—X—	Function	—X—
Ether	—O—	Amine	—NH—	Thioether	—S—	Phosphine	—PR—
Acetal	—O—C(R,R)—O—	1,3-Oxaza	—O—C(H,H)—N(H)—	Thiolactone	—S—C(=O)—	Phosphinate	—P(R)—O—
Lactone	—O—C(=O)—	Lactam	—N(H)—C(=O)—	Thionolactone	—O—C(=S)—	Phosphonite	—O—P(R)—O—
Carbonate	—O—C(=O)—O—	Urea	—N(H)—C(=O)—N(H)—	Thiocarbonate	—O—C(=S)—O—	Phosphite	—O—P(OR)—O—
Anhydride	—C(=O)—O—C(=O)—	Imide	—C(=O)—N(H)—C(=O)—	**Silicium**		Phosphonate	—O—P(=O)(R)—O—
		N-carboxy-anhydride	—N(H)—C(=O)—O—C(=O)—	**Function**	**—X—**	Phosphate	—O—P(=O)(OR)—O—
				Silane	—SiR,R—	Phophazene	—N=P(R,R)—N=
				Silaether	—Si(R,R)—O—		
				Siloxane	—O—Si(R,R)—O—		

Figure 2.9 : a) Simplified synthesis mechanism of ROP, b) Monomer groups that can be used for (-X-) [61].

Alternatively, there is a way to synthesize cyclic esters as a more environmental-friendly way by using enzymatic ring opening polymerization (eROP), in particular, has far greater benefits, because it eliminates the need for metal catalysts [31]. Enyzmes as catalysts are not only non-toxic but capable of using under moderate circumstances, in terms of temperature, pH and pressure. Moreover, immobilizing the enzyme has enabled the catalyst simply removed and reused over and over again, while product purification is not required. The leading candidate for enzymatic ring opening polymerization (eROP) presently is immobilized CALB, because it has been shown to be exceptionally efficient and adaptable for eROP of lactones with numerous sizes [62]. In addition, substantial level of regioselectivity, chemoselectivity and stereoselectivity of enzymes separate them from traditional ways [62]. Since eROP lead to lower energy usage and decreased production of hazardous byproducts, it becomes a eco-friendly strategy. Furthermore, the resultant polymer's applicability for

a range of different purposes is improved by the lack of constituents originating from metals [63]. The mechanism of eROP of δ-valerolactone via immobilized CALB could be seen from Figure 2.10.

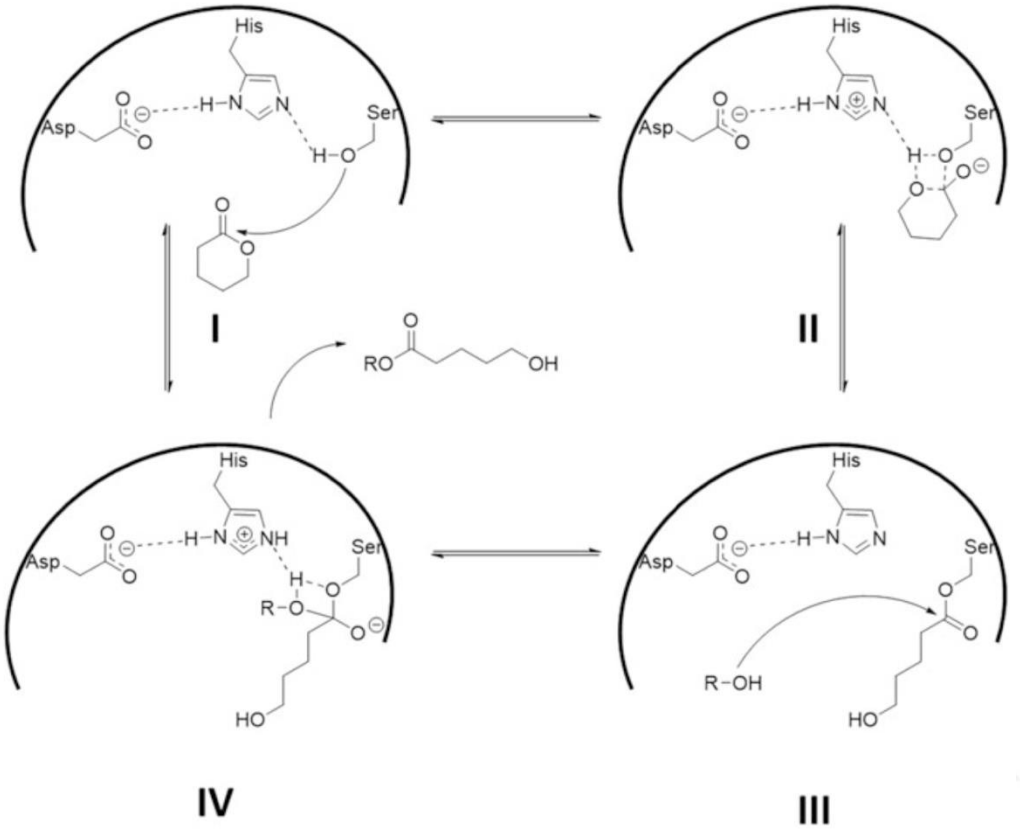

Figure 2.10 : Mechanism of eROP of δ-valerolactone via immobilized CALB (Novozyme 435) [62]**.**

2.4.1 δ-Valerolactone

The most basic but also a significant lactone molecule called δ-valerolactone is fabricated from lignocellulosic biomass that is not edible [64]. It belongs to the group of lactones with six-members [65]. δ-valerolactone can be mediated in the manufacturing of dispersion agents and protective coatings. It can be useful for the copolymerization reactions(for example: with ε-caprolactone). Since, it helps to decrease the melting temperature of the resultant product, which could be copolymer or oligomer [66]. δ-valerolactone can be also viable for the manufacturing of poly(δ-valerolactone), which is homopolymer, by using the pathway of ring opening polymerization [66,67]. PVL is not as elastic as poly(ε-caprolactone), yet it displays semi-crystalline aliphatic form, a relatively low melting temperature(~58^{o}C) and a glass transition point(-60^{o}C) [61,67]. Poly(lactone) molecules have become popular in the pharmaceutical and medical fields nowadays, incorporating tissue engineering,

surgical fibers, synthetic devices and drug delivery systems. Due to their many benefits, including biocompatibility, nontoxicity, thermoplasticity, semi-crystalline and hydrophobic form, flexibility, along with controlled decomposition, PVL is an intriguing option and frequently utilized in biomedical implementations [17,68]. In order to distribute drugs to certain areas, PVL can be adjusted in phases to maximize effectiveness and reduce side effects [69]. Thus, PVL is a fundamental component in the production of anthracycline type of antibiotics and the controlled medications (like doxorubicin (DOX)), which are prescribed to avoid different types of cancer [68]. The chemical structure of δ-valerolactone could be seen from Figure 2.11.

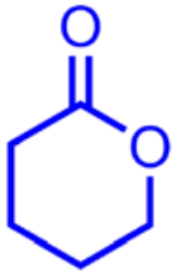

Figure 2.11 : Chemical structure of δ-valerolactone [70].

2.5 Drug Delivery Systems

A drug composition, such as tablet, ointment, capsule or solution, is referred to as a "drug delivery system". When a composition incorporates an integrated approach to regulate the drug release kinetics over an extended period, it is referred to as a controlled release drug delivery system" or "controlled drug delivery system" [71]. Systems for delivering drugs are essential to personalized treatment. These advancements enable better treatment results, less complications, and increased patient compliance by customizing the administration of drugs to each patient's specific needs. Customizing medicinal procedures is the goal of personalized medication [72]. The quick removal of conventional drug delivery systems, like tablets, syrups and capsules, from the body causes unpredictable concentrations of drugs within the therapeutic spectrum. After taking just one dose of traditional drugs, the substance is quickly metabolized, which causes the amount present to rise right away before falling exponentially [73]. This could lead to a reaction beneath the curative barrier since the window for treatment may not be long enough to have a medicinal impact. Owing to their uncertain distribution in the body and an inadequate ability to regulate drug release features, these traditional drug delivery systems, which are the gold standard

for oral drug administration, frequently produce system-wide negative reactions [73]. Controlled-release drug delivery systems are therefore critical to preserving steady bloodstream levels of the medication within the curative spectrum, which guarantees the intended medicinal impact for a prolonged amount of time. According to the four pathways of controlled release (dissolution, diffusion, osmosis, ion exchange), these systems comprise hydrogels, microparticles, polymeric implants and nanoparticles with surface modifications that aim at particular tissues and lengthen the half-life of medications [74]. Oppose to traditional drug delivery systems, targeted and controlled drug delivery systems present some opportunities, such as improved drug efficacy, location-specific distribution, increased ease of use, decreased negative outcomes and toxicity, possible preventable implementations [75]. The smart substances known as stimuli-responsive drug delivery systems are able to respond to external as well as internal inputs. Various kinds of elements, including pH, light, temperature, enzyme and ultrasound, are examples of these stimuli. Drug delivery is made flexible and adaptable by these responsive drug delivery systems, offering specific and regulated release mechanisms [73]. Some examples for drug delivery systems could be seen from Figure 2.12.

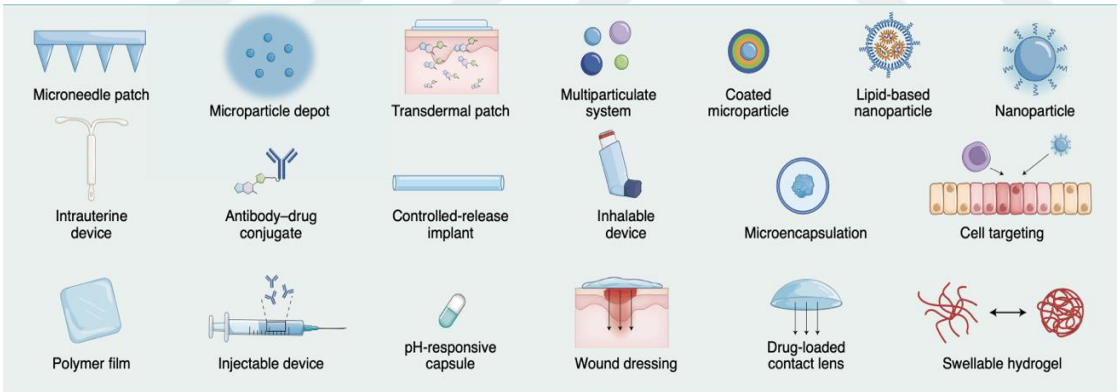

Figure 2.12 : Examples for drug delivery systems [74].

An outstanding option for serving as a drug delivery agent is polymeric compounds. Improved qualities, including ease of use, water-solubility, non-toxicity, biodegradability and biocompatibility were demonstrated by biopolymers and their derivatives of them. In addition, with a controlled drug release, these biopolymers can lessen drug toxicity [76]. Comparing synthetic biodegradable polymers to natural biodegradable polymers reveals numerous advantages, such as reproducibility. For instance, polylactic acid(PLA), polyglycolic acid (PGA), and their copolymers, which

is polylactic co-glycolic acid (PLGA), are among the most commonly employed synthetic biodegradable polymers in controlled drug delivery systems. The significant benefits of them include the ability to modify mechanical properties, decomposition rates, and ability to be formed into a variety of shapes [77]. Medicinal compounds must disperse or encapsulate in the biopolymer matrix as a carrier based mechanism in a variety of drug delivery mechanisms, including hydrogel fabrication, liposomes, micelles, polymer-drug conjugation, micro/nanocapsules and micro/nanospheres, niosomes [75,76]. Diffusion, erosion, fragmentation, and swelling/shrinking are the four primary strategies that have been identified; they vary mainly in the part that the carrier particles perform in regulating the drug's release [78]. These mechanisms could be seen from Figure 2.13.

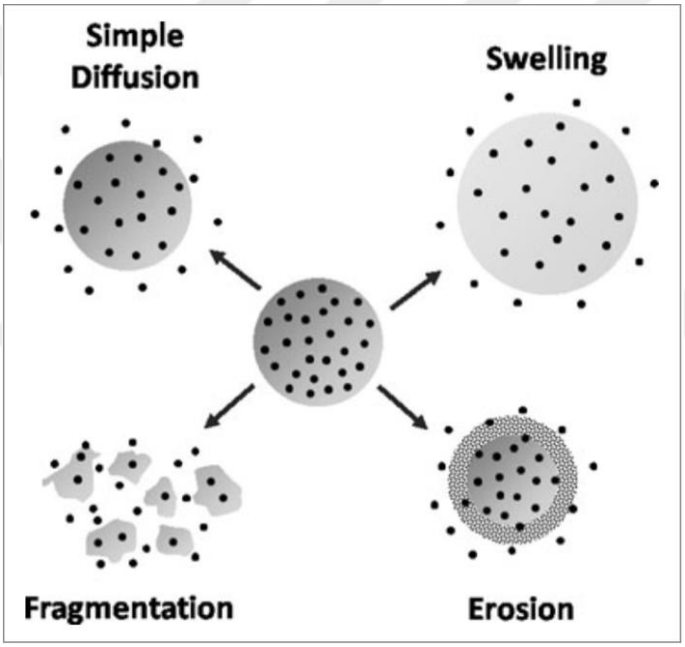

Figure 2.13 : The four strategies for drug release [79].

For a medication to be both efficient and acceptable, its levels in the blood must stay within the therapeutic limits. The range that is therapeutic is situated between the maximum toxic concentration (MTC) and the minimum effective concentration (MEC). When it comes to medications that are swiftly taken in and got rid of, just one administration leads to the drug level to increase and decrease quickly (black solid line in the Figure 2.14 represents this situation). It is possible for the medication level to go far beyond the therapeutic range for extended periods of time then frequent administration at periodic times induces oscillating levels of drugs in the bloodstream (black solid curve followed by dotted curve in the Figure 2.14 represents this

situation). The orange curve in the Figure 2.14, or zero-order release, can be adjusted to fall within the maximum toxic concentration and minimum effective concentration, which concludes in a steady drug level in bloodstream following a preliminery peak [80].

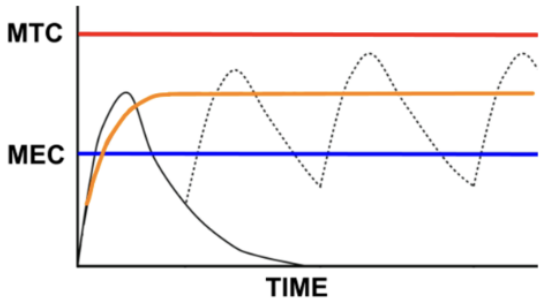

Figure 2.14 : The drug concentration as a function of time [80].

2.6 Microspheres

Having particle sizes varying from one to thousand μm in diameter, microspheres are a form of particle dispersion mechanism, where molecules of drug are incorporated in a polymer matrix by adsorption or dispersion. Numerous medical compounds, including peptides, proteins, nucleic acids and molecules of small size medicine could be encapsulated in microspheres and have the relevant therapeutic properties [81]. The microspheres have garnered a lot of interest lately upon account of their tiny size of particles, unique surface features, and substantial surface-to-volume ratio. Those features create solid-liquid interface with the enclosing liquid, and the qualities of this interface influence how well the polymeric microspheres disperse [82]. The polymeric microspheres could be fabricated by biodegradable polymers or synthetic polymers. Because of their biodegradability, biocompatibility and bioadhesivity, natural polymers, such as starch, polylactic acid etc. could be used for fabricating biodegradable polymeric microspheres [83]. On the other hand, synthetic polymeric microspheres have been also shown to be effective and biocompatible, and they are frequently used in clinical settings. They can also be used as bulking agents, embolic particles, fillers, drug delivery medium etc [83]. The two sorts of microspheres- microcapsules and micromatrixes- are distinguished by the method of encapsulating. Microcapsules are like storage systems, where a polymeric substance coats a drug core, while micromatrices include a drug that is evenly distributed throughout the polymeric matrix [84]. The microspheres have numerous upsides, especially because of their

tiny-size and spherical form, they enable to make easy injection. Besides, they ensure proper management of drug release and degradation [85]. An example picture of microspheres could be seen from Figure 2.15. Moreover, drug release rates regulated through controlled relase distribution using biodegradable microspheres, which reduces harmful adverse effects and the issues associated with frequent injections. In addition, they facilitate the dispersion of the compounds that are insoluble in water in water-based environments. The microspheres have not only a long-lasting and consistent therapeutic impact, but also assist to reduce toxicity and dosage of the drugs [86].

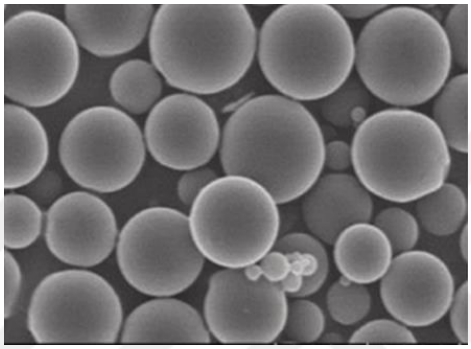

Figure 2.15 : An example picture of microspheres [85].

To fabricate polymeric microspheres for employing in biomedicine and pharmaceuticals, a number of techniques have been researched, comprising suspension polymerization, spray drying, emulsion-solvent evaporation, gelation thereafter emulsification, electrospinning, ultrasonication, separation of phases [87]. Futhermore, membrane emulsification, microfluidic technology, coacervation, supercritical fluid technique and superhydrophobic surface mediated technique could be employed for fabricating microspheres as well [82]. Some of the fabrication methods of microspheres could be seen from Figure 2.16. The drug could be released from the microspheres via two different ways, which are dissolution and diffusion. In the case of dissolution, the reduced hydrophilicity of the polymer or its slower process of dissolution in gastrointestinal fluid regulates the rate of drug dissolution. In the case of diffusion, the drug diffuses from an area with a greater levels to one with a lessened one [88].

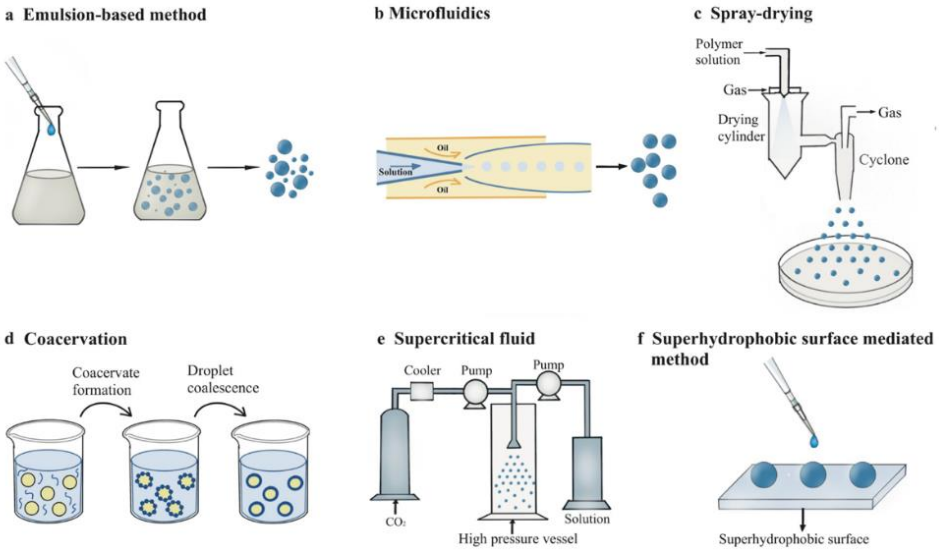

Figure 2.16 : Some of the fabrication methods of microspheres [82].

2.6.1 Emulsion/solvent evaporation method

One of the techniques for the preparation of the microspheres is emulsion/solvent evaporation technique. For microparticle fabrication, the emulsion-based solvent evaporation method has become extremely common, since it ensures substantial rate of particle formation, it is easy to use, economical and repeatable. In this method, the immissible water phase is used to emulsify a solution of a polymer and bioactive ingredient. Solid particles are left behind after the solvent evaporates, forming microparticles [89]. In other words, by taking away the volatile solvent from the emulsion's dispersed phase, the solvent evaporation process generates microspheres. With this technique, microspheres can have their dimensions regulated within the nanometric scale [90]. For implementations involving sustained drug administration, this technique offers control over particle size and enables the encapsulation of a variety of active substances [89]. The emulsion/solvent evaporation processes classified as single emulsion and double emulsion processes. Oil/water (o/w) and water/oil (w/o) emulsion/evaporation processes could be the examples for the single emulsion processes. Oil/water/oil (o/w/o) and water/oil/water (w/o/w) emulsion/evaporation processes could be the examples for the double emulsion processes [90]. Natural polymers like protein and carbohydrates are converted into microparticule carriers by using the single emulsion process [91]. In this process, a polymer is initially blended with either a solid suspension of water-soluble components (like proteins) or water-insoluble components (such those soluble in dichloromethane (DCM) or chloroform). To create the single emulsion, the resultant

mixture is subsequently sonicated or homogenized in an aqueous phase that contains an emulsifying substance that stabilizes the emulsion. Solid microparticles are left behind, when the solvent diffuses and evaporates from the droplets [92]. Due to their exceptional ability to jointly encapsulate hydrophobic and hydrophilic bioactive ingredients, double emulsions have garnered a lot of interest [93].The double emulsion method works well with water-soluble medications, proteins, peptides and vaccines, yet it requires the fabrication of several emulsions. The solution of polymers that eventually encompasses the protein presence in the dispersed aqueous phase frequently forms up the lipophilic organic continuous state, in which the protein aqueous solution is disseminated. Following the homogenization, the primary emulsified mixture is incorporated with the polyvinyl alcohol (PVA) aqueous solution. This produces a double emulsion, resulting in is subsequently eliminated by through either stirring to remove the organic phase or evaporation of the solvent, which keeps the emulsion at lower level of pressure [94]. The microsphere fabrication by single emulsion/evaporation method and double emulsion/evaporation method could be seen from Figure 2.17.

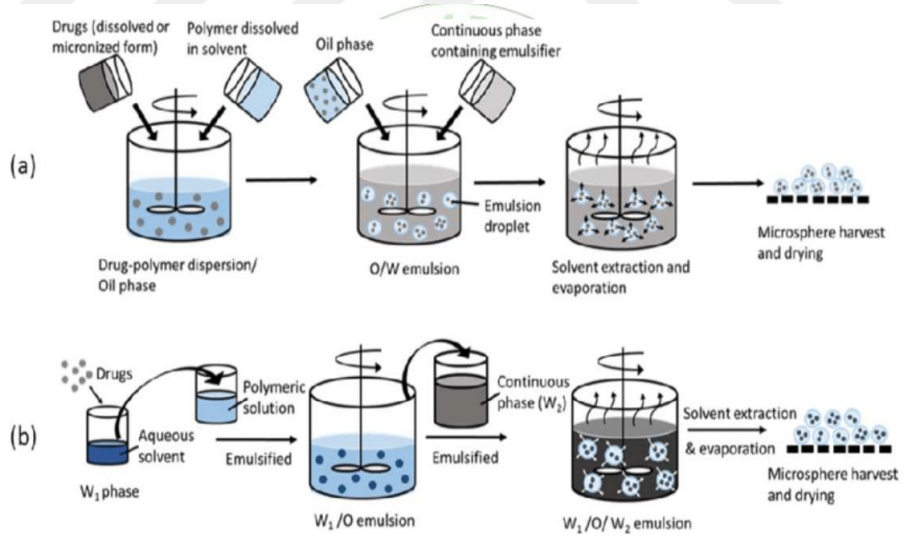

Figure 2.17 : The microsphere fabrication by a) single emulsion/evaporation method, b) double emulsion/evaporation method [90].

2.7 Nanohybrid Systems

Nanohybrid systems are composite substances constructed up of two or more different nanoscale constituents that are closely joined or blended at the molecular or atomic scale. When these elements are combined, a fresh substance with specific qualities that

may be superior to those of the constituent parts individually can be produced. The resultant nanohybrids frequently show mutually beneficial impacts, which enhance efficiency across a range of applications [95]. Different kinds of nanohybrids can be generated with the four primary categories of traditional components, which are metals, nonmetal inorganic materials, polymers and organic materials with tiny-molecules. A few instances of nanohybrids include those built with two nonmetal inorganic materials, metals and nonmetal inorganic materials, polymers and metals, two metals or metal alloys, polymers and biomolecules, respectively [96]. The categorization of nanohybrid systems based on the characteristics of the filler and the matrix components could be seen from Figure 2.18.

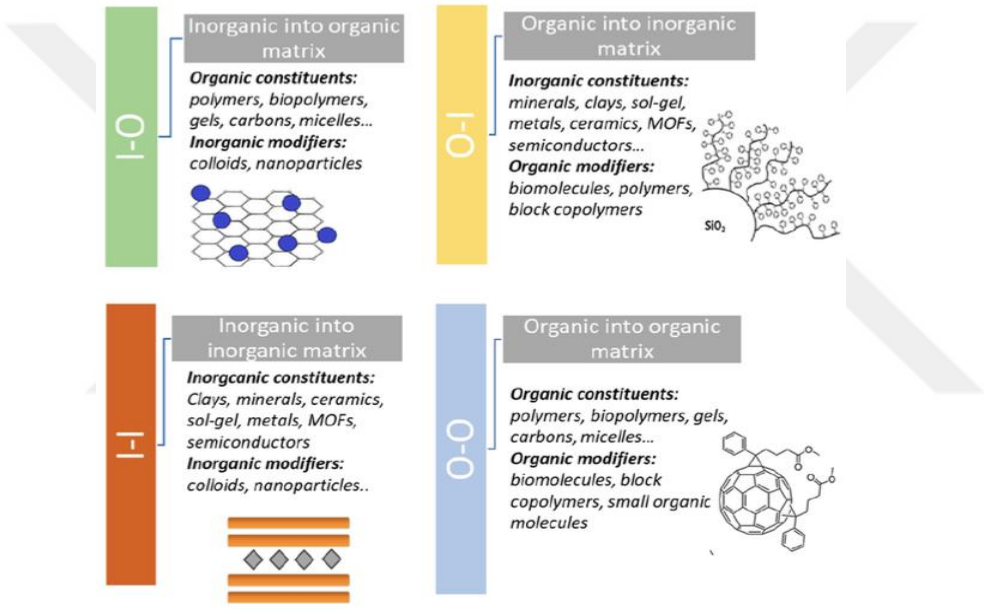

Figure 2.18 : The categorization of nanohybrid systems based on the characteristics of the filler and the matrix components [97].

Many inorganic compounds, consisting of mesoporous silica, iron oxide nanoparticles, gold and silver nanoparticles, and various clays, are employed extensively, either alone or in combination with polymers, particularly in drug delivery and controlled release implementations. The improved optical, electrical and mechanical capabilities of these inorganic compounds, along with their tiny size of particles make them desirable [98]. In drug delivery applications, these inorganic particles are typically coated, grafted or combined with biodegradable and biocompatible polymers to produce composites, Additionally, this methodology makes the particles more biocompatible, meaning it is a crucial component of a efficient system of drug delivery. These polymers can be either natural or synthetic. Poly(ε-caprolactone) (PCL), polyvinyl alcohol (PVA) and

polyethylene glycol (PEG) are the most commonly utilized polymers in organic/inorganic hybrid systems for biomedical implementations [99]. Class -I and Class-II hybrids are the two categories into which hybrid materials are usually divided based on the kind of connection that takes place between the organic and inorganic compounds. Weak connections among organic and inorganic compounds, consisting of hydrogen bonds, Van der Waals forces, or electrostatic connections, are what define Class-I hybrids [100]. These connections ensure to encapsulate or entrap inorganic particles within the polymer matrix. Both in situ and ex situ procedures can be employed to generate Class-I organic/inorganic hybrids [101]. On the other hand, Class-II hybrid materials have substantial chemical interactions between the organic and inorganic compounds, such as covalent, ionic-covalent or coordination linkages. In order to improve stability, these hybrid materials may contain alkoxy groups and metal-carbon connections that go through hydrolysis-condensation processes [100]. In situ fabrication of the polymer while inorganic particles are present, in situ fabrication of inorganic compound, or ex situ fabrication of both the polymer and the inorganic compound are the two strategies that can be used to create this covalent link [101]. Molecular-level incorporation of organic polymers and inorganic constituents is required for the fabrication of polymer/inorganic hybrid materials. Several approaches, including sol-gel procedures, melt blending, in situ polymerization and surface modification can be used to accomplish this. The intended qualities and implementations of the hybrid material determine which polymer and inorganic constituent is used [95]. In situ synthesis of the polymer component(PVL) in the existence of ex situ synthesized inorganic material (silica content in the lipase immobilized on RHA) represents the fabrication process used in this study. The polymer chains were “grafted from” or covalently bound to inorganic material’s surface by using surface modification technique. During the procedure, the monomer(δ-valerolactone) droplet enclosed inorganic material (silica content in the lipase immobilized on RHA) that were synthesized ex situ. When the polymerization reaction is finished, nanocomposite particles were fabricated [102].

2.8 Transchalcone

Drug investigations and medicinal science have paid close attention to chalcones, a category of organic molecules distinguished by their unique pharmalogical

characteristics and unique chemical structure. The open chain flavonoids found in chalcones are multipurpose molecules constituted of two aromatic rings joined by a three-carbon unsaturated carbonyl system [103]. There are two distinct types of chalcones, which are cis (Z, 2) and trans (E, 1) isomers. E isomers are the most prevalent chalcones due to their typically greater thermodynamic stability, while Z isomers are unstable due to the intermolecular interactions among ring-B and the carbonyl group [104]. The structure of the trans-chalcone molecule could be seen from Figure 2.19.

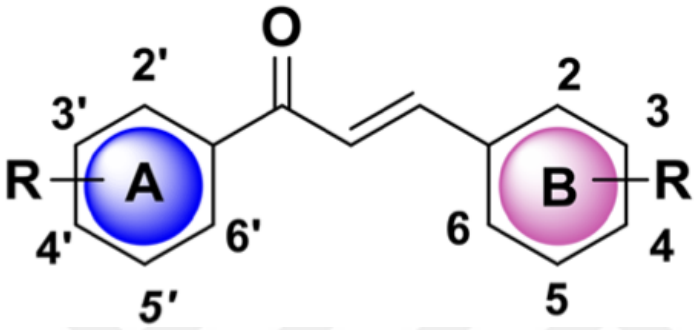

Figure 2.19 : The structure of the trans-chalcone molecule [104].

Chalcones are polyphenolic chemicals of various structures found in plants. There are several possible uses for chalcone-based compounds, including antibacterial, antiviral, antioxidant, anti-inflammatory, antidiabetic, antiulcer, anticancer properties. Chalcones provide significant pieces to the formation of crucial heterocyclic compounds that have medicinal applications for a range of illnesses [105]. Owing to their simple structures, chalcones, which are a carbon α,β-unsaturated system, reveal a variety of features in specific biological and pharmalogical domains. The Chaisen-Schmidt reaction is a widely used method for synthesizing chalcones. The reaction mechanism could be seen from Figure 2.20. It is thought to be very significant and entails the base-catalyzed condensation of an aromatic ketone with aldehyde to produce a chalcone structure [106].

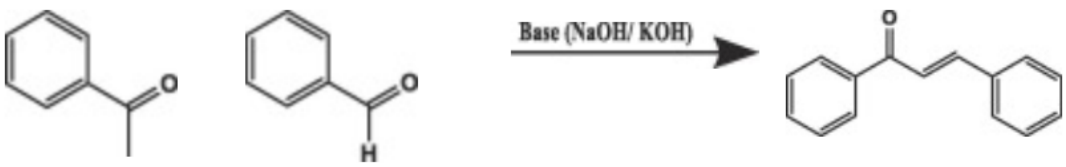

Figure 2.20 : The Chaisen-Schmidt reaction to fabricate the chalcone scaffold [106].

3. MATERIALS AND METHOD

3.1 Materials

A regional rice manufacturing factory in Edirne, Turkey generously provided the rice husks, which were then processed to generate rice husk ash(RHA). For experiments designed to modify the surface of RHA, (3-aminopropyl triethoxysilane, $C_9H_{23}NO_3Si$, 98 %, Sigma-Aldrich) was selected. To get rid of unnecessary impurities, rice husks had been washed with distilled water throughout the initial processing phase. RHA had been produced by burning the dried rice husks for six hours at 600-650^oC. Afterwards, it is utilized as a support substance for the immobilization of enzyme. The immobilized *Candida antarctica* Lipase B(CALB) (E.C. 3.1.1.3, recombinant, expressed in Aspergillus niger, Sigma) was used as a biocatalyst for the reactions. CALB was supplied in free form from Sigma Aldrich, then, immobilized onto RHA. RHA's surface was modified by treating it with (3-APTES, $C_9H_{23}NO_3Si$, 98 %, Sigma-Aldrich). For the surface modification of RHA, acetone (C_3H_6O, 100 %, Merck) was utilized as an ambient. The 0.015 M, pH=7 phosphate buffer solution was prepared by using sodium dihyrogen phosphate monohydrate (NaH_2PO_4. H_2O) (Carlo Erba) and disodium hydrogen phosphate heptahydrate (Na_2HPO_4. $7H_2O$) (Merck). In the polymerization reactions, δ-valerolactone (δ-VL) ($C_5H_8O_2$, Sigma-Aldrich) was employed as a monomer. In addition to this, toluene (C_7H_8, 99.8 %, Merck) was employed as a solvent, which is organic, in the polymerization reactions. In order to terminate the polymerization reactions and to be functional as a solvent for PVL polymer and PVL nanohybrid throughout the fabrication of microspheres, chloroform($CHCl_3$, 99 %, Merck) was utilized. Methanol (99% CH_3OH) (Emboy), which was supplied from Merck, was additionally utilized regarding the termination of polymerization reactions and the precipitation of the resultant polymer and nanohybrid. The artificially produced drug, Transchalcone (TC, $C_{15}H_{12}O$, 97%, Sigma-Aldrich), was supplied from Sigma Aldrich. Dichloromethane (CH_2Cl_2, 99 %, Carlo Erba) was utilized as the solvent of transchalcone in the internal phase of the TC-loaded microspheres throughout their fabrication. In order to prepare TC-loaded

microspheres, which were fabricated from PVL and PVL nanohybrid, an organic solvent called poly(vinyl alcohol) ($(C_2H_4O)n$, Sigma-Aldrich), was utilized. pH=7.4 phosphate buffer and pH=5.6 acetate buffer solutions (0.01 M) for enzyme immobilization and drug release studies were prepared by using sodium chloride (NaCl, 99.6 %, Carlo Erba), potassium chloride (KCl, 100 %, Merck), sodium phosphate dibasic dihydrate($Na_2HPO_4.2H_2O$, 100 %, Fluka Analytical), potassium dihydrogen phosphate (KH_2PO_4, %100, Merck), acetic acid(CH_3COOH, %100, Merck) and sodium acetate (CH3COONa, 100%, GPR).

3.2 Methods

3.2.1 Preparation of support material for the CALB immobilization

To get rid of any impurities, rice husks were initially washed with distilled water. They were rinsed and then left to dry overnight at 30^oC in an oven. Following that, the dried rice husks underwent combustion for six hours at 600-650^oC in an oven. Up until the desired burning degree was reached, the oven's temperature was continuously monitored and raised by 10^oC per minute. For the purpose of avoiding moisture after cooling, the rice husk ashes (RHA) were moved to desiccator once the combustion procedure had been done [16]. The processed rice husks are depicted in Figure 3.1 and 3.2.

Figure 3.1 : Dried rice husk after being washed with distilled water.

Figure 3.2 : Rice husk ash after the process of combustion.

According to the earlier research, the support material's surface was silanized by employing organosilane agent 3-APTES prior to the immobilization procedure. In 5 ml of acetone, 250 mg of RHA and 15% (v/v) 3-APTES were blended. For two hours, the mixture was incubated at 50^{o}C and 160 rpm in a shaking water bath (Julabo SW22) [16]. The shaking water bath instrument, which was used in the studies could be seen in Figure 3.3.

Figure 3.3 : Shaking water bath instrument used for physical adsorption.

29.25 ml 1M $NaH_2PO_4.H_2O$ and 45.75 ml 1M $NaH_2PO_4.7H_2O$ were combined with with distilled water, and the resultant mixture was diluted to 1 L with distilled water so as to produce 0.015 M, pH=7 phosphate buffer solution. A pH meter (Inolab TWT) was used for adjusting the buffer solution's pH value.

3.2.2 Immobilization of CALB

For the lipase immobilization, the prepared support were utilized. As previously mentioned, CALB was immobilized onto surface-modified RHA by using a physical

adsorption methodology[16]. For five hours at room temperature, CALB and RHA were combined in 25 ml of 0.015 M pH=7 phosphate buffer solution with an enzyme loading ratio of 2 μL/mg. Once the time expired, immobilized CALB went through a drying process for twelve hours at 300^{o}C in an oven. An apparatus used for filtration and the enzme after filtration could be seen from Figure 3.4 and 3.5, respectively.

Figure 3.4 : Apparatus used for filtration.

Figure 3.5 : Immobilized enzyme that has been filtered following immobilization via physical adsorption.

3.2.3 Enzymatic synthesis of poly(δ-valerolactone)

To facilitate the polymerization of δ-valerolactone, immobilized CALB was employed as a biocatalyst. Poly(δ-valerolactone) polymer was generated using the same polymerization process as the earlier study [17]. The reaction was conducted in a nitrogen ambient by using 1 g of toluene. There was a 20% of enzyme concentration and a 1:2 weight ratio of toluene to monomer. The reaction mixture underwent stirring at 80^{o}C and 120 rpm. According to previous study, these conditions are the best

conditions in order to produce PVL with the highest molecule weight, which was M_n=8040 g/mol [17]. Excess chloroform was employed at the end of the procedure to terminate the polymerization. Following the enyzme filtering from the polymerization media, the filtrate's chloroform was evaporated in an oven set to 50^{o}C. For purification, the polymer was subsequently precipitated in cold methanol and filtered. The final step was to dry the product overnight at 30^{o}C in the oven. The apparatus used for the reaction and the obtained polymer could be seen from Figure 3.6 and 3.7, respectively.

Figure 3.6 : Apparatus used for polymerization.

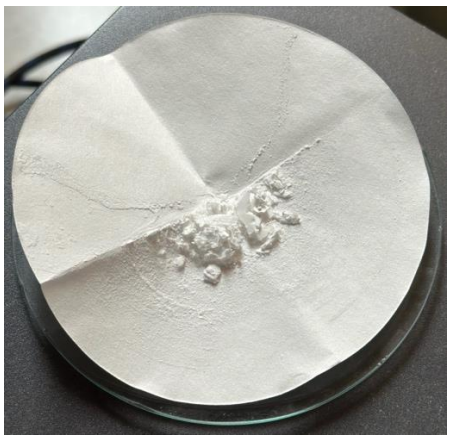

Figure 3.7 : The obtained poly(δ-valerolactone).

3.2.4 Enzymatic synthesis of poly(δ-valerolactone) nanohybrid

A lot of steps of PVL nanohybrid synthesis pratically the same as the synthesis of poly(δ-valerolactone), except the last few steps. To begin with, immobilized CALB was employed as a biocatalyst. The reaction was conducted in a nitrogen ambient by using 1 g of toluene. There was a 20% of enzyme concentration and a 1:2 weight ratio

of toluene to monomer. The reaction mixture underwent stirring at 80^{o}C and 120 rpm. Approximately 1 ml of chloroform was employed at the end of the procedure to terminate the polymerization. The resultant product was precipitated by dropping it into 300 ml of cold methanol, which was stirring at 100 rpm. Afterwards, this mixture was filtered by vacuum pump. The resultant remainings on the filter paper were dried at 50^{o}C for 24 hours [99]. After this period, the dried residuals were obtained as PVL nanohybrid. The obtained PVL nanohybrid could be seen from Figure 3.8.

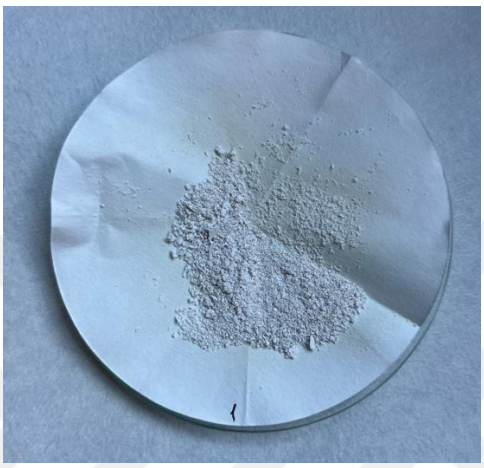

Figure 3.8 : The obtained PVL nanohybrid.

3.2.5 Preparation of TC-loaded PVL and PVL nanohybrid microspheres

The traditional O/W emulsion/solvent methodology was used to fabricate the microspheres [99]. The PVL polymer/nanohybrid with or without TC in chloroform(CH) and TC solution in dichloromethane (DCM) made up the internal phase. In order to keep the TC:PVL and TC:PVL nanohybrid ratios at 1:10, 1:5 and 1:2.5, the amount of TC:PVL or TC:PVL nanohybrid system was altered. Prior research tested a range of PVA solution concentrations (0.1, 0.5, 1(w/v)%), and it was shown that 1(w/v)% was the most effective concentration for fabricating microspheres [99]. To investigate how it affects of fluctuating concentrations on TC loading and release, the external phase consisted of a PVA solution at a fixed concentration of 1(w/v)%. By using a vortex mixer, the TC solution, PVL solution and PVL nanohybrid solution were initially thoroughly combined. For the formation of a milky-white emulsion, this solution was mixed with 50 ml of PVA solution while being stirred at 1500 rpm for five minutes. After that, 50 ml of distilled water was added to dilute emulsion, and it was agitated for 24 hours to let the solvents evaporate. Following the evaporation, the microspheres were dried in an oven set to 30^{o}C for the entire night

after the emulsion was centrifuged to extract the PVA and noncapsulated TC. By using methanol for extracting the drug content, the microsphere's encapsulation efficiencies (EC) and loading capacities (LC) were ascertained instantly [99]. The polymer did not obstruct the UV spectrophotometer absorbance measurements, mainly since methanol dissolves the chalcone present in the particles but not the polymer [99]. A UV spectrophotometer was used to measure the absorbance at 308 nm by using methanol as the blank solution subsequently the suspension that was formed had been filtered (a calibration curve is attached in Appendices A). The Equation 3.1 and Equation 3.2 shown below were used to determine encapsulation efficiency and loading capacity, respectively.

$$\text{EE (\%)} = \frac{\text{weight of TC in the microspheres}}{\text{weight of TC in the emulsion}} \text{ x } 100 \quad (3.1)$$

$$\text{LC (\%)} = \frac{\text{Actual weight of TC in the microspheres}}{\text{Total weight of microspheres}} \text{ x } 100 \quad (3.2)$$

3.2.6 In vitro TC release from loaded PVL and PVL nanohybrid microspheres

The features of drug release from microspheres were examined. As the release media, PBS solution (pH 7.4, 0.1 M) was used in drug release tests. In an incubator set to 37^{o}C and 120 rpm, 10 mg of loaded microspheres were suspended in PBS solution and shaken. A 1 ml aliquot was taken and the equivalent volume of completely fresh PBS solution was put in at the designated intervals. To get rid of any suspended microspheres that could have been present, the aliquot was filtered using syringe filters (0.45 μm), when it was needed. A UV spectrophotometer was used to measure the absorbance, once the extracted specimen had been diluted to 10 ml with PBS. By switching the release media to an acetate buffer solution (pH 5.6), the pH-responsive behaviour of the loaded microspheres was investigated. All of the release studies were carried out under sink circumstances. In Appendices A, related calibration curves were displayed.

3.2.7 Kinetic model fitting

To gain an improved comprehension of the drug release procedure for each specimen, the drug release profiles were fitted to kinetic models. Nonlinear regression was employed to fit the data to the Higuchi and Korsmeyer-Peppas kinetic models, and the

corresponding kinetic variables were identified. The Equation 3.3 and Equation 3.3 shown below were utilized for the kinetic models.

$$\text{Higuchi: } Q_t/Q_\infty = K_H \times t^{0.5} \quad (3.3)$$

$$\text{Korsmeyer-Peppas: } Q_t/Q_\infty = K_{KP} \times t^n \quad (3.4)$$

Where n is the release exponent and Q_t/Q_∞ is the fraction of drug released at time t. The Higuchi and Korsmeyer-Peppas release rate coeffcients are K_H ($t^{-0.5}$) and K_{KP}(t^{-n}), respectively.

3.3 Characterization Techniques

3.3.1 Scanning electron microscope (SEM)

A scanning electron microscope (SEM, TM4000Plus II, HITACHI) was used to examine the microsphere's surface morphology. All of the specimens were coated with gold by using the equipment's coater (SBC-800, Small Ion Sputtering Instrument) prior to the scannings. The SEM and its coater instrument used for characterization could be seen from Figure 3.9. The scannings were conducted at 5 kV, 10 kV and 15 kV.

Figure 3.9 : SEM and its coater instrument used for characterization.

3.3.2 Fourier transform infrared spectroscopy (FT-IR)

The chemical compositon and structure of PVL/PVL nanohyrid, TC-loaded PVL/PVL nanohybrid microspheres, drug-free PVL/PVL nanohybrid microspheres, and TC

specimens were examined by using SHIMADZU's IRAffinity-1 ATR-FT-IR Spectrometer. FT-IR measurement shows alterations in functional groups subsequently each stage of enzyme immobilization. Additionally, by comparing the enzymatically synthesized polymer to the unique functional groups and and linkages of PVL or PVL nanohybrid, FT-IR was used to identify them as PVL or PVL nanohybrid. With a resolution of 4 cm^{-1}, not less than 16 scans were used to get the spectra. The FT-IR instrument used for characterization could be seen from Figure 3.10.

Figure 3.10 : FT-IR instrument used for characterization.

3.3.3 Differential scanning calorimetry (DSC)

To identify the thermal properties, differential scanning calorimetry (DSC) via METTLER TOLEDO DSC 1 STAR^e System is employed. At a flow rate of 80 ml per minute, measurements were made in an inert nitrogen ambient and analysed. Heat-cool thermal cycle was used to detect the melting point (T_m) and glass transition point (T_g) of the specimens with temperatures ranging from -50 to 200°C at a rate of 10°C per minute.

3.3.4 Thermal gravimetric analysis (TGA)

Thermal gravimetric analysis (TGA) was employed to thermally characterize the surface-modified RHA, PVL specimens and PVL nanohybrid specimens. To achieve this, 1,3 – 6,9 mg of specimens underwent heating under ait flow from 25^{o}C to 500^{o}C at a rate of 10^{o}C per minute. METTLER TOLEDO TGA 1 STAR^e System was the equipment in use.

3.3.5 X-Ray diffraction analysis (XRD)

To analyze the crystal structures of PVL and PVL nanohybrid specimens, X-Ray diffraction (XRD) variations were found by using Cu-Kα radiation on a range of 5° to 70° with a 0.02° step size by using a XRD equipment (Rigaku MiniFlex).

3.3.6 Ultraviolet (UV) spectrophotometer

By detecting absorbance on an ultraviolet spectrophotometer (UV-Vis, Cary 60, Agilent Technologies), the encapsulation rate of microspheres and the total quantity of transchalcone released were ascertained. The UV-Vis instrument used for characterization could be seen from Figure 3.11. To generate the calibration graph, solutions that had varying transchalcone concentrations were made. The methanol was employed as a blank solution, along with pH 5.6 acetate buffer and pH 7.4 phosphate buffer solution.

Figure 3.11 : UV-Vis instrument used for characterization.

4. RESULTS AND DISCUSSION

4.1 Synthesis of Poly(δ-valerolactone) With Immobilized Enzyme

The earlier studies indicated that δ-valerolactone combined with handmade immobilized CALB, exhibited ring opening polymerization in toluene media. The mean molecular weight (M_n) of the synthetic PVL, which was generated, was 8040 g/mol [17]. Unlike other studies, this one investigated the effectiveness of immobilized CALB on δ-valerolactone to detect its impact on microsphere formation. In earlier research, the maximum performance was attained at a fixed temperature of 80^oC [17]. In this study, PVL is generated according to earlier research with the greatest M_n value throughout the 24 hours polymerization period at 80^oC [17].

4.2 Fabrication of PVL Microspheres

Due to its numerous pharmalogical upsides, as formerly described, the enzymatically synthesized PVL, which was generated for this study in therapeutic uses, was formed into microspheres. The emulsion/solvent evaporation methodology is used to generate both drug-free and TC-loaded PVL microsphere structures. Several microsphere formulations were generated in the earlier research to examine the impact of process factors [99]. As it was previously pointed out, PVA at different concentrations (0.1, 0.5, 1 (w/v) %) were the exterior phase of the microsphere compositions and were examined and compiled. Since the enhanced viscosity limits drug diffusion into the exterior phase, the findings displayed that a 1 (w/v) % PVA concentration in the exterior phase heightened encapsulation efficiency [99]. As a result, in this study, microspheres were generated with an exterior phase, which is PVA concentration of 1 (w/v) %. The impact of the interior phase concentration was additionally investigated in the prior research [99]. As stated in Table 4.1, multiple TC ratios on PVL were further investigated in this study.

Table 4.1 : PVA concentrations, PVL microsphere formulations, encapsulation efficiencies, loading capacities and mean particle diameters.

Sample Code	PVA concentration (%)	TC:PVL ratio (%)	Encapsulation Efficiency (%)[1]	Loading Capacity (%)	Mean Particle Diameter (μm)[2]
A-1	1	0	-	-	26.6 ± 8.8
A-2	1	20	98.6 ± 8.4	16.4 ± 1.4	30.4 ± 11.8
B-1	0.5	0	-	-	27.3 ± 6.6
B-2	0.5	20	83.6 ± 3.8	13.9 ± 0.6	41.4 ± 10.6
C-1	1	0	-	-	27.8 ± 7.5
C-2	1	10	71.2 ± 7.9	6.5 ± 0.7	42.4 ± 13.4
D-1	0.5	0	-	-	46.6 ± 13.3
D-2	0.5	10	67.2 ± 6.8	6.1 ± 0.6	39.5 ± 11.7
E-1	0.5	0	-	-	32.7 ± 8.8
E-2	0.5	40	61.6 ± 3.8	17.6 ± 1.1	25.9 ± 5.0
F-1	1	0	-	-	21.7 ± 4.6
F-2	1	40	67.3 ± 0.2	19.2 ± 0.1	35.1 ± 10.4
G-1	0.1	0	-	-	21.2 ± 6.8
G-2	0.1	20	67.6 ± 4.7	11.3 ± 0.8	24.1 ± 6.6
H-1	0.1	0	-	-	34.7 ± 10.0
H-2	0.1	10	71.6 ± 3.0	6.5 ± 0.3	28.4 ± 7.7
I-1	0.1	0	-	-	20.9 ± 4.5
I-2	0.1	40	54.1 ± 2.2	15.5 ± 0.6	32.5 ± 12.6

[1]Calculated from Equation 3.1.
[2]Measured by particle size analyzer of SEM instrument(mean±SD; n=34)

Experiments were conducted with 25 mg, 50 mg and 100 mg PVL amounts (40% = 25 mg, 20 % = 50 mg and 10 % = 100 mg amounts), with the drug mass generally held fixed at 10 mg. Simultaneously, microspheres were generated as drug-free and TC-loaded. Equation 3.1 was employed to identify encapsulation efficiency (%). The microspheres formed at a 20% TC:PVL ratio with 1 (w/v)% PVA concentration (specimen A-2) were found to have the greatest encapsulation efficiency (%), as demonstrated in Table 4.1.

It was shown that raising PVL amounts, in other words, decreasing TC:PVL ratio from 40% to 20%, at the constant concentration of PVA (1 %, 0.5 % and 0.1 %) improved the encapsulation efficiency. Besides, at the constant PVA concentrations (1% and 0.5%), it was pointed out that raising PVL amounts (by decreasing TC:PVL ratio from 40% to 10%) made the encapsulation efficiency almost unchanged. On the other hand, at the consant PVA concentration (0.1%), it was shown that raising PVL amounts (by

decreasing TC:PVL ratio from 40% to 20%) improved the encapsulation efficiency, but decreasing TC:PVL ratio from 20% to 10% made the encapsulation efficiency nearly unaffected.

Moreover, it was seen that with the constant amounts of PVL (when the TC:PVL ratios are %40 and 20%), increasing the PVA concentration (%) made the encapsulation efficiency higher. However, with the constant amount of PVL (when the TC:PVL ratio is 10%), raising PVA concentration (%) made the encapsulation efficiency almost unvaried.

The one significant factor influencing the encapsulation efficiency is the particle size. The mean particle size diameters varied between 24.1 - 42.4 μm. A larger particle size results from a decrease in the emulsification capability owing to a decrease in a PVA concentration [107]. When the PVA concentration was decreased from 0.5% to 0.1% with the constant amount of PVL (when the TC:PVL ratio is 40%), it was seen that particle size of the microspheres became larger (from 25.9 ± 5.0 μm to 32.5 ± 12.6 μm). When the PVA concentration was decreased from 1% to 0.5% with the constant amount of PVL (when the TC:PVL ratio is 20%), it was seen that particle size of the microspheres also became larger (from 30.4 ± 11.8 μm to 41.4 ± 10.6 μm). Besides, in general, it seems that the particle size of the TC-loaded PVL microspheres became more larger than drug-free PVL microspheres.

Furthermore, larger particles formed as a result of the interior phase being more viscous thanks to an increase in polymer concentration [108]. Especially, at constant PVA concentration of 0.5%, with the increase of PVL amount (when the TC:PVL ratio decreased from 40% to 20%), the particle size was elevated from 25.9 ± 5.0 μm to 41.4 ± 10.6 μm. In addition, at constant PVA concentration of 1%, with the increase of PVL amount (when the TC:PVL ratio decreased from 20% to 10%), the particle size was elevated from 30.4 ± 11.8 μm to 42.4 ± 13.4 μm.

The diffusion of the encapsulated drug from the matrix system is facilitated by enhancing porosity of the microshere. In the earlier research, it was shown that the drug was released more quickly from the smaller microsphere [109]. Due to their tiny spherical size, microspheres can possibly be inserted into the body with simplicity. This kind of therapeutic insertation will increase bioavailability and reduce the

likehood side effects. That is why, smaller particle size is the preferred parameter for the controlled drug release systems [109].

4.3 Characterization of PVL Microspheres

The chemical and mechanical characteristics of the fabricated PVL, TC-loaded PVL microspheres, drug-free PVL microspheres were examined by using SEM, FT-IR, DSC, TGA and XRD analyses.

4.3.1 SEM results of PVL microspheres

The samples codes, different PVA concentrations and TC:PVL ratios can be seen from Table 4.2.

Table 4.2 : Sample codes, PVA concentrations and TC ratios in order to PVL.

Sample Code	PVA concentration (%)	TC:PVL ratio (%)
A-1	1	0
A-2	1	20
B-1	0.5	0
B-2	0.5	20
C-1	1	0
C-2	1	10
D-1	0.5	0
D-2	0.5	10
E-1	0.5	0
E-2	0.5	40
F-1	1	0
F-2	1	40
G-1	0.1	0
G-2	0.1	20
H-1	0.1	0
H-2	0.1	10
I-1	0.1	0
I-2	0.1	40

As shown in Figure 4.1, a multitude of scanning electron microscope images were employed to evaluate the shape of the microspheres and identify the particle size. Every formulation of microspheres resulted in a shpherical form. As expected for a solvent evaporation methodology, drug-free and TC-loaded PVL microspheres had a spherical form and a porous surface [82].

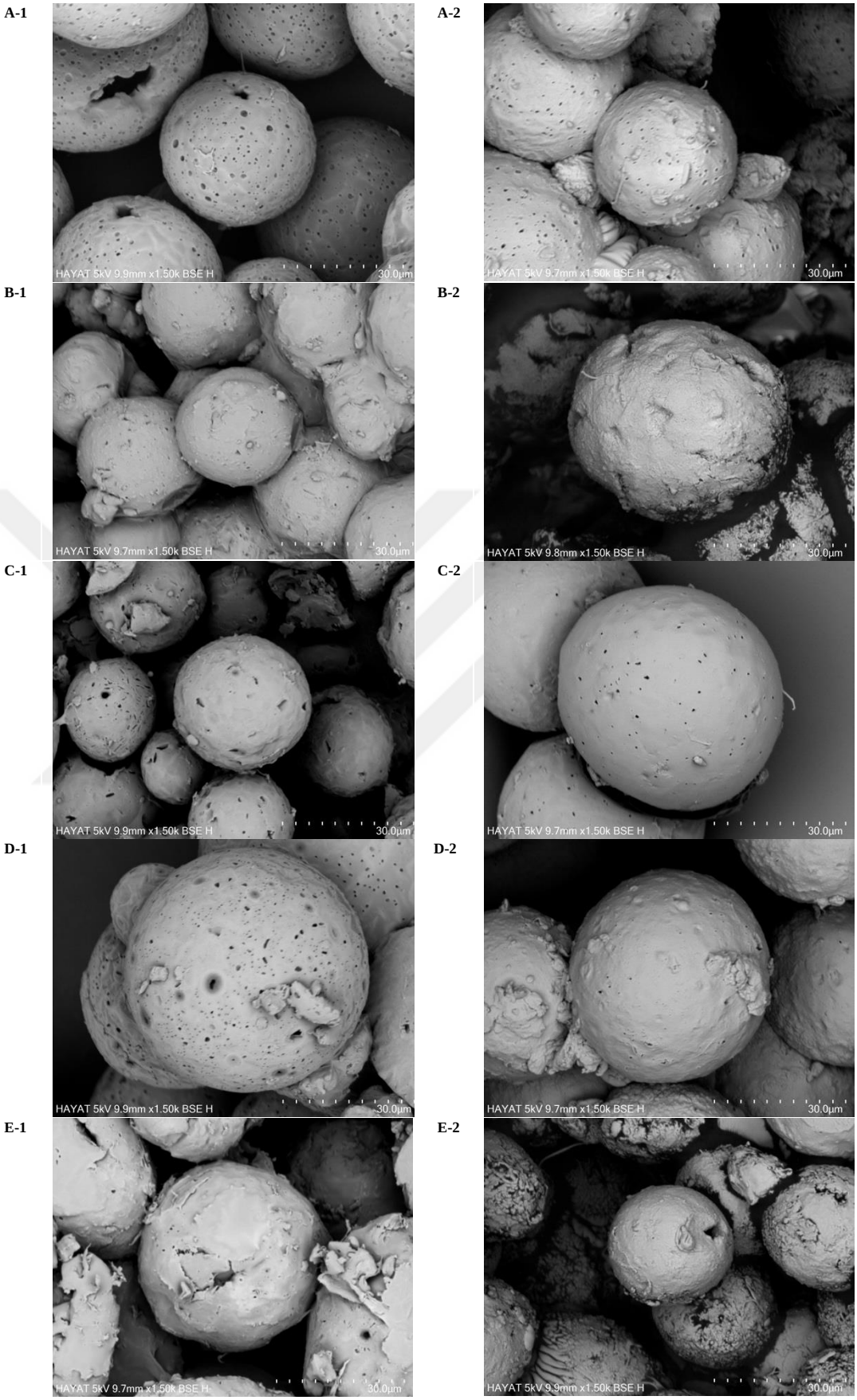

Figure 4.1 : SEM images of : Drug-free and TC-loaded PVL microspheres (Magnification 1500x, scale bar 30 µm).

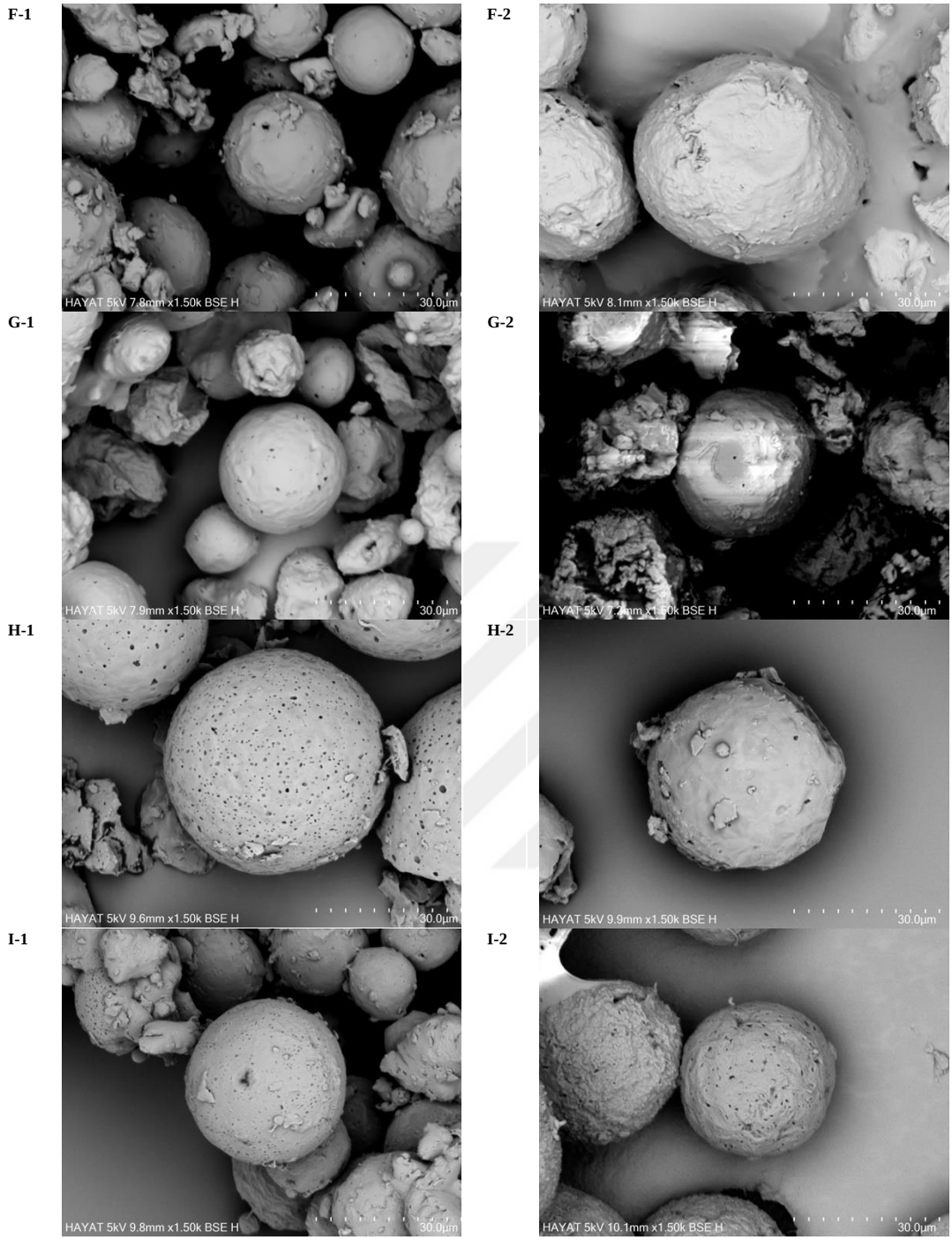

Figure 4.1 (continued) : SEM images of : Drug-free and TC-loaded PVL microspheres (Magnification 1500x, scale bar 30 µm).

4.3.2 FT-IR results of PVL microspheres

FT-IR analysis was implemented to additional characterize PVL, drug-free PVL microspheres, TC-loaded PVL microspheres and TC. The FT-IR spectra of these specimens could be seen from Figure 4.2. The asymmetrical and symmetrical CH_2 groups in the structure of the synthesized PVL have peaks of 2958 cm^{-1} and 2876 cm^{-1}. Also, the C=O streching in the PVL structure have peaks of 1723 cm^{-1}, the C-O and

C-C bonds have peaks of 1322 cm^{-1} and the symmetrical C-O-C bonds have peaks of 1165 cm^{-1}. Besides, both drug-free and TC-loaded PVL microspheres exhibit all of these distinctive peaks, which are consistent with the previous researches [17,68].

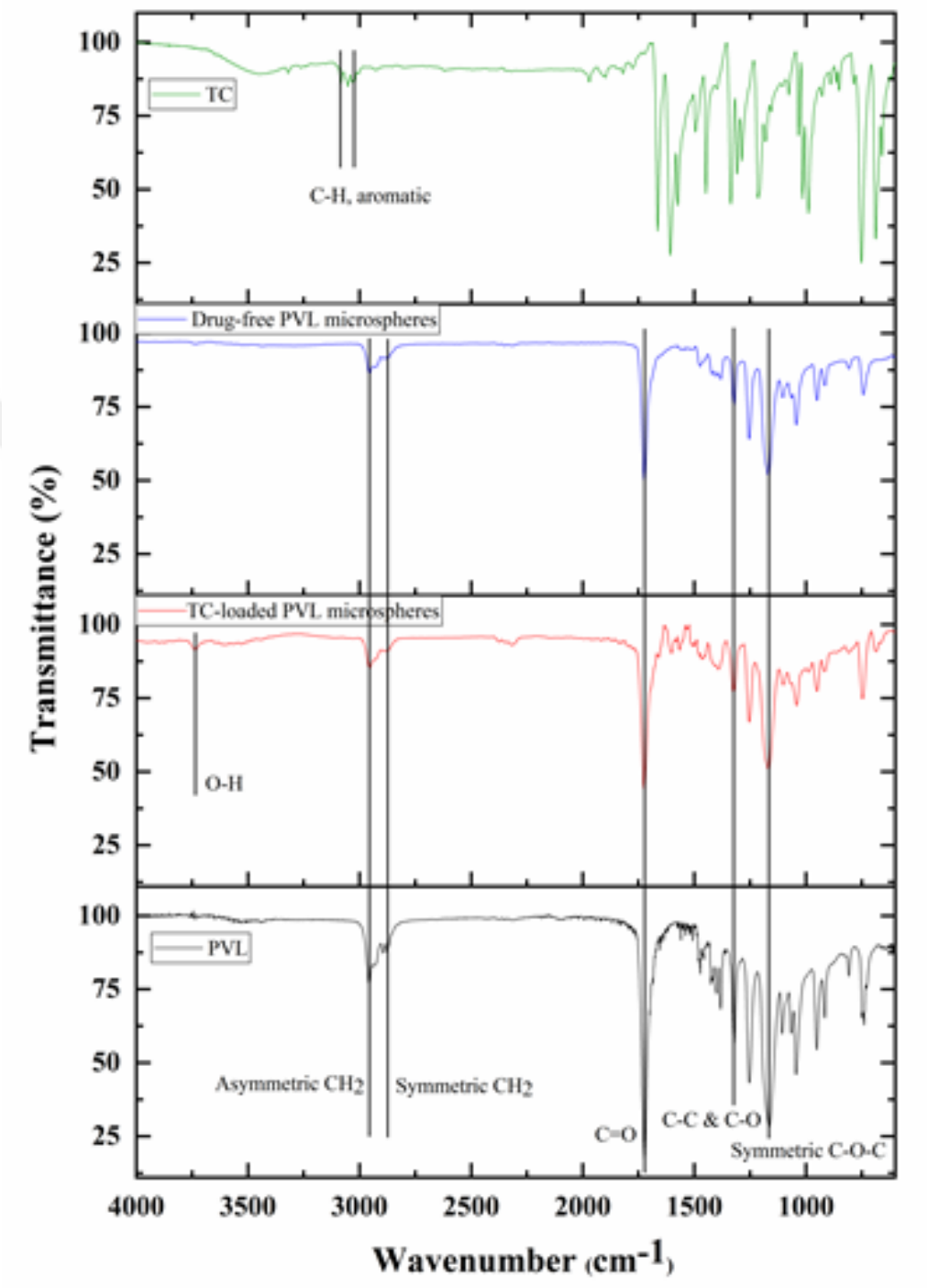

Figure 4.2 : FT-IR spectra of TC, drug-free PVL microspheres, TC-loaded PVL microspheres, PVL.

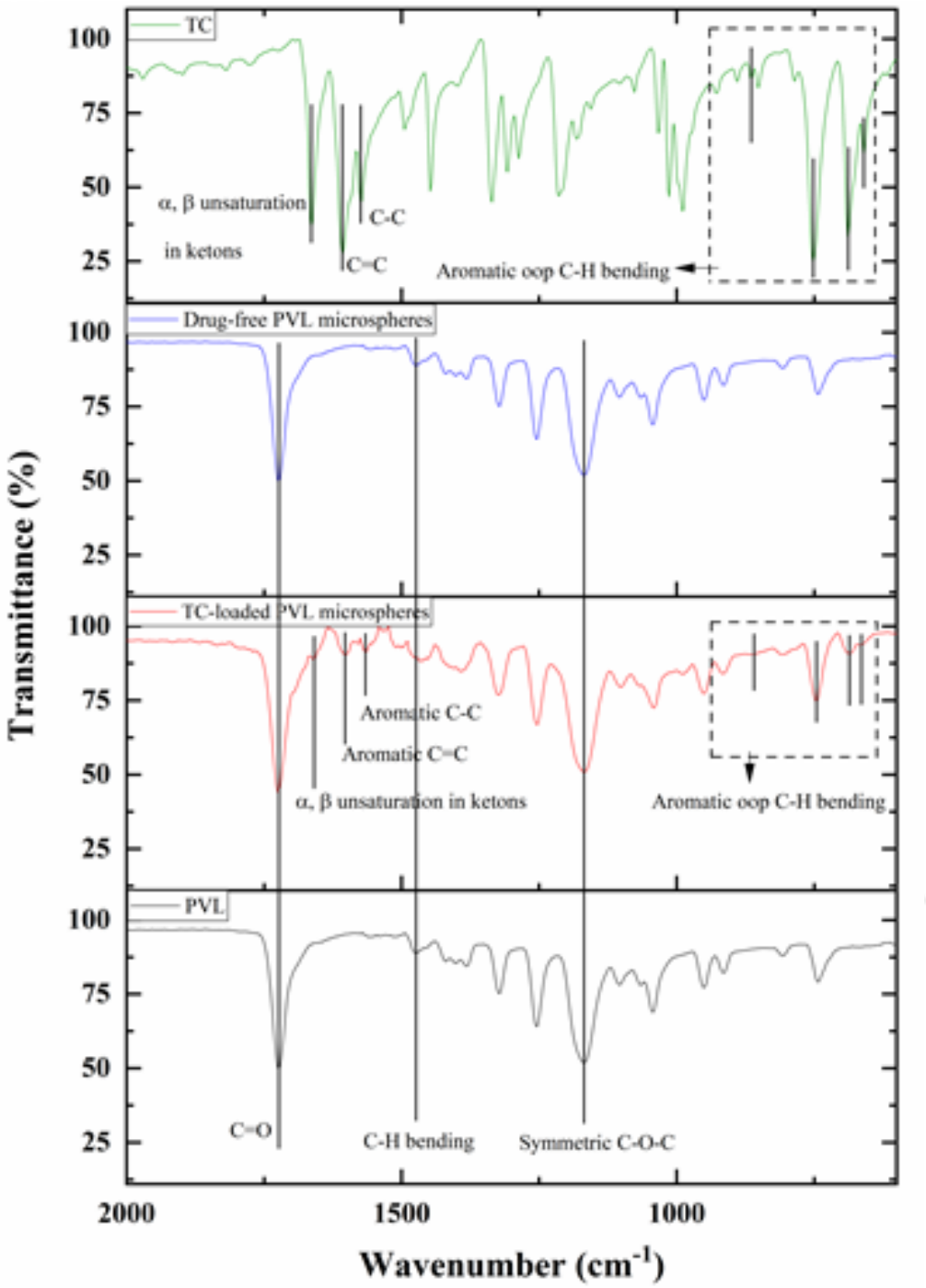

Figure 4.2 (continued) : FT-IR spectra of TC, drug-free PVL microspheres, TC-loaded PVL microspheres, PVL.

Moreover, the signals for an O-H stretching have detected at 3736 cm^{-1} in the TC-loaded PVL microspheres's structure. It is equivalent to the -OH group, which was intermolecularly H-bonded.

The peaks of C-H bending at 1473 cm^{-1} and symmetric C-O-C bond at 1170 cm^{-1} also observed in the drug-free and TC-loaded PVL microspheres, like in the structure of the PVL. In the spectra of TC, the peaks have shown at 1663 cm^{-1} because of the α, β

unsaturation in ketones of the drug, at 675-900 cm^{-1} because of aromatic oop C-H bending, at 3025-3084 cm^{-1} because of aromatic C-H bond, and in addition, at 1607 cm^{-1} and 1575 cm-1, due to the stretching of C=C and C=O, respectively [99]. When it was compared the spectra of TC and TC-loaded PVL microspheres, it is clearly said that the spectras are looking alike without any signicant difference. It means that TC is successfully encapsulated in the structure of PVL microspheres.

4.3.3 DSC results of PVL microspheres

Drug-free PVL microspheres and after TC were added into them, the thermochemical alterations in the PVL structure were observed by using DSC analysis. The specimens' temperatures of melting are demonstrated by the DSC plots in Figure 4.3.

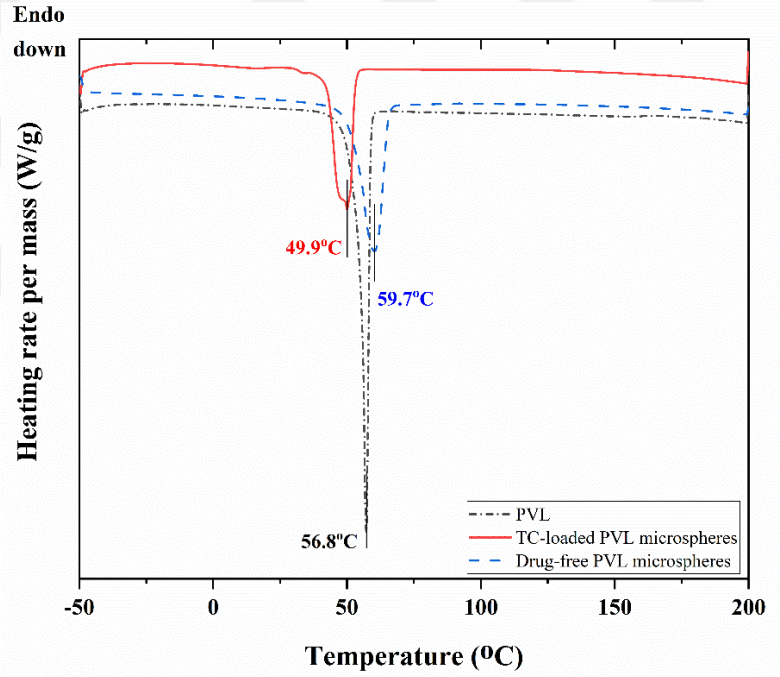

Figure 4.3 : Melting temperatures of the specimens: DSC melting endotherm, PVL, TC-loaded PVL microspheres, drug-free PVL microspheres.

The T_m value of the PVL is approximately 58°C, according to published studies [61]. With this perspective, it can be seen that the measured T_m data of the drug-free PVL microspheres are close to this data, as expected.

From the regions beneath the melting peaks, the entalphy values of PVL, TC-loaded PVL microspheres and drug-free PVL microspheres were determined to be 124.6 J/g, 86.4 J/g and 109.1 J/g, respectively. Table 4.3 displays the computed results. With loaded TC, it can be claimed that the melting temperature and entalphy values decreased.

Table 4.3 : T_m and enthalpy values of PVL, TC-loaded PVL microspheres and drug-free PVL microspheres.

	T_m (℃)	ΔH_m (J/g)
PVL	56.8	124.6
TC-loaded PVL microspheres	49.9	86.4
Drug-free PVL microspheres	59.7	109.1

The melting temperature of the industrial TC was found to be 59^{o}C in the prior research [99]. Since there is not any second melting peak on the DSC curve of the TC-loaded PVL microspheres, it can be said that TC is sufficiently molecularly dispersed in the TC-loaded PVL microspheres [110]. In this case, as it was shown in the another previous study, no addional melting peak close to drug's melting point means TC's surface morphology is amorphous [111]. Besides, since the melting temperature of TC-loaded PVL microspheres (T_m : 49.9^{o}C) are less than the melting temperatures of both PVL (T_m ~ 58^{o}C) and TC (T_m : 59^{o}C), it can be said that there is an eutectic system was occurred [99].

4.3.4 TGA results of PVL microspheres

The thermal decomposition profiles of drug-free PVL microspheres and TC-loaded PVL microspheres in comparison to PVL was examined by using TGA analysis. The temperature change leads to weight losses. Hence, absorption, adsorption, vaporization, sublimation, decomposition are among the thermal processes that TGA is primarily used to examine [112]. In this analysis, weight changes of the three specimens were deducted. According to the curves in Figure 4.4, PVL started to decompose at approximately 180^{o}C, as it was expected [17].

The specimen of neat-PVL showed two steps of degradation. Its primarily degradation was at 310.8^{o}C with 66.3% weight loss. The secondary degradation of the PVL was at 445.3^{o}C, where it decomposed as 32%. With the exception of water/solvent evaporation interval, the specimens of drug-free and TC-loaded PVL microspheres degraded in two and three steps, respectively. The primarily degradation of TC-loaded PVL microspheres was at 235.5^{o}C with 42.5% weight loss, which was almost the half of the specimen. This temperature (235.5^{o}C) is less than first degradation of neat-PVL (310^{o}C) and drug-free PVL microspheres (347.7^{o}C), due to addition of TC. This suggests that the degradation temperature is lowered by an incorporation of additional substances [113]. Compared to drug-free PVL microsphere-specimen, TC-loaded

microsphere-specimen's initial degrading step began more promptly and took place over a larger temperature span.

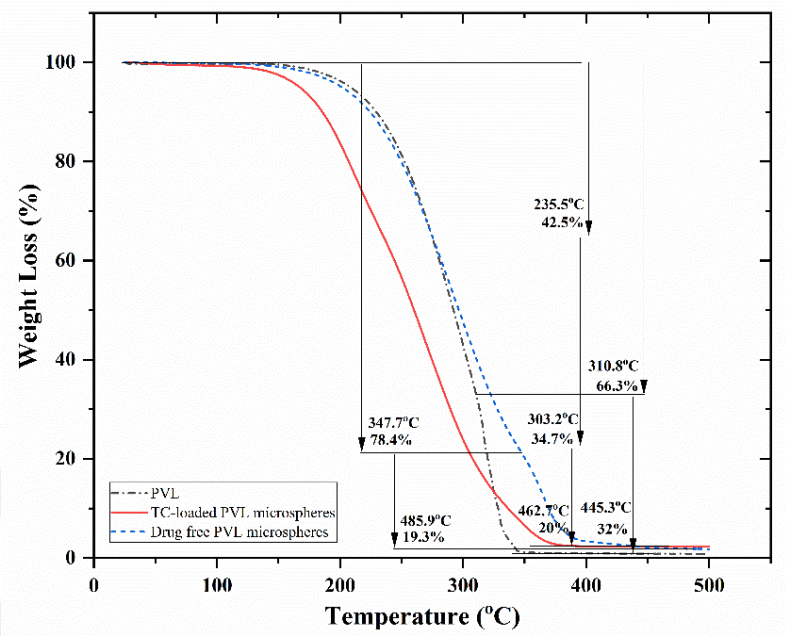

Figure 4.4 : TGA and derivative of weight losses results; PVL (black), TC-loaded PVL microspheres(red), drug-free PVL microspheres (blue).

4.3.5 XRD results of PVL microspheres

By using XRD analysis, the impact of the TC-loading on the crystalline structures and crystallinity of microspheres were examined. The diffraction peaks can be seen from Figure 4.5.

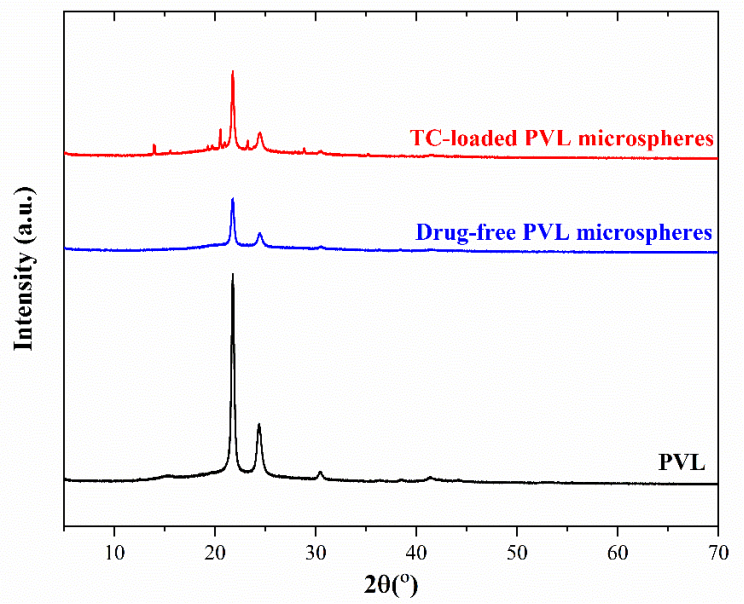

Figure 4.5 : XRD measurement of : TC- loaded PVL microspheres (red), Drug-free PVL microspheres (blue), PVL (black).

Two unique diffraction peaks at $2\theta = 21.8^{o}$ and 24.4^{o} were seen in PVL, TC-loaded PVL microsphere-specimen and drug-free PVL microsphere-specimen; they assigned to the PVL. The neat PVL has semicrystalline structure as predicted, and amorphism rises when TC are added. Following TC-loading, it was seen that the intensities of the distintive crystalline peaks went down. The pattern gets noisier as the crystalline peak's intensity value reduces. In other words, crystallinity is thus diminishes.

4.4 pH Dependent Drug Release From PVL Microspheres

The drug release mechanism is significantly influenced by the properties of the release media. Among these characteristics is pH, which was investigated in relation to microsphere release. As demonstrated in Figure 4.6, two unique pH levels are were used in this research to simulate the contexts of different bodily parts while examining the release behaviour of varying concentration of PVL in the TC-loaded PVL microspheres at pH 5.6 and pH 7.4. While pH 7.4 represents healthy body, pH 5.6 represents cancer cell [114].

At the constant PVA concentration of 1% and TC amount (10 mg), different amounts of PVL (25 mg, 50 mg, 100 mg) were used to form microspheres, as it was previously mentioned.

To begin with, the first burst release was noted to have taken place over the first 4 hours for pH 7.4. At this pH value, For the TC:PVL ratio of 10%, initial burst release was examined as 26.3 ± 2.6 (%), while the initial burst release was examined as 7.5 ± 0.9 (%) for the TC:PVL ratio of 20%, and 7.7 ± 3.2 (%) for the TC:PVL ratio of 40%. It means, the initial burst release with 10% of TC:PVL ratio has shown higher rate than the other ratios. These three distinct PVL microspheres formed with varying ratio of PVL were found to have equivalent release patterns. There was a burst release at the beginning of the drug release behaviour, followed by a steady release. The results of the 744-hour drug release studies showed that PVL microspheres formed with 10% TC:PVL ratio have the highest release percentage at 42.1 ± 10.8 (%). The remaining two specimens' cumulative release percentages are 20.0 ± 2.3 (%) with TC:PVL ratio of 20% and 16.8 ± 0.6 (%) with TC:PVL ratio of 40%. These findings indicate that the most ideal formulation for TC-loaded PVL microspheres is 10% ratio of TC:PVL.

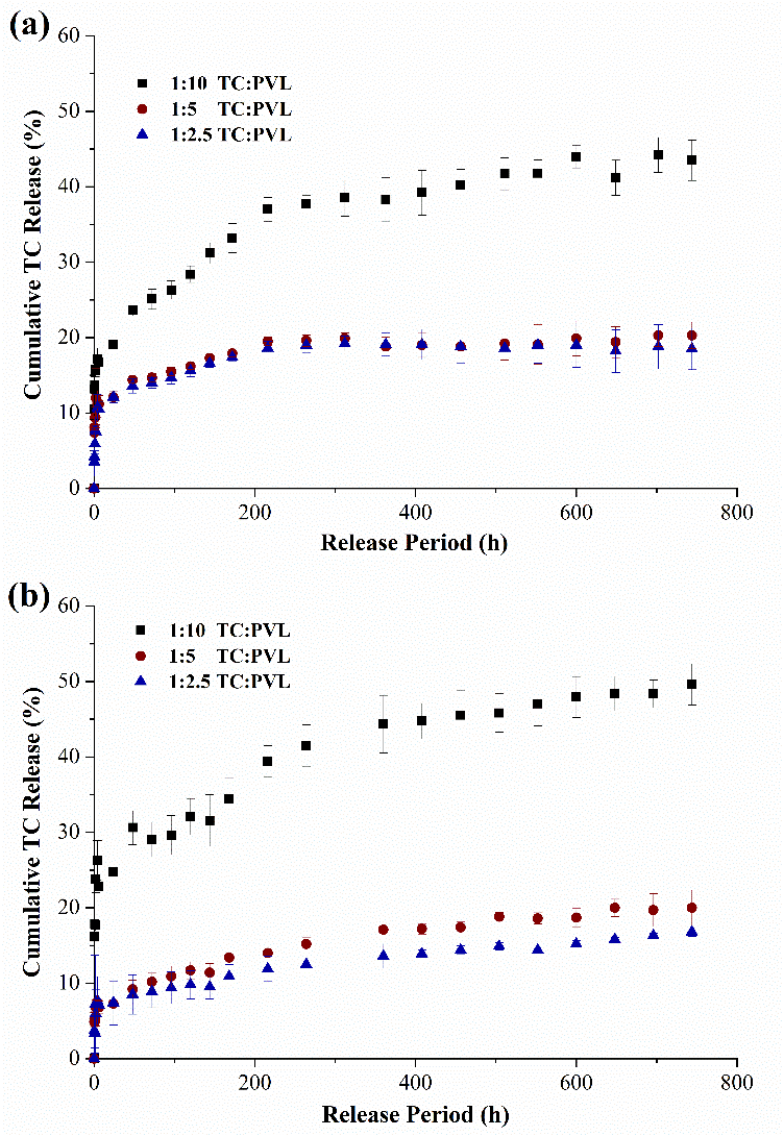

Figure 4.6 : Effect of PVL concentration on cumulative TC release (%) in two different pH media (pH 5.6 and pH 7.4, respectively).

The second of all, the first burst release was noted to have taken place over the first 6 hours for pH 5.6. At this pH value, For the TC:PVL ratio of 10%, initial burst release was examined as 16.7 ± 0.4 (%), while the initial burst release was examined as 11.2 ± 1.1 (%) for the TC:PVL ratio of 20%, and 10.5 ± 1.0 (%) for the TC:PVL ratio of 40%. It means, the initial burst release with 10% of TC:PVL ratio has shown higher rate than the other ratios. These three distinct PVL microspheres formed with varying ratio of PVL were also found to have equivalent release patterns like pH 7.4 plots. There was a burst release at the beginning of the drug release behaviour, followed by a steady release. The results of the 744-hour drug release studies showed that PVL microspheres formed with 10% TC:PVL ratio have the highest release percentage at 43.5 ± 2.7 (%). The remaining two specimens' cumulative release percentages are 20.3

± 1.8 (%) with TC:PVL ratio of 20% and 18.5 ± 2.7 (%) with TC:PVL ratio of 40%. These findings pointed that the most ideal formulation for TC-loaded PVL microspheres is 10% ratio of TC:PVL like it was found in the pH 5.6 results.

It can be inferred from a comparison of drug release profiles at two pH values that the release percentages at pH 5.6 are greater than those at pH 7.4. In pH 7.4 it was discovered that TC-loaded PVL microspheres with the 10% ratio of TC:PVL exhibited a greater burst release rate. One may argue that the pH 5.6 media enables for a more controlled release of these specimens.

4.5 Kinetic Modelling and Release Mechanism for PVL Microspheres

To gain additional insight into the drug release mechanism for every specimen, as detailed in section 3.2.7, the drug release patterns are fitted to two kinetic models, named the Higuchi and Korsmeyer-Peppas models of math. The computed variables for the fitted kinetic model are displayed in Figure 4.7.

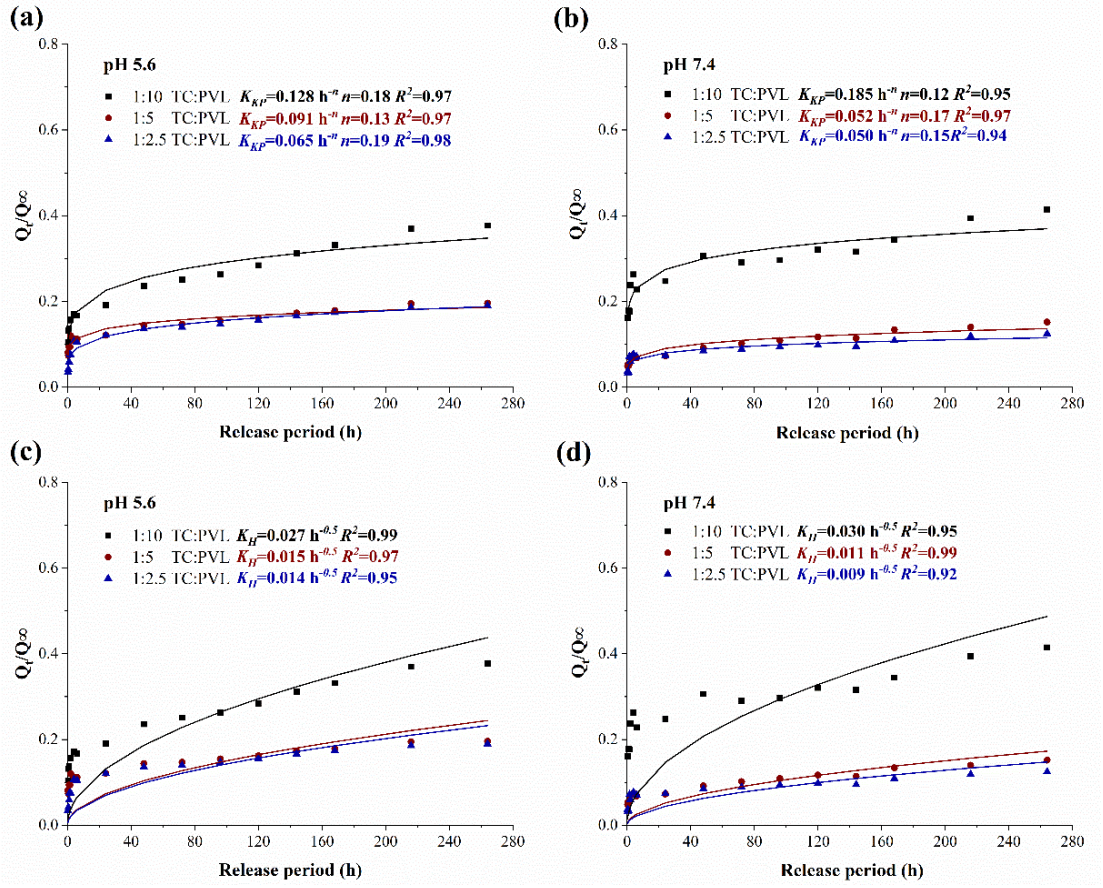

Figure 4.7 : Kinetic modelling and calculations of release mechanisms in two different pH media (pH 5.6 and pH 7.4) with TC-loaded PVL nanohybrid microspheres.

The correlation coefficient of the Korsmeyer-Peppas model was greater ($R^2 > 94$) in comparison to other kinetic model. The release exponent (n) in the model of Korsmeyer-Peppas provides information about drug release profile. It is derived from the linearized equation's (Equation 3.4) slope [115]. A diffusion release mechanism called Fickian is inferred in the occasion of spherical shape of drug carrier, if n is smaller than 0.43. In addition, anomalous transport mechanism is followed, if there n is between 0.43 and 0.85. Besides, the release mechanism called Case-II occurred, if n is greater than 0.85 [116]. As shown in the Figure 4.7, the calculated numerical value of n for each of the PVL microsphere combinations are less than 0.43. Therefore, a diffusion release mechanism called Fickian is valid for all [117]. Additionally, this research demonstrates that the primary release system of the microsphere combinations was unaffected by the alterations in the pH of the release ambient. As a result, it was discovered that the mathematical model of Korsmeyer-Peppas worked effectively for every specimen and each pH ambients.

4.6 Synthesis of Poly(δ-valerolactone) Nanohybrid Microspheres With Immobilized Enzyme

The earlier studies indicated that δ-valerolactone combined with handmade immobilized CALB, exhibited ring opening polymerization in toluene media [17]. Unlike other studies, this one also investigated the effectiveness of immobilized CALB on δ-valerolactone to detect its impact on microsphere formation via nanohybrid system. In the earlier research, the maximum performance was attained at a fixed temperature of 80^{o}C [17]. In this study, PVL-nanohybrid was throughout 24 hours and at 80^{o}C polymerization period to get attain the greatest M_n value.

4.7 Fabrication of PVL Nanohybrid Microspheres

Due to its numerous pharmalogical upsides, as formerly described, the enzymatically synthesized PVL nanohybrid, which was generated for this study in biomedical uses, was formed into microspheres. The emulsion/solvent evaporation methodology is used to generate both drug-free and TC-loaded PVL nanohybrid microsphere structures. Several microsphere formulations were generated in the earlier research to examine the impact of process factors [99]. As it was previously pointed out, PVA at different concentrations (0.1, 0.5, 1 (w/v) %) were the exterior phase of the microsphere

compositions and were examined and compiled. Since the enhanced viscosity limits drug diffusion into the exterior phase, the findings displayed that a 1 (w/v) % PVA concentration in the exterior phase heightened encapsulation efficiency [99]. As a result, in this study, microspheres were generated with an exterior phase, which is PVA concentration of 1 (w/v) %. The impact of the interior phase concentration was additionally investigated in the prior research [99]. As stated in Table 4.4, multiple TC ratios on PVL nanoybrid were further investigated in this study.

Experiments were conducted with 25 mg, 50 mg and 100 mg PVL nanohybrid amounts (40% = 25 mg, 20% = 50 mg and 10% = 100 mg amounts), with the drug mass generally held fixed at 10 mg. Simultaneously, nanohybrid microspheres were generated as drug-free and TC-loaded. Equation 3.1 was employed to identify encapsulation efficiency (%). The microspheres formed at a 10% TC:PVL nanohybrid ratio with 1 (w/v)% PVA concentration (specimen C-2) were found to have the greatest encapsulation efficiency (%), as demonstrated in Table 4.4.

Table 4.4 : PVA concentrations, PVL nanohybrid microsphere formulations, encapsulation efficiencies, loading capacities, mean particle diameters.

Sample Code	PVA concentration (%)	TC:PVL nanohybrid ratio (%)	Encapsulation Efficiency (%)[1]	Loading Capacity (%)	Mean Particle Diameter (μm)[2]
A-1	1	0	-	-	27.3 ± 10.4
A-2	1	20	78.0 ± 9.3	13.0 ± 1.6	32.2 ± 15.0
B-1	0.5	0	-	-	19.9 ± 6.8
B-2	0.5	20	71.6 ± 7.3	11.9 ± 1.2	26.3 ± 10.2
C-1	1	0	-	-	17.8 ± 4.9
C-2	1	10	82.7 ± 6.4	7.5 ± 0.6	28.8 ± 16.9
D-1	0.5	0	-	-	19.4 ± 9.0
D-2	0.5	10	65.7 ± 5.8	6.0 ± 0.5	28.4 ± 9.4
E-1	0.5	0	-	-	14.2 ± 5.9
E-2	0.5	40	78.8 ± 6.2	22.5 ± 1.8	23.8 ± 7.1
F-1	1	0	-	-	19.9 ± 11.1
F-2	1	40	61.3 ± 3.2	17.5 ± 0.9	23.5 ± 7.6
G-1	0.1	0	-	-	15.1 ± 6.1
G-2	0.1	20	68.6 ± 9.4	11.4 ± 1.6	28.0 ± 12.2
H-1	0.1	0	-	-	19.1 ± 6.6
H-2	0.1	10	75.3 ± 1.3	6.8 ± 0.1	22.8 ± 10.0
I-1	0.1	0	-	-	14.4 ± 5.7
I-2	0.1	40	79.9 ± 5.9	22.8 ± 1.7	13.7 ± 6.0

[1]Calculated from Equation 3.1.
[2]Measured by particle size analyzer of SEM instrument (mean±SD; n=58-76)

It was shown that raising PVL nanohybrid amounts, in other words, decreasing TC:PVL nanohybrid ratio at the constant concentration of PVA (1%) improved the

encapsulation efficiency. Besides, at the constant PVA concentrations (0.1% and 0.5%), it was pointed out that raising PVL nanohybrid amounts made the encapsulation efficiency almost unchanged.

Moreover, it was seen that with the constant amounts of PVL nanohybrid (when the TC:PVL nanohybrid ratios are 40%), increasing the PVA concentration (%) made the encapsulation efficiency lower. However, with the constant amount of PVL nanohybrid (when the TC:PVL nanohybrid ratio is 20%), raising PVA concentration (%) made the encapsulation efficiency reduced. Yet, with the constant amount of PVL nanohybrid(when the TC:PVL nanohybrid ratio is 10%), raising PVA concentration (%) made the encapsulation efficiency almost unvaried.

The one significant factor influencing the encapsulation efficiency is the particle size. The mean particle size diameters varied between 13.7 – 32.2 μm. When the PVA concentration was decreased from 0.5% to 0.1% with the constant amount of PVL nanohybrid (when the TC:PVL nanohybrid ratio is 40%), it was seen that particle size of the microspheres became smaller (from 23.8 ± 7.1 μm to 13.7 ± 6.0 μm). When the PVA concentration was decreased from 1% to 0.5% with the constant amount of PVL nanohybrid (when the TC:PVL nanohybrid ratio is 20%), it was seen that particle size of the microspheres also became smaller (from 32.2 ± 15.0 μm to 26.3 ± 10.2 μm). Besides, in general, it seems that the particle size of the TC-loaded PVL nanohybrid microspheres became more larger than drug-free PVL nanohybrid microspheres.

Furthermore, larger particles formed as a result of the interior phase being more viscous thanks to an increase in polymer concentration [108]. Especially, at constant PVA concentration of 0.5%, with the increase of PVL nanohybrid amount (when the TC:PVL nanohybrid ratio decreased from 40% to 10%), the particle size was elevated from 23.8 ± 7.1 μm to 28.4 ± 9.4 μm. In addition, at constant PVA concentration of 1%, with the increase of PVL nanohybrid amount (when the TC:PVL nanohybrid ratio decreased from 40% to 20%), the particle size was elevated from 23.5 ± 7.6 μm to 32.2 ± 15.0 μm.

The diffusion of the encapsulated drug from the matrix system is facilitated by enhancing porosity of the microshere. In the earlier research, it was shown that the drug was released more quickly from the smaller microsphere [109]. Due to their tiny spherical size, microspheres can possibly be inserted into the body with simplicity.

This kind of therapeutic insertation will increase bioavailability and reduce the likehood side effects. That is why, smaller particle size is the preferred parameter for the controlled drug release systems [109].

4.8 Characterization of PVL Nanohybrid Microspheres

The chemical and mechanical characteristics of the fabricated PVL nanohybrid, TC-loaded PVL nanohybrid microspheres, drug-free PVL nanohybrid microspheres were examined by using SEM, FT-IR, DSC, TGA and XRD analyses.

4.8.1 SEM results of PVL nanohybrid microspheres

The samples codes, different PVA concentrations and TC:PVL nanohybrid ratios can be seen from Table 4.5.

Table 4.5 : Sample codes, PVA concentrations and TC ratios in order to PVL nanohybrid.

Sample Code	PVA concentration (%)	TC:PVL nanohybrid ratio (%)
A-1	1	0
A-2	1	20
B-1	0.5	0
B-2	0.5	20
C-1	1	0
C-2	1	10
D-1	0.5	0
D-2	0.5	10
E-1	0.5	0
E-2	0.5	40
F-1	1	0
F-2	1	40
G-1	0.1	0
G-2	0.1	20
H-1	0.1	0
H-2	0.1	10
I-1	0.1	0
I-2	0.1	40

As shown in Figure 4.8, a multitude of scanning electron microscope images were employed to evaluate the shape of the microspheres and identify the particle size. Every formulation of microspheres resulted in a shpherical form. As expected for a solvent evaporation methodology, drug-free and TC-loaded PVL nanohybrid microspheres had a spherical form and a porous surface [82].

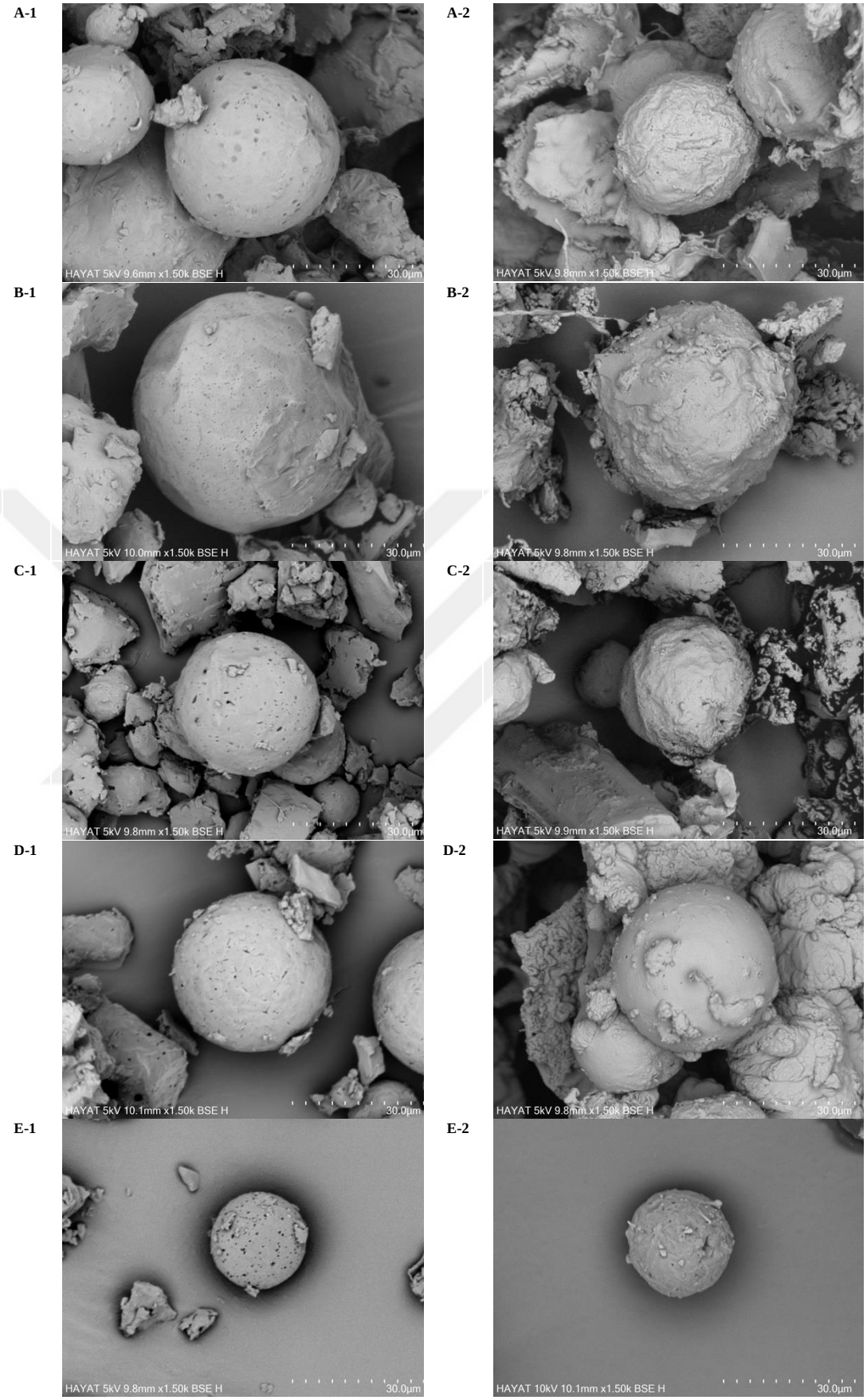

Figure 4.8 : SEM images of : Drug-free and TC-loaded PVL nanohybrid microspheres (Magnification 1500x, scale bar 30 µm).

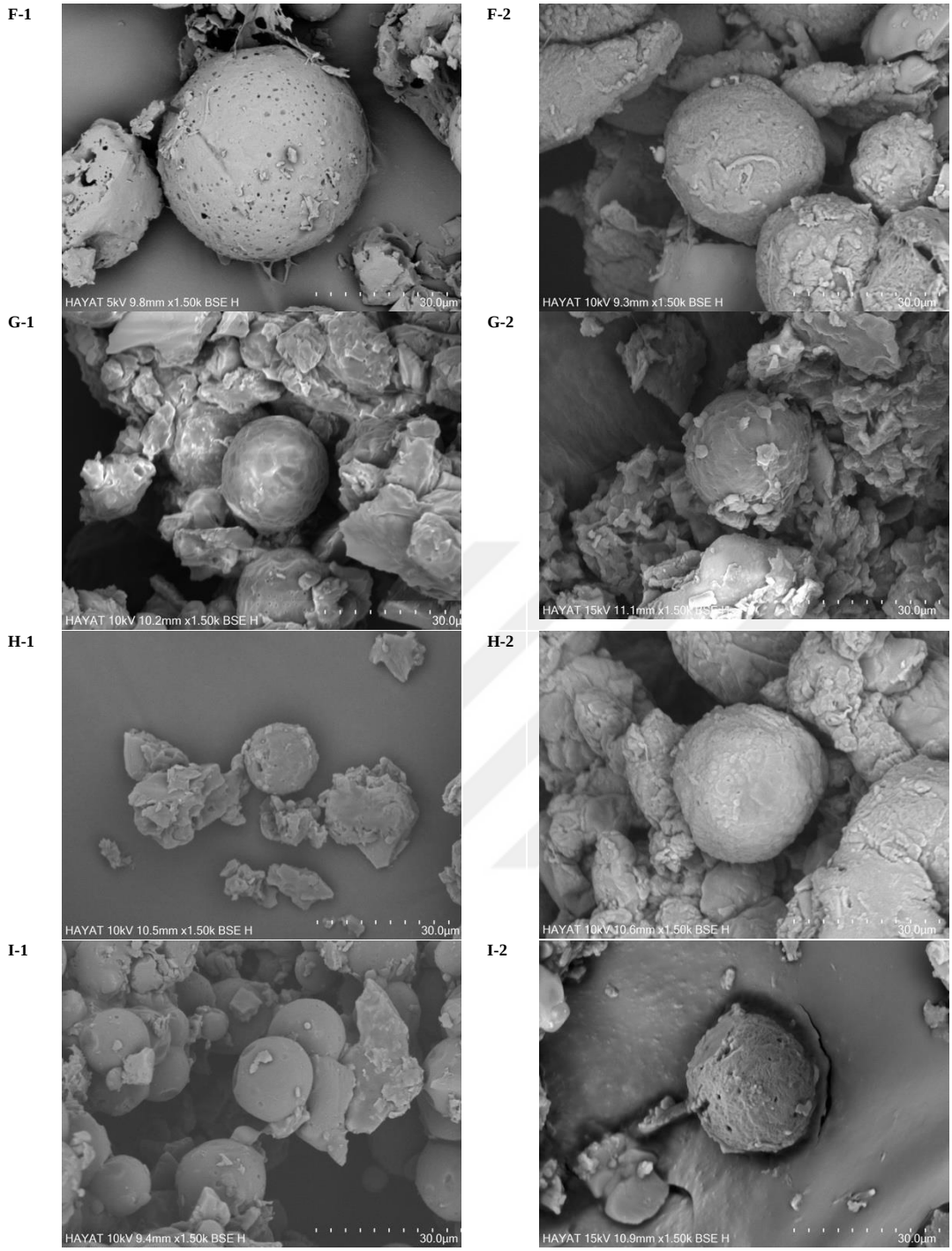

Figure 4.8 (continued) : SEM images of : Drug-free and TC-loaded PVL nanohybrid microspheres (Magnification 1500x, scale bar 30 µm).

4.8.2 FT-IR results of PVL nanohybrid microspheres

FT-IR analysis was implemented to additional characterize PVL nanohybrid, drug-free PVL nanohybrid microspheres, TC-loaded PVL nanohybrid microspheres and TC. The FT-IR spectra of these specimens could be seen from Figure 4.9. The asymmetrical and symmetrical CH_2 groups in the structure of the synthesized PVL nanohybrid have peaks of 2957 cm^{-1} and 2880 cm^{-1}. Also, the C=O streching in the

PVL nanohybrid structure have peaks of 1724 cm^{-1}, the C-O and C-C bonds have peaks of 1254 cm^{-1} and the symmetrical C-O-C bonds have peaks of 1169 cm^{-1}. Besides, both drug-free and TC-loaded PVL nanohybrid microspheres exhibit all of these distinctive peaks, which are consistent with the previous researches [17,68].

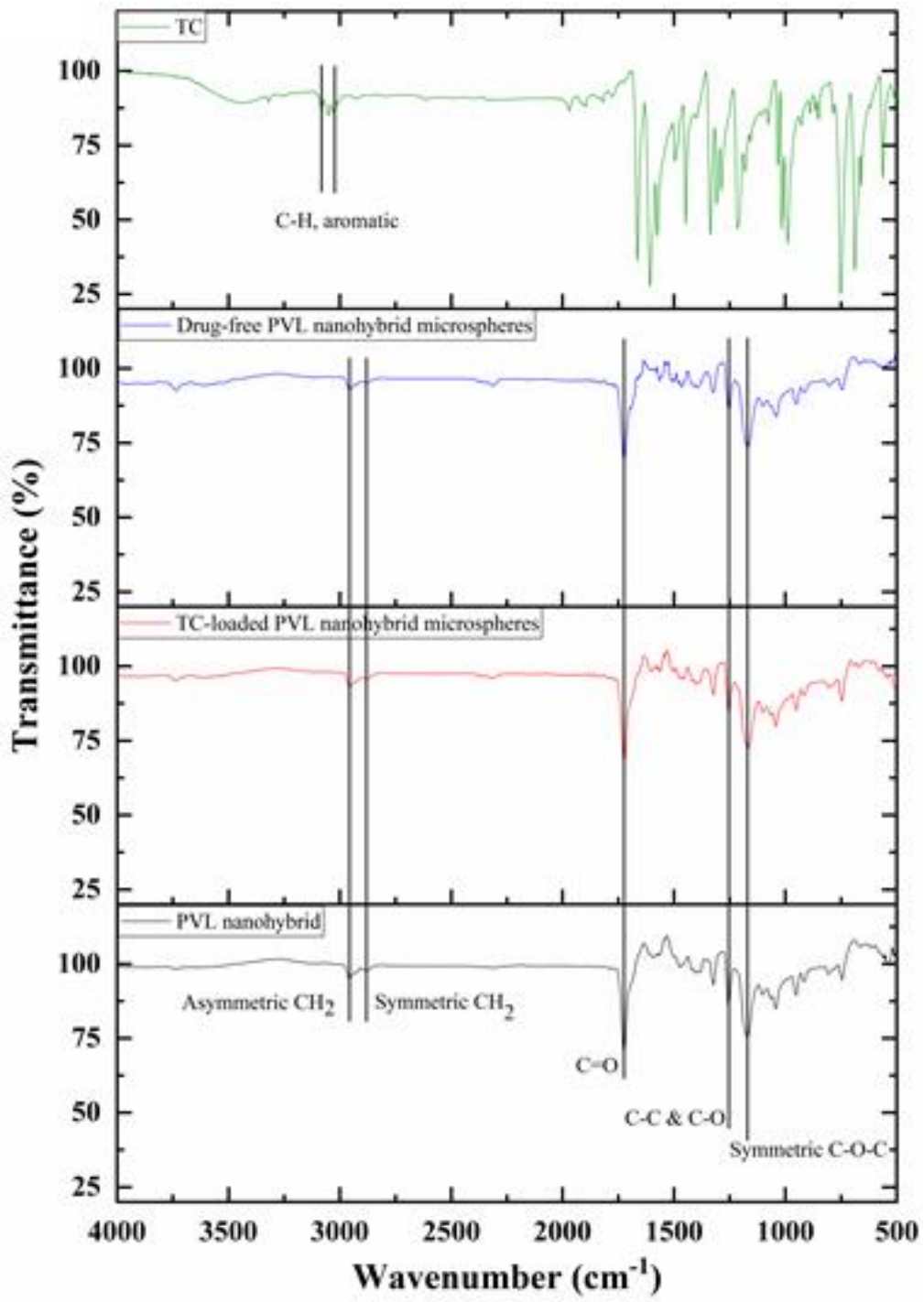

Figure 4.9 : FT-IR spectra of TC, drug-free PVL nanohybrid microspheres, TC-loaded PVL nanohiybrid microspheres, PVL nanohybrid.

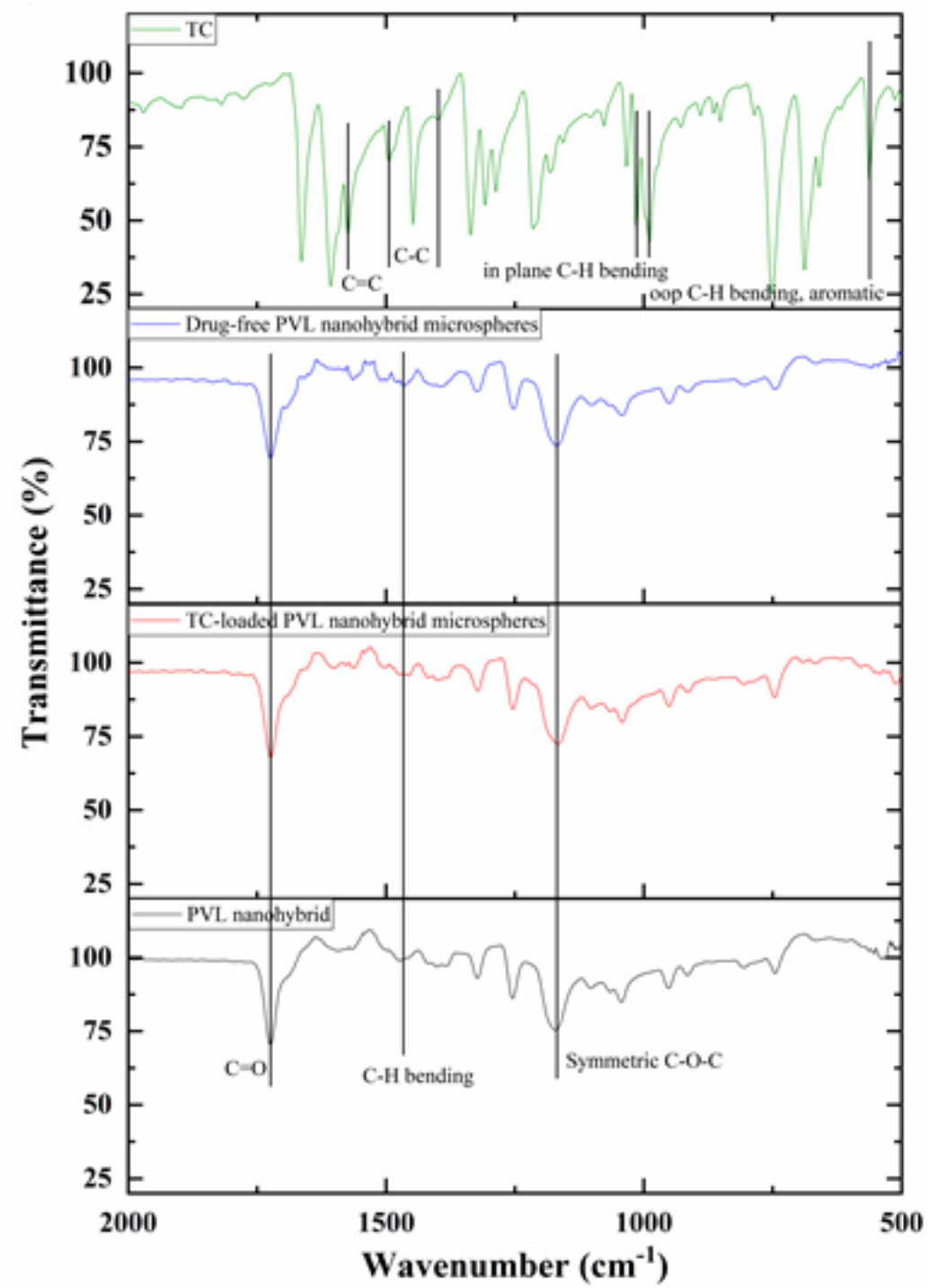

Figure 4.9 (continued) : FT-IR spectra of TC, drug-free PVL nanohybrid microspheres, TC-loaded PVL nanohiybrid microspheres, PVL nanohybrid.

The peaks of C-H bending at 1467 cm^{-1} and symmetric C-O-C bond at 1169 cm^{-1} also observed in the drug-free and TC-loaded PVL nanohybrid microspheres, like in the structure of the PVL nanohybrid. In the spectra of TC, the peaks have shown at 1663 cm^{-1} because of the α, β unsaturation in ketones of the drug, at 675-900 cm^{-1} because of aromatic oop C-H bending, at 3025-3084 cm^{-1} because of aromatic C-H bond, and

in addition, at 1607 cm^{-1} and 1575 cm-1, due to the stretching of C=C and C=O, respectively [99]. When it was compared the spectra of TC and TC-loaded PVL nanohybrid microspheres, it is clearly said that the spectras are looking alike without any signicant difference. It means that TC is successfully encapsulated in the structure of PVL nanohybrid microspheres.

4.8.3 DSC results of PVL nanohybrid microspheres

Drug-free PVL nanohybrid microspheres and after TC were added into them, the thermochemical alterations in the PVL nanohybrid structure were observed by using DSC analysis. The specimens' temperatures of melting are demonstrated by the DSC plots in Figure 4.10.

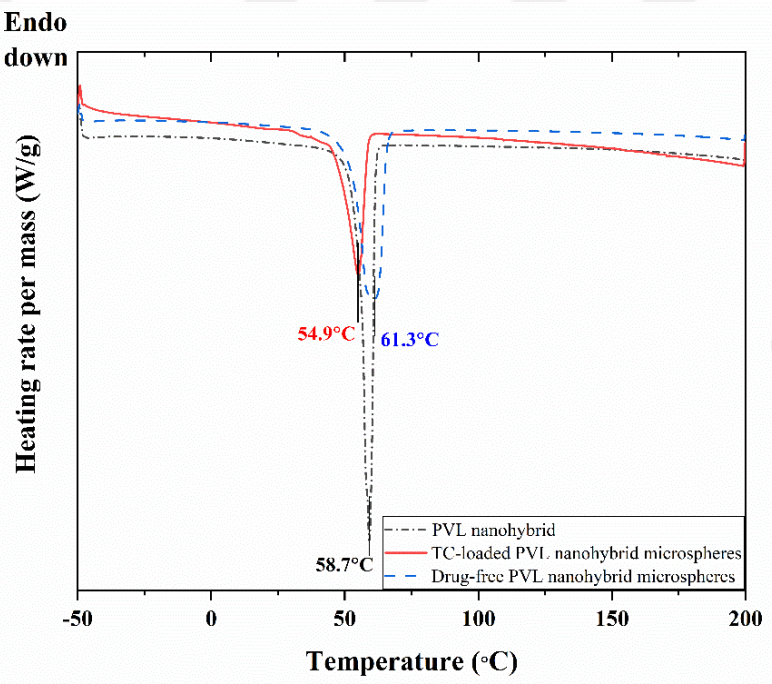

Figure 4.10 : Melting temperatures of the specimens: DSC melting endotherm, PVL nanohybrid, TC-loaded PVL nanohybrid microspheres, drug-free PVL nanohybrid microspheres.

The T_m value of the PVL nanohybrid is 58.7°C. It can be seen that the measured T_m data of the drug-free PVL nanohybrid microspheres are close to this data.

From the regions beneath the melting peaks, the entalphy values of PVL nanohybrid, TC-loaded PVL nanohybrid microspheres and drug-free PVL nanohybrid microspheres were determined to be 99.1 J/g, 57.0 J/g and 89.4 J/g, respectively. Table 4.6 displays the computed results. With loaded TC, it can be claimed that the melting temperature and entalphy values decreased.

Table 4.6 : T_m and enthalpy values of PVL nanohybrid, TC-loaded PVL nanohybrid microspheres and drug-free PVL nanohybrid microspheres.

	T_m (℃)	ΔH_m (J/g)
PVL nanohybrid	58.7	99.1
TC-loaded PVL nanohybrid microspheres	54.9	57.0
Drug-free PVL nanohybrid microspheres	61.3	89.4

The melting temperature of the industrial TC was found to be 59^{o}C in the prior research [99]. Since there is not any second melting peak on the DSC curve of the TC-loaded PVL nanohybrid microspheres, it can be said that TC is sufficiently molecularly dispersed in the TC-loaded PVL nanohybrid microspheres [110]. In this case, as it was shown in the another previous study, no addional melting peak close to drug's melting point means TC's surface morphology is amorphous [111]. Besides, since the melting temperature of TC-loaded PVL nanohybrid microspheres (T_m : 54.9^{o}C) are less than the melting temperatures of both PVL nanohybrid (T_m : 58.7^{o}C) and TC (T_m : 59^{o}C), it can be said that there is an eutectic system was occurred [99].

4.8.4 TGA results of PVL nanohybrid microspheres

The thermal decomposition profiles of drug-free PVL nanohybrid microspheres and TC-loaded PVL nanohybrid microspheres in comparison to PVL nanohybrid was examined by using TGA analysis. The temperature change leads to weight losses. Hence, absorption, adsorption, vaporization, sublimation, decomposition are among the thermal processes that TGA is primarily used to examine [112]. In this analysis, weight changes of the three specimens were deducted. According to the curves in Figure 4.11, PVL nanohybrid started to decompose at approximately 30^{o}C.

The specimen of PVL nanohybrid showed two steps of degradation. Its primarily degradation was at 346.1^{o}C with 58.2% weight loss. The secondary degradation of the PVL nanohybrid was at 499.2^{o}C, where it decomposed as 19.2%. With the exception of water/solvent evaporation interval, the specimens of drug-free and TC-loaded PVL nanohybrid microspheres both degraded in three steps. The primarily degradation of TC-loaded PVL nanohybrid microspheres was at 256.6^{o}C with 27.8% weight loss. This temperature (256.6^{o}C) is less than first degradation of PVL nanohybrid (346.1^{o}C) and drug-free PVL nanohybrid microspheres (347.7^{o}C), due to addition of TC. This suggests that the degradation temperature is lowered by an incorporation of additional substances [113]. Compared to drug-free PVL nanohybrid microsphere-specimen, TC-

loaded microsphere-specimen's initial degrading step began more promptly and took place over a larger temperature span.

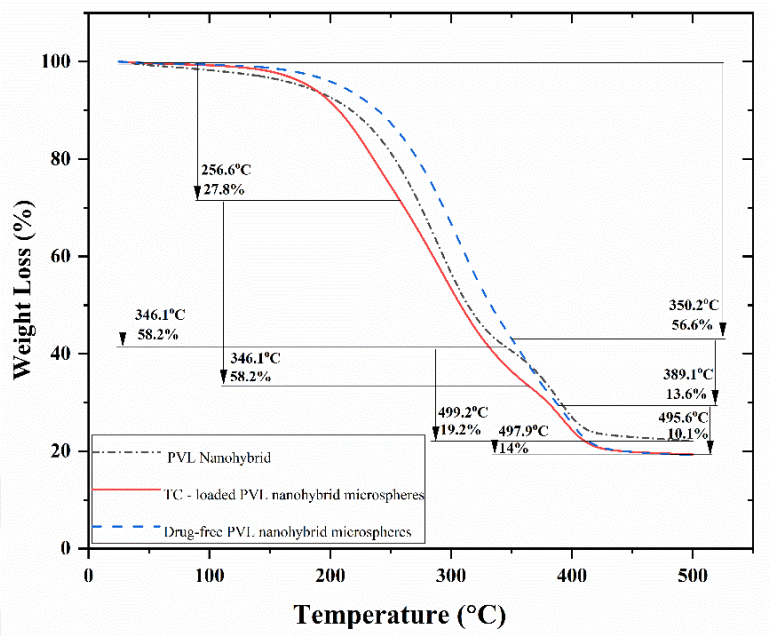

Figure 4.11 : TGA and derivative of weight losses results; PVL nanohybrid (black), TC-loaded PVL nanohybrid microspheres(red), drug-free PVL nanohybrid microspheres (blue).

4.8.5 XRD results of PVL nanohybrid microspheres

By using XRD analysis, the impact of the TC-loading on the crystalline structures and crystallinity of nanohybrid microspheres were examined. The diffaction peaks can be seen from Figure 4.12.

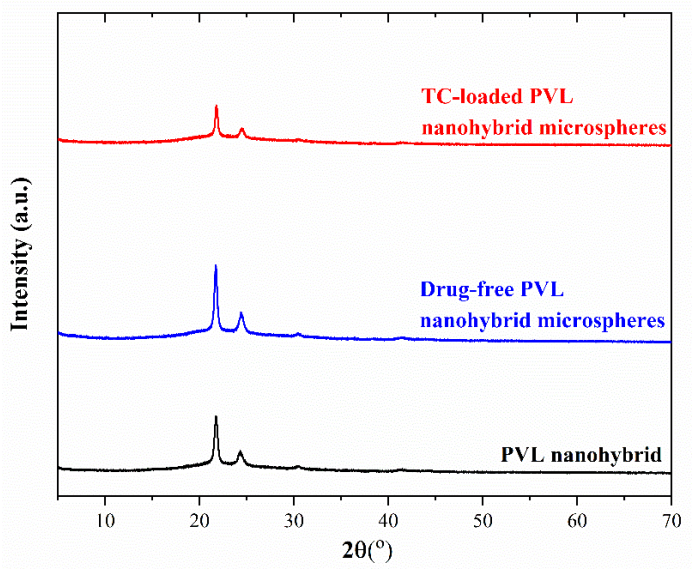

Figure 4.12 : XRD measurement of : TC-loaded PVL nanohybrid microspheres (red), Drug-free PVL nanohybrid microspheres (blue), PVL nanohybrid (black).

Two unique diffraction peaks at $2\theta = 21.8^{o}$ and 24.4^{o} were seen in PVL nanohybrid, TC-loaded PVL nanohybrid microsphere-specimen and drug-free PVL nanohybrid microsphere-specimen; they assigned to the PVL nanohybrid. Following TC-loading, it was seen that the intensities of the distintive crystalline peaks went down. The pattern gets noisier as the crystalline peak's intensity value reduces. In other words, crystallinity is thus diminishes.

4.8.6 pH dependent drug release of PVL nanohybrid microspheres

The drug release mechanism is significantly influenced by the properties of the release media. Among these characteristics is pH, which was investigated in relation to microsphere release. As demonstrated in Figure 4.13, two unique pH levels are were used in this research to simulate the contexts of different bodily parts while examining the release behaviour of varying concentration of PVL nanohybrid in the TC-loaded PVL nanohybrid microspheres at pH 5.6 and pH 7.4 . While pH 7.4 represent healthy body, pH 5.6 represents cancer cell [114].

At the constant PVA concentration of 1% and TC amount (10 mg), different amounts of PVL nanohybrid (25 mg, 50 mg, 100 mg) were used to form microspheres, as it was previously mentioned.

To begin with, the first burst release was noted to have taken place over the first 6 hours for pH 7.4. At this pH value, For the TC:PVL nanohybrid ratio of 10%, initial burst release was examined as 7.9 ± 1.3 (%), while the initial burst release was examined as 6.0 ± 0.7 (%) for the TC:PVL nanohybrid ratio of 20%, and 4.7 ± 2.1 (%) for the TC:PVL nanohybrid ratio of 40%. It means, the initial burst release with 10% of TC:PVL nanohybrid ratio has shown higher rate than the other ratios. These three distinct PVL nanohybrid microspheres formed with varying ratio of PVL nanohybrid were found to have equivalent release patterns. There was a burst release at the beginning of the drug release behaviour, followed by a steady release. The results of the 744-hour drug release studies showed that PVL nanohybrid microspheres formed with 10% TC:PVL nanohybrid ratio have the highest release percentage at 39.4 ± 5.0 (%). The remaining two specimens' cumulative release percentages are 15.3 ± 2.5 (%) with TC:PVL nanohybrid ratio of 20% and 16.3 ± 0.7 (%) with TC:PVL nanohybrid ratio of 40%. These findings indicate that the most ideal formulation for TC-loaded PVL nanohybrid microspheres is 10% ratio of TC:PVL nanohybrid.

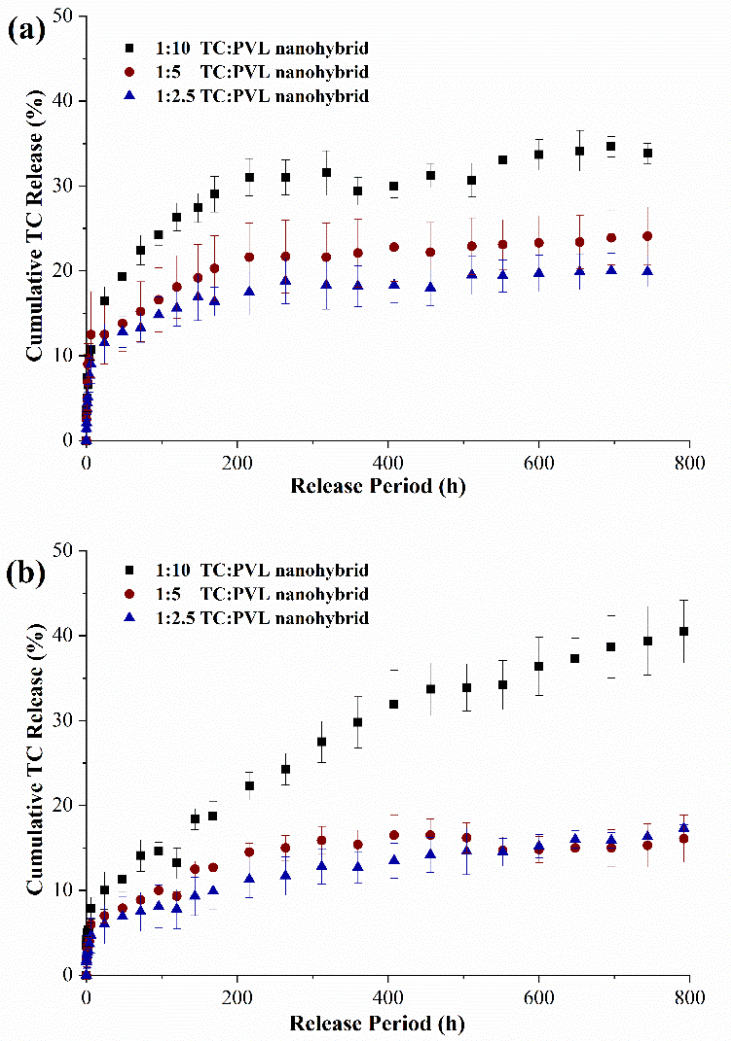

Figure 4.13 : Effect of PVL nanohybrid concentration on cumulative TC release (%) in two different pH media (pH 5.6 and pH 7.4, respectively).

The second of all, the first burst release was noted to have taken place over the first 6 hours for pH 5.6. At this pH value, For the TC:PVL nanohybrid ratio of 10%, initial burst release was examined as 10.8 ± 1.3 (%), while the initial burst release was examined as 12.5 ± 5.1 (%) for the TC:PVL nanohybrid ratio of 20%, and 9.0 ± 2.2 (%) for the TC:PVL nanohybrid ratio of 40%. It means, the initial burst release with 10% of TC:PVL nanohybrid ratio has shown higher rate than the other ratios. These three distinct PVL nanohybrid microspheres formed with varying ratio of PVL nanohybrid were also found to have equivalent release patterns like pH 7.4 plots. There was a burst release at the beginning of the drug release behaviour, followed by a steady release. The results of the 744-hour drug release studies showed that PVL nanohybrid microspheres formed with 10% TC:PVL nanohybrid ratio have the highest release percentage at 34.2 ± 12.8 (%). The remaining two specimens' cumulative release percentages are 24.1 ± 3.4 (%) with TC:PVL nanohybrid ratio of 20% and 19.9 ± 1.8

(%) with TC:PVL nanohybrid ratio of 40%. These findings pointed that the most ideal formulation for TC-loaded PVL nanohybrid microspheres is 10% ratio of TC:PVL nanohybrid like it was found in the pH 7.4 results.

It can be inferred from a comparison of drug release profiles at two pH values that the release percentages at pH 7.4 are greater than those at pH 5.6. In pH 5.6, it was discovered that TC-loaded PVL microspheres with the 10% ratio of TC:PVL nanohybrid exhibited a greater burst release rate. One may argue that the pH 7.4 media enables for a more controlled release of these specimens.

4.9 Kinetic Modelling and Release Mechanism for PVL Nanohybrid Microspheres

To gain additional insight into the drug release mechanism for every specimen, as detailed in section 3.2.7, the drug release patterns are fitted to two kinetic models, named the Higuchi and Korsmeyer-Peppas models of math. The computed variables for the fitted kinetic model are displayed in Figure 4.14.

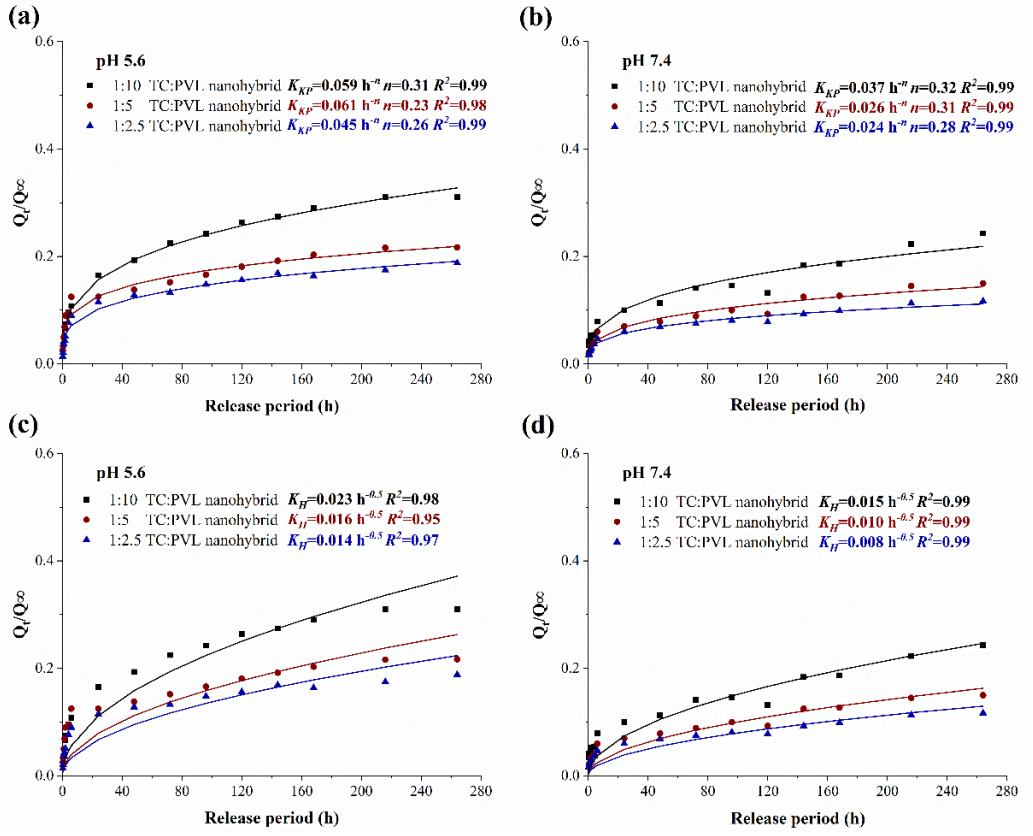

Figure 4.14 : Kinetic modelling and calculations of release mechanisms in two different pH media (pH 5.6 and pH 7.4) with TC-loaded PVL nanohybrid microspheres.

The correlation coefficient of the Korsmeyer-Peppas model was greater ($R^2 > 98$) in comparison to other kinetic model. The release exponent (n) in the model of Korsmeyer-Peppas provides information about drug release profile. It is derived from the linearized equation's (Equation 3.4) slope [115]. A diffusion release mechanism called Fickian is inferred in the occasion of spherical shape of drug carrier, if n is smaller than 0.43. In addition, anomalous transport mechanism is followed, if there n is between 0.43 and 0.85. Besides, the release mechanism called Case-II occurred, if n is greater than 0.85 [116]. As shown in the Figure 4.14, the calculated numerical value of n for each of the PVL nanohybrid microsphere combinations are less than 0.43. Thus, a diffusion release mechanism called Fickian is valid for all [117]. Additionally, this research demonstrates that the primary release system of the microsphere combinations was unaffected by the alterations in the pH of the release ambient. In summary, it was discovered that the mathematical model of Korsmeyer-Peppas worked effectively for every specimen and each pH ambients.

5. CONCLUSSION AND RECOMMENDATIONS

This research could be summarized by three main subjects. Physical adsorption was employed in the first part to immobilize lipase on surface-modified RHA. The silica based material underwent surface modification when amine groups were added to its surface by utilizing 3-aminopropyltriethoxysilane. As stated before, physical adsorption was used to immobilize the free form of *Candida antarctica* lipase B [16]. By using the monomer ratios from prior study, poly(δ-valerolactone) and poly(δ-valerolactone) nanohybrid were generated by enzymatic ring opening polymerization in the second part. The reactions are conducted at 80^{o}C for 24 hours to get the highest molecular mass for both polymer and nanohybrid. These resultant materials were ultimately found to be applied in the fabrication of microspheres. As following, the methodology of O/W emulsion was employed to fabricate TC-loaded PVL microspheres, TC-loaded PVL nanohybrid microspheres, drug-free PVL microspheres and drug free PVL nanohybrid microspheres. Afterwards, drug release mechanism of these fabricated microspheres were investigated. For this investigation, with three different PVA concentrations (0.1, 0.5, 1 (w/v)%), three different TC:PVL ratios (10, 20, 40%) and TC:PVL nanohybrid ratios (10, 20, 40%) have been evaluated in order to ascertain greatest encapsulation efficiency, and thereby drug release profile. To define the thermal and chemical properties, TGA, DSC, SEM and XRD were applied to these microspheres. As it can be seen from Table 4.1 and 4.4, the greatest encapsulation efficiencies were observed with specimen A-2 (1% PVA and 20% ratio of TC:PVL) as 98.6 ± 8.4 (%) and specimen C-2 (1% PVA and 20% ratio of TC:PVL nanohybrid) as 82.7 ± 6.4 (%). The lowest encapsulation efficiencies were observed with specimen I-2 (0.1% PVA and 40% ratio of TC:PVL) as 54.1 ± 2.2 (%) and specimen F-2 (1% PVA and 40% ratio of TC:PVL nanohybrid) as 61.3 ± 3.2 (%). The second greatest encapsulation efficiencies were observed with specimen B-2 (0.5% PVA and 20% ratio of TC:PVL) as 83.6 ± 3.8 (%) and specimen I-2 (0.1% PVA and 40% ratio of TC:PVL nanohybrid) as 79.9 ± 5.9 (%). It was shown that raising PVL amounts, in other words, decreasing TC:PVL ratio from 40% to 20%, at the constant concentration of PVA (1%, 0.5% and 0.1%) improved the encapsulation efficiency.

Moreover, it was seen that with the conctant amounts of PVL (when the TC:PVL ratios are 40% and 20%), increasing the PVA concentration (%) made the encapsulation efficiency higher. Besides, it was shown that raising PVL nanohybrid amounts, in other words, decreasing TC:PVL nanohybrid ratio at the constant concentration of PVA (1%) improved the encapsulation efficiency. This research also demonstrates that drug release mechanisms are not affected majorly by the pH-changes. The DSC analysis shows that addition of TC into microspheres has lowered the melting points but there were no any extra TC-peak on the curves, so it is concluded that TC is successfully encapsulated and molecularly dispersed into PVL microspheres and PVL nanohybrid microspheres. The eutectic system was observed for both PVL microspheres and PVL nanohybrid microspheres.

TGA analyses were used to compare the thermal degradation pattern of drug-free and TC-loaded PVL microspheres with PVL. Additionally, TGA analyses were used to compare the thermal degradation pattern of drug-free and TC-loaded PVL nanohybrid microspheres with PVL nanohybrid. Decompositions and weight losses have been evaluated and interpreted based on the scientific literature and the analyses that were conducted. The chemical groups that indicate the existence of TC, PVL, TC-loaded PVL microspheres, drug-free PVL microspheres, PVL nanohybrid, TC-loaded PVL nanohybrid microspheres, and drug-free PVL nanohybrid microspheres were all observed by using FT-IR as characterization technique. In the sections of 4.3.2 and 4.8.2, each of the distinctive peaks were analyzed and described. TC was determined to be encapsulated within the microspheres. XRD analyses were used besides to several other characterizations to investigate the impact of TC loading on the crystalline structures and the crystallinity of microspheres. The characteristic peaks were examined. The SEM images reveal that every single one of the microsphere formulations had spherical shape. To observe the drug release behaviour of the microspheres fabricated in various surroundings, pH-dependent drug release investigations were conducted in the present research by employing two pH levels that were 5.6 and 7.4. The total cumulative release of TC was enhanced by the PVL microsphere formulations, reaching 42.1% in pH 7.4 ambient and 43.5% in pH 5.6 ambient. It is evident that the pH 5.6 release percentages are considerably greater than the pH 7.4 release percentages when compared to the drug release behaviours at two pH levels. It was demonstrated that PVL microspheres fabricated with a 10% TC:PVL

ratio exhibited a greater burst release rate in a pH 7.4 ambient. Moreover, the total cumulative release of TC was enhanced by the PVL nanohybrid microsphere formulations, reaching 39.4% in pH 7.4 ambient and 34.2% in pH 5.6 ambient. It is evident that the pH 7.4 release percentages are considerably greater than the pH 5.6 release percentages when compared to the drug release behaviours at two pH levels. It was demonstrated that PVL nanohybrid microspheres fabricated with a 10% TC:PVL nanohybrid ratio exhibited a greater burst release rate in a pH 5.6 ambient. The TC release was conducted for an overall duration of 744 hours in each case. Finally, the release kinetics were examined. The release was found to be compatible with the kinetic model of Korsmeyer-Peppas. This mathematical model had a greater correlation coefficient ($R^2 > 94$ for PVL microspheres and $R^2 > 98$ for PVL nanohybrid microspheres) than the other mathematical model of Higuchi, when the release rate constants were evaluated. Furthermore, it was discovered that the kinetic model of Korsmeyer-Peppas worked well with all samples and pH levels. All microsphere formulations had TC release that was controlled by Fickian diffusion, according to the calculated n value. In conclusion, the goal of this study is to develop new controlled drug delivery systems by integrating a transchalcone into biological in origin polymeric carriers. A biocompatible, environmentally friendly, high-molecular-weight polymer and nanohybrid containing home-made immobilized enzymes that are compatible for human body will be produced in order to fabricate microspheres. Transchalcone will be incorporated with the polymer and nanohybrid generated by biocatalyst for use in therapy. Following the completion of all characterization tests and investigation of drug release profiles, it can be clearly said that this research's findings suggest that PVL microsheres or PVL-nanohybrid microspheres may find implementation in prolonged therapeutic applications.

REFERENCES

[1] **George, A., Sanjay, M. R., Srisuk, R., Parameswaranpillai, J., & Siengchin, S.** (2020). A comprehensive review on chemical properties and applications of biopolymers and their composites. *International Journal of Biological Macromolecules, 154*, 329–338. https://doi.org/10.1016/j.ijbiomac. 2020.03.120.

[2] **Bilal, M., & Iqbal, H. M. N.** (2019). Naturally-derived biopolymers: Potential platforms for enzyme immobilization. *International Journal of Biological Macromolecules, 130*, 462–482. https://doi.org/10.1016/ j.ijbiomac.2019.02.152.

[3] **Asri, N. A., Sezali, N. A. A., Ong, H. L., Mohd Pisal, M. H., Lim, Y. H., Fang, J.** (2024). Review on Biodegradable Aliphatic Polyesters: Development and Challenges. *Macromolecular Rapid Communications*, *45*(23), 2400475. https://doi.org/10.1002/marc.202400475.

[4] **Zhao, H.** (2019). Enzymatic polymerization to polyesters in nonaqueous solvents. In *Methods in Enzymology* (Vol. 627, pp.1-21). Elsevier Inc. https://doi.org/10.1016/bs.mie.2019.03.002.

[5] **Hevilla, V., Sonseca, A., Echeverría, C., Muñoz-Bonilla, A., & Fernández-García, M.** (2021). Enzymatic synthesis of polyesters and their bioapplications: Recent advances and perspectives. *Macromolecular Bioscience, 21*(10), 2100156. https://doi.org/10.1002/mabi.202100156.

[6] **Kobayashi, S.** (2009). Recent developments in lipase-catalyzed synthesis of polyesters. *Macromolecular Rapid Communications*, *30*(4-5), 237–266. https://doi.org/10.1002/marc.200800690.

[7] **Liu, Y., Song, L., Feng, N., Jiang, W., Jin, Y., & Li, X.** (2020). Recent advances in the synthesis of biodegradable polyesters by sustainable polymerization: lipase-catalyzed polymerization. *RSC Advances*, *10*, 36230–36240. https://doi.org/10.1039/d0ra07138b.

[8] **Santos, R. D., Rebelatto, E. A, Guindani, C., Madalosso, H. B., Scorsin, L., Mayer, D. A., & Oliveira, J. V.** (2025). Lipase-catalyzed synthesis of poly (ω-pentadecalactone-co-globalide) in supercritical carbon dioxide. *The Journal of Supercritical Fluids*, *215*, 106409. https://doi.org/10.1016/j.supflu.2024.106409.

[9] **Gkountela, C. I., & Vouyiouka, S. N.** (2022). Enzymatic polymerization as a green approach to synthesizing bio-based polyesters. *Macromol*, *2*(1), 30–57. https://doi.org/10.3390/macromol2010003.

[10] **Lu, Y., Lv, Q., Liu, B., & Liu, J.** (2019). Immobilized Candida antarctica lipase B catalyzed synthesis of biodegradable polymers for biomedical applications. *Biomaterials Science*, *7*(12), 4963–4983. https://doi.org/10.1039/c9bm00716d.

[11] **Shafi, S., Zafar, S., Sarwar, Z., Rasool, M. H., & Rasheed, T.** (2022). Organic–Inorganic Nanohybrids in Medicine. In Rizwan, K., Bilal, M., Rasheed, T. & Nguyen, T. A. (Eds.), *Hybrid Nanomaterials: Biomedical, Environmental and Energy Applications* (pp. 77-106). Springer Singapore. https://doi.org/10.1007/978-981-19-4538-0_5.

[12] **Fazal, T., Murtaza, B. N., Shah, M., Iqbal, S., Rehman, M., Jaber, F., Dera, A. A., Awwad, N. S. & Ibrahium, H. A.** (2023). Recent developments in natural biopolymer based drug delivery systems. *RSC Advances*, *13*, 23087–23121. https://doi.org/10.1039/d3ra03369d.

[13] **Peng, Y., Chen, L., Ye, S., Kang, Y., Liu, J., Zeng S., & Yu, L.** (2020). Research and development of drug delivery systems based on drug transporter and nano-formulation. *Asian Journal of Pharmaceutical Sciences*, *15*(2), 220–236. https://doi.org/10.1016/j.ajps.2020.02.004.

[14] **Dhaliwal, J. S., Moshawih, S., Goh, K. W., Loy, M. J., Hossain, M. S., Hermansyah, A., Kotra, V., Kifli, N., Goh, H. P., Dhaliwal, S. K. S., Yassin, H. & Ming, L. C.** (2022). Pharmacotherapeutics applications and chemistry of chalcone derivatives. *Molecules*, *27*(20), 7062. https://doi.org/10.3390/molecules27207062.

[15] **Santos, A. M., Carvalho Nascimento Júnior, J. A., Silva Cezar, S. V., Santana Júnior, C. C, Santos Oliveira, A. M., Picot, L., dos Passos Menezes, P., & Serafini, M. R.** (2024). Exploring the therapeutic potential and chemical properties of trans-chalcone: a comprehensive review. *Future Medicinal Chemistry*, *16*(23), 2547–2562. https://doi.org/10.1080/17568919.2024.2424148.

[16] **Ulker, C., Gokalp, N., & Guvenilir, Y.** (2016). Immobilization of Candida antarctica lipase B (CALB) on surface-modified rice husk ashes (RHA) via physical adsorption and cross-linking methods. *Biocatalysis Biotransformation*, *34*(4), 172–180. https://doi.org/10.1080/10242422.2016.1247818.

[17] **Ulker, C., Gok, Z., & Guvenilir, Y.** (2019). Performance Comparison of Commercial and Home-Made Lipases for Synthesis of Poly (δ-Valerolactone) Homopolymers. *Journal of Renewable Materials*, *7*(4), 335–343. https://doi.org/10.32604/jrm.2019.03819.

[18] **M., R. V., & Edison, L. K.** (2022). Safety issues, environmental impacts, and health effects of biopolymers. In Thomas, S., AR, A., Jose Chirayil, C. & Thomas, B. (Eds.), *Handbook of biopolymers* (pp. 1-27). Springer Singapore. https://doi.org/10.1007/978-981-16-6603-2_54-1.

[19] **Das, A., Ringu, T., Ghosh, S., & Pramanik, N.** (2023). A comprehensive review on recent advances in preparation, physicochemical characterization, and bioengineering applications of biopolymers. *Polymer Bulletin*, *80*, 7247–7312. https://doi.org/10.1007/s00289-022-04443-4.

[20] **Getahun, M. J., Kassie, B. B., & Alemu, T. S.** (2024). Recent advances in biopolymer synthesis, properties, & commercial applications: A review. *Process Biochemistry*, *145*, 261-287. https://doi.org/10.1016/j.procbio.2024.06.034.

[21] **Thomas, B., & Melethil, K.** (2023). Biopolymers: State of the Art and New Challenges. In Thomas, S., AR, A., Jose Chirayil, C., & Thomas, B. (Eds.), *Handbook of Biopolymers* (pp. 1–22). Springer Singapore. https://doi.org/10.1007/978-981-16-6603-2_1-1.

[22] **Jabeen, N., & Atif, M.** (2024). Polysaccharides based biopolymers for biomedical applications: A review. *Polymers for Advanced Technologies*, *35*(1), e6203. https://doi.org/10.1002/pat.6203.

[23] **Cherian, R. M., Varghese, R. T., Joy, J., Jose, C., & Thomas, S.** (2024). Synthetic Biopolymers: Properties, Fabrication, and Applications. In Reghunadhan, A., H., A. & Thomas, S. (Eds.), *Applications of Biopolymers in Science, Biotechnology, and Engineering* (pp. 31-56). John Wiley & Sons Inc. https://doi.org/10.1002/9781119783473.ch2.

[24] **Shi, C., Quinn, E. C., Diment, W. T., & Chen, E. Y.-X.** (2024). Recyclable and (Bio) degradable polyesters in a circular plastics economy. *Chemical Reviews*, *124*(7), 4393–4478. https://doi.org/10.1021/acs.chemrev.3c00848.

[25] **Sahu, P., Sharma, L., Dawsey, T., & Gupta, R. K.** (2024). Insight into the synthesis and thermomechanical properties of "short-long" type biobased aliphatic polyesters. *Journal of Applied Polymer Science*, *141*(8), e54972. https://doi.org/10.1002/app.54972.

[26] **Asri, N. A., Sezali, N. A. A., Ong, H. L., Mohd Pisal, M. H., Lim, Y. H., & Fang, J.** (2024). Review on Biodegradable Aliphatic Polyesters: Development and Challenges. *Macromolecular Rapid Communications*, *45*(23), 2400475. https://doi.org/10.1002/marc.202400475.

[27] **Mishra, N., Gandhi, R., & Vasava, D.** (2021). The thermo-mechanical and fluorescent properties of polyesters: a review. *Polymer Science, Series B*, *63*(6), 621–639. https://doi.org/10.1134/S1560090421060191.

[28] **Opriş, O., Mormile, C., Lung, I., Stegarescu, A., Soran, M.-L., & Soran, A.** (2024). An overview of biopolymers for drug delivery applications. *Applied Sciences*, *14*(4), 1383. https://doi.org/10.3390/app14041383.

[29] **Righetti, G. I. C., Faedi, F., & Famulari, A.** (2024). Embracing Sustainability: The World of Bio-Based Polymers in a Mini Review. *Polymers (Basel, Switzerland)*, *16*(7), 950. https://doi.org/10.3390/polym16070950.

[30] **Kim, S., Ga, S., Bae, H., Sluyter, R., Konstantinov, K., Shrestha, L. K., Kim, Y. H., & Ariga, K.** (2024). Multidisciplinary approaches for enzyme biocatalysis in pharmaceuticals: protein engineering, computational biology, and nanoarchitectonics. *EES Catalysis*, *2*(1), 14–48. https://doi.org/10.1039/d3ey00239j.

[31] **Freije García, F., & García Liñares, G.** (2024). Use of Lipases as a Sustainable and Efficient Method for the Synthesis and Degradation of Polymers. *Journal of Polymers and the Environment*, *32*, 2484–2516. https://doi.org/10.1007/s10924-023-03118-z.

[32] **Vardar-Yel, N., Tütüncü H. E., & Sürmeli Y.** (2024). Lipases for targeted industrial applications, focusing on the development of biotechnologically significant aspects: A comprehensive review of recent trends in protein engineering. *International Journal of Biological Macromolecules*, *273*(1), 132853. https://doi.org/10.1016/j.ijbiomac.2024.132853.

[33] **Eskandari, A., Leow, T. C, Rahman, M. B. A., & Oslan, S. N.** (2024). Recent insight into the advances and prospects of microbial lipases and their potential applications in industry. *International Microbiology*, *27*, 1597-1631. https://doi.org/10.1007/s10123-024-00498-7.

[34] **Alves, V., Furtado, G. F., & Alves Macedo, G.** (2024). Lipases as Biocatalysts for Enzymatic Interesterification. In Parisi, S. & Pereira, R. (Eds.), *Chemical and Enzymatic Interesterification for Food Lipid Production* (pp. 17-24). Springer Switzerland. https://doi.org/10.1007/978-3-031-67405-1_2.

[35] **Akram, F., Mir, A. S., Haq, I., Roohi, A.** (2023). An appraisal on prominent industrial and biotechnological applications of bacterial lipases. *Molecular Biotechnology*, *65*, 521–543. https://doi.org/10.1007/s12033-022-00592-z.

[36] **Fahim, Y. A., El-Khawaga, A. M., Sallam, R. M., Elsayed, M. A., & Assar, M. F. A.** (2024). A review on Lipases: sources, assays, immobilization techniques on nanomaterials and applications. *BioNanoScience*, *14*, 1780–1797. https://doi.org/10.1007/s12668-024-01319-x.

[37] **Shrestha, S., Sharma, S., Sahney, R., & Dahiya, P.** (2024). Candida antarctica lipases as an industrial biocatalyst for sustainable industrial applications. In *Enzyme Biotechnology for Environmental Sustainability* (pp. 497-512). Elsevier Inc. https://doi.org/10.1016/B978-0-443-22072-2.00007-3.

[38] **Benea, I. C., Dăescu, D., Todea, A., Nagy, L., Keki, S., Păușescu, I., Pellis, A. & Peter, F.** (2024). Efficient biotransformation of biobased raw materials into novel polyesters/polyesteramides; comparative investigation of enzymatic synthesis of block and random copolymers and terpolymers. *International Journal of Biological Macromolecules*, *282*(4), 137046. https://doi.org/10.1016/j.ijbiomac.2024.137046.

[39] **Rodríguez-Núñez, K., Bernal, C., & Bolívar, J. M.** (2023). The enzyme, the support, and the immobilization strategy: The key findings to a desirable biocatalyst. In *Biocatalyst Immobilization* (pp. 1-16). Elsevier Inc. https://doi.org/10.1016/B978-0-323-91317-1.00015-3.

[40] **Jiang, Y., Zheng, J., Wang, M., Xu, W., Wang, Y., Wen, L., & Dong, J.** (2024). Pros and cons in various immobilization techniques and carriers for enzymes. *Applied Biochemistry and Biotechnology*, *196*, 5633-5655. https://doi.org/10.1007/s12010-023-04838-7.

[41] **Attique, S. A., Hussain, N., Bilal M., & Iqbal, H. M. N.** (2023). Enzyme immobilization approaches. In *Biocatalyst Immobilization* (pp. 37-54). Elsevier Inc. https://doi.org/10.1016/B978-0-323-91317-1.00007-4.

[42] **Bullo, G. T., Marasca, N., Almeida, F. L. C., & Forte, M. B. S.** (2024). Lipases: market study and potential applications of immobilized derivatives. *Biofuels, Bioproducts and Biorefining*, *18*(5), 1676-1689. https://doi.org/10.1002/bbb.2607.

[43] **Silva Almeida, C., Simão Neto, F., da Silva Sousa, P., da Silva Aires, F. I., de Matos Filho, J. R., Gama Cavalcante, A. L, de Sousa Junior, P., G., Melo, R. L. F., & dos Santos, J. C. S.** (2024). Enhancing Lipase Immobilization via Physical Adsorption: Advancements in Stability, Reusability, and Industrial Applications for Sustainable Biotechnological Processes. *ACS Omega*, 9(47), 46698-46732. https://doi.org/10.1021/acsomega.4c07088.

[44] **Li, J., Shi, X., Qin, X., Liu, M., Wang, Q., & Zhong, J.** (2024). Improved lipase performance by covalent immobilization of Candida antarctica lipase B on amino acid modified microcrystalline cellulose as green renewable support. *Colloids and Surfaces B: Biointerfaces*, *235*, 113764. https://doi.org/10.1016/j.colsurfb.2024.113764.

[45] **Zhao, L., Zhang, Y., Yang, Y., & Yu, C.** (2022). Silica-based nanoparticles for enzyme immobilization and delivery. *Chemistry–An Asian Journal*, *17*(17), e202200573. https://doi.org/10.1002/asia.202200573.

[46] **Onoka, I., & Makangara, J. J.** (2025). Micro-and nanocarriers for immobilization of enzymes. In *Marine Biopolymers* (pp. 545-572). Elsevier Inc. https://doi.org/10.1016/B978-0-443-15606-9.00019-X.

[47] **Girelli, A. M., & Chiappini, V.** (2023). Renewable, sustainable, and natural lignocellulosic carriers for lipase immobilization: A review. *Journal of Biotechnology*, *365*, 29–47. https://doi.org/10.1016/j.jbiotec.2023.02.003.

[48] **Hussain, M., Khan, I., Jiang, B., Zheng, L., Pan, Y., Hu, J., Ashraf, A., Din, A. S. U., AL-Ansi, W., Khan, A. & Zou, X.** (2023). Lipases: Sources, immobilization techniques, and applications. *International Journal of Environment, Agriculture and Biotechnology*, *8*(6), *94-121*. https://doi.org/10.22161/ijeab.86.12.

[49] **Ismail, A. R., & Baek, K-H.** (2020). Lipase immobilization with support materials, preparation techniques, and applications: Present and future aspects. *International Journal of Biological Macromolecules*, *163*, 1624–1639. https://doi.org/10.1016/j.ijbiomac.2020.09.021.

[50] **Seroka, N. S., & Khotseng, L.** (2024). New Source of Biogenic Silicon from Sugarcane Bagasse. In de Mello Prado, R., Etesami, H. & Srivastava, A. K. (Eds.), *Silicon Advances for Sustainable Agriculture and Human Health: Increased Nutrition and Disease Prevention* (pp. 209-221). Springer Switzerland. https://doi.org/10.1007/978-3-031-69876-7_10.

[51] **McLean, B., & Yarovsky, I.** (2024). Structure, Properties, and Applications of Silica Nanoparticles: Recent Theoretical Modeling Advances, Challenges, and Future Directions. *Small*, *20*(51), 2405299. https://doi.org/10.1002/smll.202405299.

[52] **Fernandes, I. J., Moraes, C. A. M., Egea, J. R. J., & Sousa, V. C.** (2024). Production and characterization of silica materials from rice husk ash by different combustion processes. *Powder Technology*, *436*, 119473. https://doi.org/10.1016/j.powtec.2024.119473.

[53] **Vesoloski, J. F., Todero, A. S., Macieski, R. J., de Oliveira Pereira, F., Dallago, R. M., & Mignoni, M. L.** (2022). Immobilization of lipase from Candida antarctica B (CALB) by sol–gel technique using rice Husk ash as silic source and ionic liquid as additive. *Applied Biochemistry and Biotechnology*, *194*, 6270–6286. https://doi.org/10.1007/s12010-022-04096-z.

[54] **Kordi, M., Farrokhi, N., Pech-Canul, M. I., & Ahmadikhah, A.** (2024). Rice husk at a glance: from agro-industrial to modern applications. *Rice Science*, *31*(1), 14–32. https://doi.org/10.1016/j.rsci.2023.08.005.

[55] **Liu, C., Han, Y., Wang, Z., Zhang, L., & Yang, W.** (2024). Preparation of (3-Aminopropyl) triethoxysilane-Modified Silica Particles with Tunable Isoelectric Point. *Langmuir*, *40*(24), 12565-12572. https://doi.org/10.1021/acs.langmuir.4c01027.

[56] **Sypabekova, M., Hagemann, A., Rho, D., & Kim, S.** (2022). 3-Aminopropyltriethoxysilane (APTES) deposition methods on oxide surfaces in solution and vapor phases for biosensing applications. *Biosensors (Basel, Switzerland)*, *13*(1), 36. https://doi.org/10.3390/bios13010036.

[57] **Aziz, T., Ullah, A., Fan, H., Jamil, M. I., Khan, F. U., Ullah, R., Iqbal, M., Ali, A. & Ullah, B.** (2021). Recent progress in silane coupling agent with its emerging applications. *Journal of Polymers and the Environment*, *29*, 3427-3443. https://doi.org/10.1007/s10924-021-02142-1.

[58] **Fopase, R., Paramasivam, S., Kale, P., & Paramasivan, B.** (2020). Strategies, challenges and opportunities of enzyme immobilization on porous silicon for biosensing applications. *Journal of Environmental Chemical Engineering*, *8*(5), 104266. https://doi.org/10.1016/j.jece.2020.104266.

[59] **Munzeiwa, W. A., Omondi, B. O., & Nyamori, V. O.** (2024). A perspective into ring-opening polymerization of ε-caprolactone and lactides: effect of, ligand, catalyst structure and system dynamics, on catalytic activity and polymer properties. *Polymer Bulletin*, *81*, 9419-9464. https://doi.org/10.1007/s00289-024-05149-5.

[60] **Mankaev, B. N., Serova, V. A., Agaeva, M. U., Lyssenko, K. A., Fakhrutdinov, A. N., Churakov, A. V., Chernikova, E. V., Egorov, M. P., & Karlov, S. S.** (2024). Aluminum and titanium complexes bearing 2, 6-Bis (2-hydroxyphenyl) pyridines for ring-opening polymerization of lactide, ε-caprolactone and their copolymerization: Effect of a ligand on coordination chemistry and reactivity. *Journal of Organometallic Chemistry*, *1005*, 122973. https://doi.org/10.1016/j.jorganchem.2023.122973.

[61] **Narmon, A. S., Jenisch, L. M., Pitet, L. M., & Dusselier, M.** (2022). Ring-Opening Polymerization Strategies for Degradable Polyesters. In Dusselier, M. & Lange, J.-P. (Eds.), *Biodegradable Polymers in the Circular Plastics Economy* (1st ed., pp. 205–271). Wiley-VCH GmbH. https://doi.org/10.1002/9783527827589.ch7.

[62] **Al-Shok, L., Haddleton, D. M., & Adams, F.** (2022). Progress in catalytic ring-opening polymerization of biobased lactones. In Künkel, A., Battagliarin, G., Winnacker, M., Rieger B., & Coates, G. (Eds.), *Synthetic biodegradable and biobased polymers: Industrial aspects and technical products* (Vol. 293, pp. 197-267). Springer Switzerland. https://doi.org/10.1007/12_2021_111.

[63] **Posada, N. C., Sierra, C. A., & Perez, L. D.** (2025). Synthesis of lipid-modified copolymers based on caprolactone via enzymatic ring-opening polymerization and click chemistry and evaluation of their potential as vehicles in drug delivery. *Journal of Applied Polymer Science*, *142*(1), e56325. https://doi.org/10.1002/app.56325.

[64] **Wang, H., Ding, G., Li, X., She, H., Zhu, Y., & Li, Y.** (2021). Sustainable production of γ-valerolactone and δ-valerolactone through the coupling of hydrogenation and dehydrogenation. *Sustainable Energy and Fuels*, *5*(4), 930–934. https://doi.org/10.1039/d0se01776k.

[65] **Dong, R., Guo, J., Sun, H., & Xu, T.** (2024). Circular Polyesters Based on Lactones. *ChemCatChem*, *17*(1), e202401319. https://doi.org/10.1002/cctc.202401319.

[66] **Bińczak, J., Dziuba, K., & Chrobok, A.** (2021). Recent developments in lactone monomers and polymer synthesis and application. *Materials*, *14*(11), 2881. https://doi.org/10.3390/ma14112881.

[67] **Badwelan, M., Alkindi, M., Alghamdi, O., Saeed, W. S., Al-Odayni, A.-B., Alrahlah, A., & Aouak, T.** (2020). Poly (δ-valerolactone)/Poly (ethylene-co-vinylalcohol)/β-Tricalcium Phosphate Composite as Scaffolds: Preparation, Properties, and In Vitro Amoxicillin Release. *Polymers (Basel, Switzerland)*, *13*(1), 46. https://doi.org/10.3390/polym13010046.

[68] **Yusuf, M., Nurfajriani, Siregar, R., Eddiyanto, & Nugraha, A. W.** (2023). Determination of HOMO and LUMO of bis (β-diketonate) zirconium (IV) compound used as a catalyst in the ring opening polymerization of ε-Caprolactone and δ-Valerolactone. *Journal of Macromolecular Science, Part A*, *60*(12), 865–874. https://doi.org/10.1080/10601325.2023.2273842.

[69] **Yusuf, M., Nurfajriani, Siregar, R. M., Eddiyanto, & Nugraha, A. W.** (2024). The role of Lewis acidity in bis (β-diketonate) zirconium (IV) complexes as catalysts for the ring-opening polymerization of δ-valerolactone. *Journal of Macromolecular Science, Part A*, *61*(12), 1030–1040. https://doi.org/10.1080/10601325.2024.2423236.

[70] **Wang, K., Li, C., Man, L., Zhang, M., Jia, Y.-G., & Zhu, X. X.** (2023). Lipase-catalyzed ring-opening polymerization of natural compound-based cyclic monomers. *Chemical Communications*, *59*(60), 9182–9194. https://doi.org/10.1039/d3cc02114a.

[71] **Park, H., Otte, A., & Park, K.** (2022). Evolution of drug delivery systems: From 1950 to 2020 and beyond. *Journal of Controlled Release*, *342*, 53–65. https://doi.org/10.1016/j.jconrel.2021.12.030.

[72] **Puccetti, M., Pariano, M., Schoubben, A., Giovagnoli, S., & Ricci, M.** (2024). Biologics, theranostics, and personalized medicine in drug delivery systems. *Pharmacological Research*, *201*, 107086. https://doi.org/10.1016/j.phrs.2024.107086.

[73] **Alavi, S. E., Alharthi, S., Alavi, S. Z., Raza, A., Shahmabadi, & H. E.** (2024). Bioresponsive drug delivery systems. *Drug Discovery Today*, *29*(1), 103849. https://doi.org/10.1016/j.drudis.2023.103849.

[74] **Vargason, A. M., Anselmo, A. C., & Mitragotri, S.** (2021). The evolution of commercial drug delivery technologies. *Nature Biomedical Engineering*, *5*, 951–967. https://doi.org/10.1038/s41551-021-00698-w.

[75] **Jain, S., Kirar, M., Bindeliya, M., Sen, L., Soni, M., Shan, M., Purohit, A., & Jain, P. K.** (2022). Novel drug delivery systems: an overview. *Asian Journal of Dental and Health Sciences*, *2*(1), 33–39. https://doi.org/10.22270/ajdhs.v2i1.14.

[76] **Biswas, M. C., Jony, B., Nandy, P. K., Chowdhury, R. A., Halder, S., Kumar, D., Ramakrishna, S., Hassan, M., Ahsan, M. A., Hoque, M. E. & Imam, M. A.** (2022). Recent advancement of biopolymers and their potential biomedical applications. *Journal of Polymers and the Environment*, *30*, 51-74. https://doi.org/10.1007/s10924-021-02199-y.

[77] **Rajput, A., Pingale, P., Bagad, P., Patil, R., & Musale, S.** (2025). Biodegradable Polymers in Sustained and Controlled Drug Delivery. In Ahmed, S., & Osmani, R. A. M. (Eds.), *Handbook of Biodegradable Polymers* (pp. 67-104). Jenny Stanford Publishing Pte. Ltd. https://doi.org/10.1201/9781032693309.

[78] **HPS, A. K., MR, N. F., & Nurazzi, M.** (2024). Biopolymers and Biopolymer Blends: Fundamentals, Processes, and Emerging Applications, 331–350. https://doi.org/10.1201/9781003416043.

[79] **Jones, O. G., & McClements, D. J.** (2010). Functional biopolymer particles: design, fabrication, and applications. *Comprehensive Reviews in Food Science and Food Safety*, *9*(4), 374–397. https://doi.org/10.1111/j.1541-4337.2010.00118.x.

[80] **Kamaly, N., Yameen, B., Wu, J., & Farokhzad, O. C.** (2016). Degradable controlled-release polymers and polymeric nanoparticles: mechanisms of controlling drug release. *Chemical Reviews*, *116*(4), 2602–2663. https://doi.org/10.1021/acs.chemrev.5b00346.

[81] **Xue, R., Wu, H., Li, S., Pu, N., Wei, D., Zhao, N., Cui, Y., Li, H., Song, Z. & Tao, Y.** (2024). Biodegradable microspheres come into sight: A promising biomaterial for delivering drug to the posterior segment of the eyeball. *Materials Today Bio, 27*, 101126. https://doi.org/10.1016/j.mtbio.2024.101126.

[82] **Li, X., Li, L., Wang, D., Zhang, J., Yi, K., Su, Y., Luo, J., Deng, X. & Deng F.** (2024). Fabrication of polymeric microspheres for biomedical applications. *Material Horizons, 11*(12), 2820-2855. https://doi.org/10.1039/d3mh01641b.

[83] **Samanta, M. S., Gautam, D., Chandel, M. W., Sawant, G., & Sharma, K.** (2021). A review on microspheres as a novel controlled drug delivery system. *Asian Journal of Pharmaceutical Clinical Research*, *14*(4), 3–11. https://doi.org/10.22159/ajpcr.2021v14i4.40634.

[84] **Uyen, N. T. T., Hamid, Z. A. A., Tram, N. X. T., & Ahmad, N.** (2020). Fabrication of alginate microspheres for drug delivery: A review. *International Journal of Biological Macromolecules, 153*, 1035–1046. https://doi.org/10.1016/j.ijbiomac.2019.10.233.

[85] **Alavi, M., & Webster, T. J.** (2021). Recent progress and challenges for polymeric microsphere compared to nanosphere drug release systems: Is there a real difference? *Bioorganic and Medicinal Chemistry, 33*, 116028. https://doi.org/10.1016/j.bmc.2021.116028.

[86] **Verma, R., Verma, S., & Kumar, S.** (2019). Microsphere-a novel drug delivery system. *Research Chronicle in Health Sciences*, *5*(1), 5–14.

[87] **Hossain, K. M. Z., Patel, U., & Ahmed, I.** (2015). Development of microspheres for biomedical applications: a review. *Progress in Biomaterials, 4*, 1–19. https://doi.org/10.1007/s40204-014-0033-8.

[88] **Lengyel, M., Kállai-Szabó, N., Antal, V., Laki, A. J., & Antal, I.** (2019). Microparticles, microspheres, and microcapsules for advanced drug delivery. *Scientia Pharmaceutica, 87*(3), 20. https://doi.org/10.3390/scipharm87030020.

[89] **Panigrahi, S. K., Das, S., & Majumdar, S.** (2024). Unveiling the potentials of hydrophilic and hydrophobic polymers in microparticle systems: Opportunities and challenges in processing techniques. *Advances in Colloid and Interface Science, 326*, 103121. https://doi.org/10.1016/j.cis.2024.103121.

[90] **Rupali, S. P., Anuja, G. G., Vrunda, R. J., Subodh, U. A., & Atram, S. C.** (2024). A Technical Note: on Microspheres. *Asian Journal of Pharmaceutical Research and Development*, *12*(1), 65–76. https://doi.org/10.22270/ajprd.v12i1.1350.

[91] **Kerkar, N., Barse, R., & Jagtap, V.** (2024). A Comprehensive Overview of Microspheres as A Novel Drug Delivery System. *International Journal of Pharmaceutical Sciences*, *2*(11), 824–835. https://doi.org/10.5281/zenodo.14187784.

[92] **Bentley, E. R., Subick, S., Pezzillo, M., Balmert, S. C., Herbert, A., & Little, S. R.** (2024). Identification and Characterization of Critical Processing Parameters in the Fabrication of Double-Emulsion Poly (lactic-co-glycolic) Acid Microparticles. *Pharmaceutics*, *16*(6), 796. https://doi.org/10.3390/pharmaceutics16060796.

[93] **Wei, X., Yao, X., Yue, J., Li, G., Liu, N., Li, D., Yang, D., Fang, Y., Nishinari, K., & Zhao, M.** (2024). Recent Advances on the Generation, Stabilization, and Potential Applications of Double Emulsions Based on the Microfluidic Strategy. *Food Engineering Reviews*, *16*, 129–145. https://doi.org/10.1007/s12393-023-09361-3.

[94] **Vaidya, S. N., Gulghane, V., Satote, V., Vaghede, S., & Kale, S.** (2024). A Review on Microspheres as Drug Carriers. *Asian Journal of Pharmaceutics (AJP)*, *18*(4), 1004-1011.

[95] **Rane, A. V., Prajitha, V., Jibin, K. P., Moyo, M., Abitha, V. K., Kanny, K., & Thomas, S.** (2024). Specific interactions in nanohybrid systems. In Thomas, S., Saiter-Fourcin, A. & Jibin, K. P. (Eds.), *Hybrid Nanofillers for Polymer Reinforcement* (pp. 73-133). Elsevier Inc. https://doi.org/10.1016/B978-0-323-99132-2.00003-0.

[96] **Wang, J., & Song, Y.** (2017). Microfluidic synthesis of nanohybrids. *Small*, *13*(18), 1604084. https://doi.org/10.1002/smll.201604084.

[97] **Gomez-Romero, P., Pokhriyal, A., Rueda-García, D., Bengoa, L. N., & González-Gil, R. M.** (2023). Hybrid Materials: A Metareview. *Chemistry of Materials*, *36*(1), 8–27. https://doi.org/10.1021/acs.chemmater.3c01878.

[98] **Manatunga, D. C., Godakanda, V. U., De Silva, R. M., & De Silva, K. M. N.** (2020). Recent developments in the use of organic–inorganic nanohybrids for drug delivery. *Wiley Interdisciplinary Reviews: Nanomedicine and Nanobiotechnology*, *12*(3), e1605. https://doi.org/10.1002/wnan.1605.

[99] **Kaptan, Y.,** (2022). Controlled delivery of Chalcone via Biopolyester Nanohybrid, *PhD. Thesis*, ITU, Institute of Science and Technology, Istanbul.

[100] **Abtahi, S., Hendeniya, N., Mahmud, S. T., Mogbojuri, G., Iheme, C. L., & Chang, B.** (2025). Metal-Coordinated Polymer–Inorganic Hybrids: Synthesis, Properties, and Application. *Polymers (Basel, Switzerland)*, *17*(2), 136. https://doi.org/10.3390/polym17020136.

[101] **Faustini, M., Nicole, L., Ruiz-Hitzky, E., & Sanchez, C.** (2018). History of organic–inorganic hybrid materials: prehistory, art, science, and advanced applications. *Advanced Functional Materials*, *28*(27), 1704158. https://doi.org/10.1002/adfm.201704158.

[102] **Hood, M. A., Mari, M., & Muñoz-Espí, R.** (2014). Synthetic strategies in the preparation of polymer/inorganic hybrid nanoparticles. *Materials (Basel, Switzerland)*, *7*(11), 7583-7614. https://doi.org/10.3390/ma7117583.

[103] **Narwal, S., Devi, B., Dhanda, T., Kumar, S., & Tahlan, S.** (2024). Exploring chalcone derivatives: synthesis and their therapeutic potential. *Journal of Molecular Structure*, *1303*, 137554. https://doi.org/10.1016/j.molstruc.2024.137554.

[104] **Shalaby, M. A., Rizk, S. A., & Fahim, A. M.** (2023). Synthesis, reactions and application of chalcones: A systematic review. *Organic and Biomolecular Chemistry*, *21*(26), 5317–5346. https://doi.org/10.1039/d3ob00792h.

[105] **Mazumder, R., Ichudaule, Ghosh, A., Deb, S., & Ghosh, R.** (2024). Significance of chalcone scaffolds in medicinal chemistry. *Topics in Current Chemistry*, *382*, 22. https://doi.org/10.1007/s41061-024-00468-7.

[106] **Sheetal, Singh, A. K., Anadebe, V. C., Singh, M., Arshad, N., Barik, R. C., Qureshi, M. A. U. R., Quadri, T. W., Akpan, E. D., Olasunkanmi, L. O., Shukla, S. K., Tuteja, J., Thakur S., Pani, B. & Ebenso, E. E.** (2024). Coordination chemistry of chalcones and derivatives and their use as corrosion inhibitors: A comprehensive review. *Coordination Chemistry Reviews*, *517*, 215985. https://doi.org/10.1016/j.ccr.2024.215985.

[107] **Farahmandghavi, F., Imani, M., & Hajiesmaeelian, F.** (2019). Silicone matrices loaded with levonorgestrel particles: Impact of the particle size on drug release. *Journal of Drug Delivery Science and Technology*, *49*, 132–142. https://doi.org/10.1016/j.jddst.2018.10.029.

[108] **Tirado, D. F., Latini, A., & Calvo, L.** (2021) .The encapsulation of hydroxytyrosol-rich olive oil in Eudraguard® protect via supercritical fluid extraction of emulsions. *Journal of Food Engineering*, *290*, 110215. https://doi.org/10.1016/j.jfoodeng.2020.110215.

[109] **Jaiswal, H., Ansari, M. T., Mahmood, T., Ahsan, F., Ansari, V. A., & Ahmad, U.** (2024). Aceclofenac loaded microspheres: Formulation and evaluation of novel preprogrammed drug delivery for the treatment of arthritis. *Intelligent Pharmacy*, *2*(1), 69–82. https://doi.org/10.1016/j.ipha.2023.10.010.

[110] **Nawaz, T., Iqbal, M., Khan, B. A., Nawaz, A., Hussain, T., Hosny, K. M., Abualsunun, W. A. & Rizg, W. Y.** (2021). Development and optimization of acriflavine-loaded polycaprolactone nanoparticles using box–behnken design for burn wound healing applications. *Polymers (Basel, Switzerland)*, *14*(1), 101. https://doi.org/10.3390/polym 140101 01.

[111] **Yu, B., Meng, L., Fu, S., Zhao, Z., Liu, Y., Wang, K., & Fu, Q.** (2018). Morphology and internal structure control over PLA microspheres by compounding PLLA and PDLA and effects on drug release behavior. *Colloids and Surfaces B: Biointerfaces*, *172*, 105–112. https://doi.org/10.1016/j.colsurfb.2018.08.037.

[112] **Loganathan, S., Valapa, R. B., Mishra, R. K., Pugazhenthi, G., & Thomas, S.** (2017). Thermogravimetric analysis for characterization of nanomaterials. In Holt, S. (Ed.), *Thermal and Rheological Measurement Techniques for Nanomaterials Characterization* (pp. 67-108). Elsevier Inc. https://doi.org/10.1016/B978-0-323-46139-9.00004-9.

[113] **Radomska, E., Mika, L., & Sztekler, K.** (2020). The impact of additives on the main properties of phase change materials. *Energies (Basel, Switzerland)*, *13*(12), 3064. https://doi.org/10.3390/en13123064.

[114] **Gao, W., Chan, J. M., & Farokhzad, O. C.** (2010). pH-responsive nanoparticles for drug delivery. *Molecular Pharmaceutics*, *7*(6), 1913–1920. https://doi.org/10.1021/mp100253e.

[115] **Ulker Turan, C., & Guvenilir, Y.** (2021). Fabrication and characterization of electrospun biopolyester/gelatin nanofibers. *Journal of Biomedical Materials Research Part B: Applied Biomaterials*, *109*(10), 1478–1487. https://doi.org/10.1002/jbm.b.34807.

[116] **Supramaniam, J., Adnan, R., Kaus, N. H. M., & Bushra, R.** (2018). Magnetic nanocellulose alginate hydrogel beads as potential drug delivery system. *International Journal of Biological Macromolecules*, *118*, 640–648. https://doi.org/10.1016/j.ijbiomac.2018.06.043.

[117] **Fard, M. M., & Fard, A. M. M.** (2022). Modeling drug release. *Eurasian Journal of Science and Technology*, *2*(1), 14–33. https://doi.org/10.22034/EJST.2022.1.2.

APPENDICES

APPENDIX A: Calibration Curves

APPENDIX A : Calibration Curves

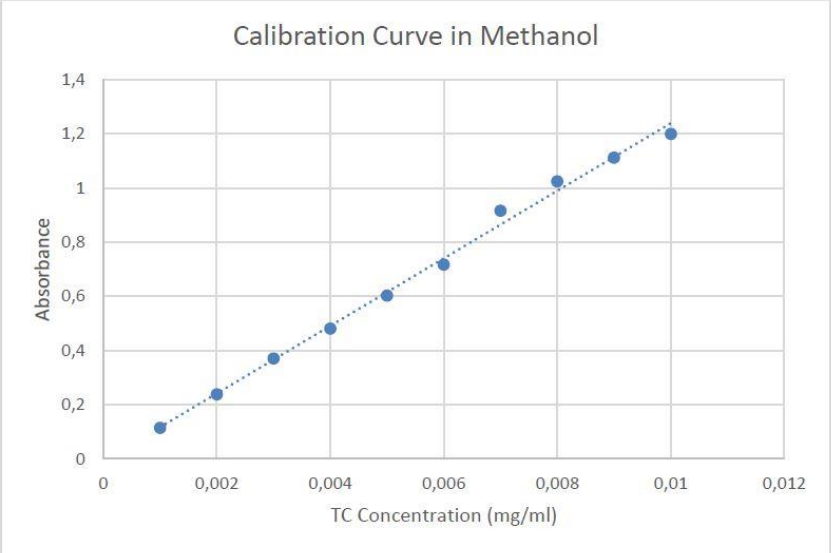

Figure A.1 : Calibration curve of TC in Methanol.

$$y = 124.72 \times x - 0.0084$$
$$R^2 = 0.9952$$

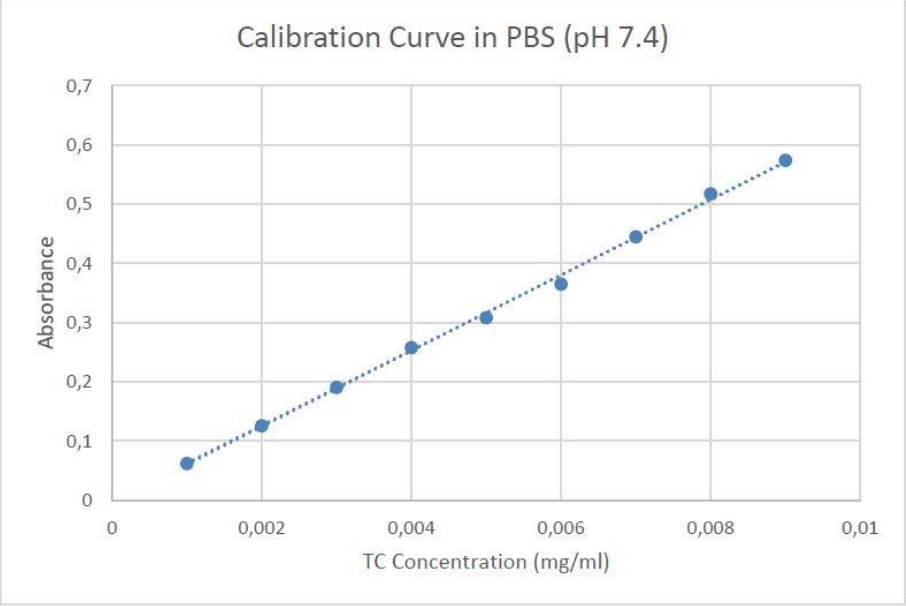

Figure A.2 : Calibration curve of TC in PBS (pH 7.4).

$$y = 63.95 \times x - 0.0036$$
$$R^2 = 0.9982$$

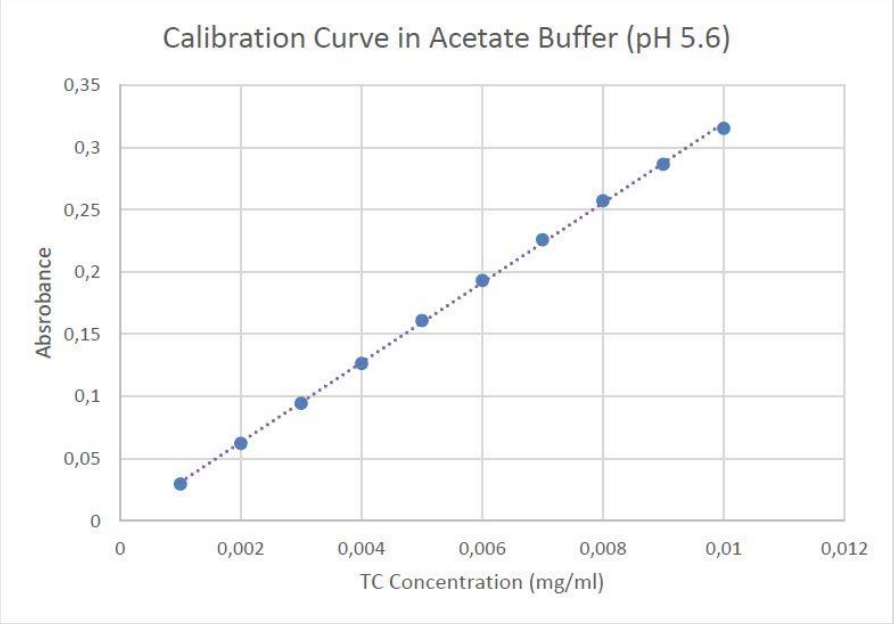

Figure A.3 : Calibration curve of TC in acetate buffer solution (pH 5.6).

$$y = 32.03 \times x - 0.0009$$
$$R^2 = 0.9995$$

CURRICULUM VITAE

Name Surname **:** Zeynep KEÇE

EDUCATION:

- **B.Sc.** **:** 2020, Istanbul Technical University, Faculty of Chemical and Metallurgical Engineering, Deparment of Chemical Engineering.

PUBLICATIONS, PRESENTATIONS AND PATENTS ON THE THESIS:

- **Keçe, Z.,** Ulker Turan, C. and Guvenilir, Y. 2024: Enzymatically Synthesized Poly(δ-valerolactone) Usage In Controlled Drug Release Systems, International Graduate Research Symposium – IGRS'24, May 8-10, 2024, Turkey. (Abstract submitted, Oral presentation)